ISBN 978-82-471-1468-1 (printed ver.)
ISBN 978-82-471-1469-8 (electronic ver.)
ISSN 1503-8181

Heidi Moe
Doctoral Thesis

Doctoral theses at NTNU, 2009:48

Heidi Moe

Strength analysis of net structures

NTNU
Norwegian University of
Science and Technology

Thesis for the degree of
philosophiae doctor
Faculty of Engineering Science and Technology
Department of Structural Engineering

NTNU
Norwegian University of
Science and Technology

Doctoral theses at NTNU, 2009:48

NTNU

Heidi Moe

Strength analysis of net structures

Thesis for the degree of philosophiae doctor

Trondheim, March 2009

Norwegian University of
Science and Technology
Faculty of Engineering Science and Technology
Department of Structural Engineering

NTNU
Norwegian University of
Science and Technology

NTNU
Norwegian University of Science and Technology

Thesis for the degree of philosophiae doctor

Faculty of Engineering Science and Technology
Department of Structural Engineering

ISBN 978-82-471-1468-1 (printed ver.)
ISBN 978-82-471-1469-8 (electronic ver.)
ISSN 1503-8181

Doctoral Theses at NTNU, 2009:48

Printed by Tapir Uttrykk

Heidi Moe

Strength analysis of net structures

Thesis for the degree of philosophiae doctor

Trondheim, December 2008

Norwegian University of Science and Technology
Faculty of Engineering Science and Technology
Department of Structural Engineering

Abstract

The main goal of this PhD project was to develop a method for non-linear strength analysis of net structures applied in the aquaculture and fishing industries, e.g. net cages and trawls. The work focused on the aquaculture net cage, which was applied in experiments and analyses, and included research to establish knowledge within material properties and failure modes of traditional netting materials for aquaculture. It was chosen to focus on tensile properties and to study elastic and plastic behaviour, fracture, creep behaviour and cod bite damage. The project consisted of three main activities: tensile testing of netting materials, studies and testing of cod bite damage and resistance, and structural analysis of aquaculture net cages.

Net cages are built as a system of ropes and netting. They are designed to transfer and carry all major forces through the ropes. Loads from current, waves, weights and handling induce forces in the net cage, which must be dimensioned to withstand this. Analyzing an aquaculture net cage is both complex and time consuming due to non-linear effects, detailed geometry and dynamic loads. The behaviour of the net cage is dominated by very large deformations and displacements, and materials with non-linear properties. There is a need for verified analysis methods and specific guidance on how to reduce the complexity of a net cage analysis.

In order to perform a strength analysis of a net cage, it is crucial to know the material properties of the netting material. Traditionally, the material property of major interest for the aquaculture industry has been the tensile breaking strength of netting (mesh) and ropes, and comparatively little focus has been on their detailed stiffness properties and general behaviour prior to fracture. A new test method was established to determine the uniaxial tensile properties of knotless netting materials. It was applied on a variety of netting materials and stress-strain relations were developed. Data on temporary creep properties, recovery of strain post creep and post creep tensile properties of a selection of Raschel knitted netting materials was presented. Post creep tensile testing showed that the length and force at break were not significantly affected by the creep load history.

Cod farmers have reported that cod interact with the cage netting through biting and thereby create wear and tear. The nature of the cod bite attack on traditional, multifilament netting materials was described based on studies of cod interaction with traditional knotless netting and resulting fracture

damage on netting fibres. Field experiments were performed, subjecting panels of netting to cod bite in commercial cod cages. In addition, a test method was developed to simulate damage on traditional netting from cod bite, and a prototype bite-jig was designed and assembled. It was concluded that netting materials for cod aquaculture must be resistant to cod bite or be repellent or uninteresting for cod.

A method for numerical analysis of net cages in constant uniform current was developed and verified for limited solidity, deformations and current velocities. Various new designs for aquaculture net cages were presented and compared to a traditional net cage with regard to stresses in the netting material and deformation of the net cage.

Acknowledgements

This work has been carried out under the supervision of professor Odd Sture Hopperstad at NTNU and Senior Scientist Dr. Arne Fredheim at SINTEF Fisheries and aquaculture. I am very thankful for their skilled guidance and great engagement in the project.

I would like to thank colleagues at SINTEF for sharing their expertise with me and taking time for discussions. Many have contributed in increasing the quality of this work. Dr. Anna Olsen has helped me in the performance of the initial tensile tests, she has given advice on statistical methods and contributed in post processing of test results. She has also contributed in the cod bite field experiments, the initial planning of the bite-jig and studies of cod teeth. Dr. Østen Jensen has contributed in the planning and post processing of tensile tests. Dr. Tim Dempster has contributed in documentation of cod bites and presentation of the initial cod escape studies. Cand. scient. Leif Magne Sunde and Cand. real. Ulf Winther have contributed in planning and presentation of the project work within escape of cod. M.Sc. Rune Gaarder has designed and assembled the bite-jig and contributed in the planning and application of the bite-jig and studies of cod bite fractures. The studied new net cage designs were suggested by Dr. Arne Fredheim and M.Sc. Mats Heide. M.Sc. Egil Lien, Dr. Pål Lader, M.Sc. Birger Enerhaug and M.Sc. Martin Føre also deserve to be mentioned in this context. My boss at the Aquaculture Technology Department, M.Sc. Jostein Storøy, receives my thanks for making this possible and supporting me all the way.

The PhD-project was funded by the Norwegian Research Council through the IntelliSTRUCT programme (Intelligent Structures in Fisheries and Aquaculture) at SINTEF Fisheries and Aquaculture. The project work was carried out during 2005-2008.

Thanks to my family and friends, who have always had faith in me and that I would be able to carry this project through. It has meant a lot to me. A special thanks to Martin and Frida for filling my spare time with happiness, love and wonderful adventures, charging my batteries for another day at work.

Contents

Synopsis:

Papers:

Appendices:

Introduction

Sea-based aquaculture technology

The sea-based aquaculture industry had its origin in Norway in the sixties and is rather new compared to the traditional catch of fish. Typical fish farms consist of three main components: the net cage, a cage collar and the mooring system (Figure 1, Figure 2 and Figure 3). These different components are equipped with buoyant elements and weights in order to keep the farm floating and to ensure that the net cage maintains its volume.

Net cages are built as a system of ropes and netting. They are designed to transfer and carry all major forces through the ropes. The netting is attached to the ropes and its intended function is to keep the fish in place. Design of net cages enclosing the fish is based on technology from the fisheries, such as fishing nets and purse seines, and developed through experience.

Figure 1: Norwegian fish farm with circular Polyethylen cage collars.

Escape of farmed fish

Millions of cultured fish have escaped from Norwegian fish farms. The main reasons for escape of the dominating species in Norwegian aquaculture, salmon (*Salmo salar*) and trout (*Oncorhynchus mykiss*), are structural failure, collisions, attacks from predators, drifting ice, propeller damage and handling (The Norwegian Directorate of Fisheries, 2008). This cultured fish may have a negative impact on wild fish through cross

breeding and spreading of diseases and parasites. Over the last years, the aquaculture industry has worked towards decreasing the number of escaped fish, with the goal of no escape. This work has been the driving force behind the introduction of the NYTEK-regulation in 2004, which refers to the Norwegian standard NS9415 "Marine fish farms -Requirements for design dimensioning, production, installation and operation" (Standard Norway, 2003).

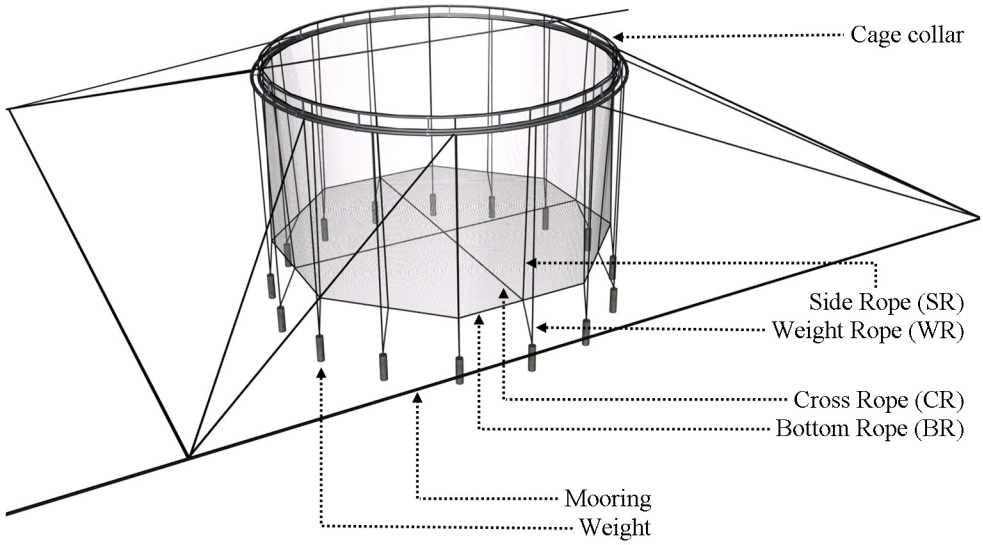

Figure 2: Sketch of circular fish farm.

Figure 3: Section of steel cage. Right picture shows net handling.

The net cage plays an important role in most escape episodes, either directly through holes in the net cage from over-loading or contact with other objects, or indirectly by transferring major loads to the fish farm (Moe et al. 2003, Paper 1, Jensen 2006, Norwegian Fisheries Directorate 2007). As the component that physically encloses the fish and the main contributor to loading of the fish farm, it is natural to focus research efforts on understanding net cage properties and behaviour to prevent further escapes.

*Escape of cultured cod (*Gadus morhua*)*

Introduction of new species in aquaculture, like Atlantic cod, creates new challenges in the development of suitable technologies for their culture. Problems may arise when technologies developed for culturing one species (e.g. salmon) are used, with little modification, to culture a new species. The Norwegian Directorate of Fisheries (2008) has estimated that cod are 10 to 20 times more likely to escape from sea-based fish farms than salmon. Cod seem to be willing to squeeze through small holes, and cod farmers have reported that cod interact with the cage netting through biting and thereby create wear and tear (Figure 4 and Moe et al., 2005). It is important to establish knowledge on how and why cultured cod escape, and to find strategies that can minimize escapes. The net cage producers have responded to this challenge by introducing new net materials intended for cod culture. However, none of these products have a documented resistance against cod bite, which is due to the fact that knowledge of wear and tear on nets due to cod bite has been insufficient.

Figure 4: Atlantic cod may try to squeeze through small holes and they bite at the netting, creating wear and tear.

Strength analysis of net cages

The net cage must be dimensioned to withstand loads from current, waves, weights and handling. The net cage is a very flexible structure with potentially large displacements as shown for a model in Figure 5.

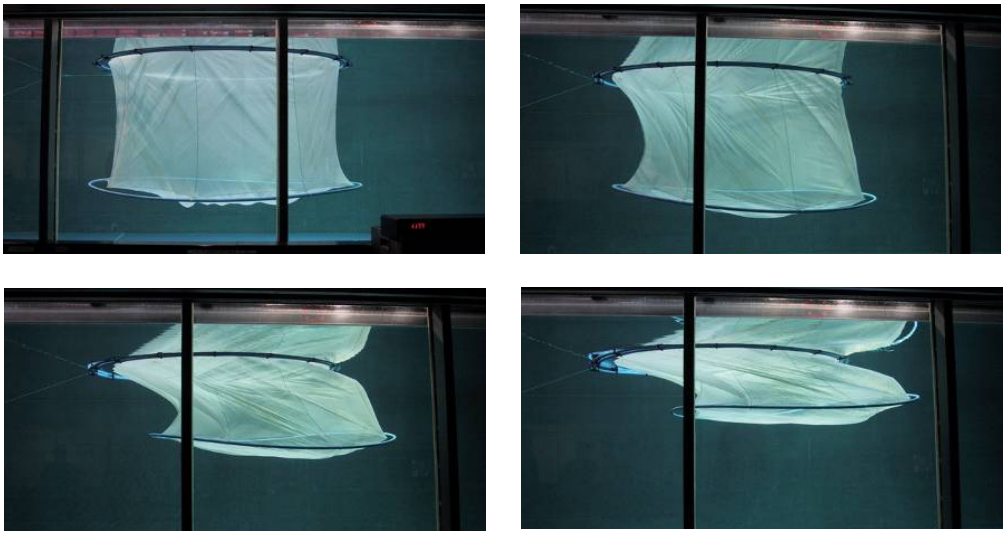

Figure 5: Model tests of circular net cage with bottom ring in a flume tank with current of varying (increasing) velocity.

The Norwegian net cage producers have developed empirical standards for design of net cages, which are implemented in NS 9415. The standard gives requirements to the tensile strength of the applied netting (combination of mesh width and mesh breaking strength), the number of ropes and their minimal tensile strength. The specific requirements are given based on the depth and circumference of the net cage. For large cages and heavy loading, the standard requires that calculations are performed to prove that the net cage has the necessary strength.

Strength analysis of aquaculture net cages is both complex and time consuming due to non-linear effects, detailed geometry and dynamic loads. The behaviour of the net cage can be dominated by non-linear effects due to very large deformations and materials with non-linear properties. The net cage is subjected to dynamic loads dependent on the relative velocity and acceleration of the different parts of the net cage. There is a need for

verified analysis methods and specific guidance on how to reduce the complexity of a net cage analysis.

In order to perform a strength analysis of a net cage, it is crucial to know the material properties of the netting material. Traditionally, the material property of major interest for the aquaculture industry has been the tensile breaking strength of netting (mesh) and ropes, and comparatively little focus has been on their detailed stiffness properties and general behaviour prior to fracture (Klust, 1982 and Sala et al., 2004). To be able to perform a strength analysis, extended knowledge of the material properties of netting and ropes applied in aquaculture is required.

During a structural analysis, not only distributions of stresses and strains can be studied, but also net cage shape and volume. Ensuring sufficient net cage volume is important for fish welfare and growth. Structural analysis can be a useful tool in developing new net cage design and operational strategies (like handling, Figure 3).

Previous work within these topics is discussed further in the attached papers.

Objectives and scope

This PhD-project was funded by the Norwegian Research Council through the IntelliSTRUCT programme (Intelligent Structures in Fisheries and Aquaculture, 2004-2008) at SINTEF Fisheries and Aquaculture. The overall goal of this programme was to develop intelligent structures for the fishing and aquaculture industries. Intelligent structures are structures that adapt to the environment and applied forces through active control and / or specific construction properties. The main focus of IntelliSTRUCT was modelling and active control of flexible structures through a synthesis of knowledge and research within cybernetics, hydrodynamics, structural mechanics and ethology.

The main goal of this PhD work was to develop a method for non-linear strength analysis of net structures applied in the aquaculture and fishing industries, e.g. net cages and trawls. During this work, the aquaculture net cage was in focus and applied in experiments and analyses. The results may also be of interest to other net structures such as trawls. In order to comply with the focus of the IntelliSTRUCT programme, the analysis method allows for easy import of hydrodynamic loading and prescribed displacements.

Net cages in operation are subjected to loads from waves, current, weights, handling, cod bite, conflicts with external bodies etc. These loads will introduce internal stresses in the net cage structure and subject the materials to wear and tear. The knowledge of the magnitude of internal stresses and damages, their critical values and possible failure modes has been insufficient to perform a precise strength analysis. Failure mechanisms that should be considered are tensile fracture, shear fracture, fatigue, creep, chemical wear and abrasion. This work includes research to establish knowledge within material properties and failure modes of traditional netting materials for aquaculture. It was chosen to focus on tensile properties and to study elastic and plastic behaviour, fracture, creep behaviour and cod bite damage. The project consisted of three main activities: tensile testing of netting materials, studies and testing of cod bite damage and resistance, and structural analysis of aquaculture net cages.

Materials and methods

Raschel knitted netting materials

The netting used in net cages varies in raw material, size, structure and surface treatment. Traditionally, most netting materials have been produced of knitted bundles of Nylon (Polyamide 6) multifilaments ('knotless' netting, Figure 6) or twines of twisted multifilament bundles connected by knots ('knotted' netting, Figure 1 in Paper 4). A trade standard exists that defines the number of filaments required to produce netting with a given minimum breaking strength. A variety of other netting materials are available, but knotless square mesh Nylon netting is by far the dominating material in Norwegian aquaculture net cages.

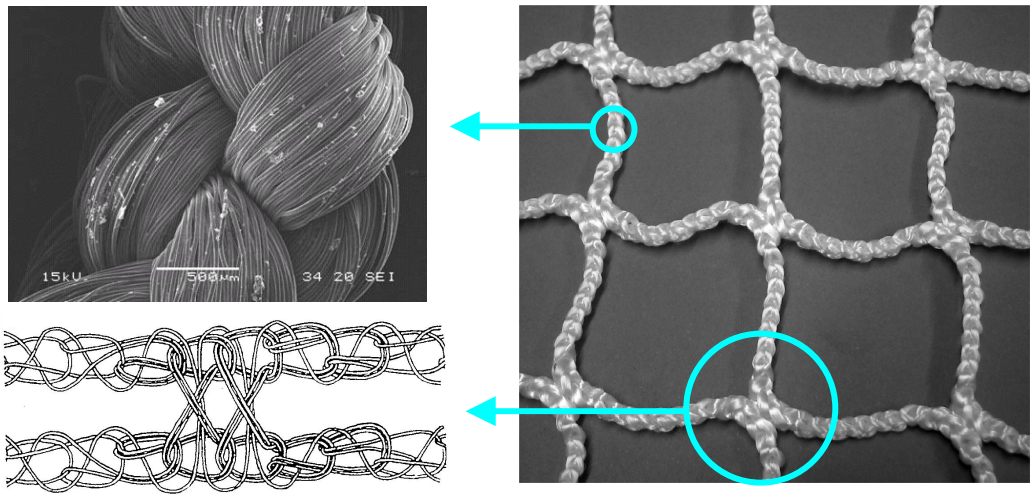

Figure 6: Typical netting used in net cages (super-knot Raschel knitted netting with multifilaments). Details are shown by an electron microscope picture (SINTEF Materials and chemistry) and a sketch of the applied knitting pattern (Klust, 1982).

This work focuses on the super-knot Raschel knitted netting. Raschel knitted netting was introduced into the fishing equipment industry in the 1950s. Raschel knitted netting proved to have several qualities superior to

the traditionally knotted netting materials, especially due to the lower amount of material in the knot. As a result, Raschel netting is often preferred over knotted netting materials for small mesh widths (Klust, 1982). The mesh widths in netting for traditional Norwegian aquaculture net cages are considered small in this context.

Several different knitting patterns for Raschel netting exist (von Brandt, 1964 and Damiani, 1964). The preferred pattern in Norwegian aquaculture netting production is the super-knot pattern, where the knot is strengthened to reduce the risk of laddering of the netting (Figure 6). Although the netting is called knotless, the connection between twines is still called a knot. The twines are knitted of three strands, each consisting of one to three bundles of multifilaments (more than 100 fibres in each bundle), as shown in Figure 6.

The knitted netting has a significant geometric flexibility; the elongation of the twines and knots will be larger than the elongation of the filaments. This contributes to the fact that netting materials are highly flexible structures with a non-linear stiffness that increases with increased displacement. In addition, the filaments are made of polymers that are known to have large strain at break and non-linear material properties. Netting materials made of Polyamide 6 multifilaments have a negligible bending stiffness (Klust, 1982) and will in practise take no compression.

Tensile tests

A new test method was developed to determine the tensile properties of knotless netting. Tests were performed using a single column testing machine with single bollard grips to reduce the build up of stress at the clamp point. A travel extensometer was used to measure the elongation of the test specimen. The test specimen was a thread consisting of several twines and knots cut out of the netting material, and it was loaded in direction parallel to the twines. A detailed description of the test method with illustrations is given in Paper 1.

Tensile testing was performed on various dimensions of wet netting, netting with anti-fouling treatment and dry netting materials (in Paper 1 and Paper 2). The method was verified by comparing the results to the establish mesh strength test (ISO 2002, Appendix B).

Cod bite damage and resistance

Surveys

Employees at 19 cod farming companies throughout Norway were surveyed to collect information on their experiences with net culture technologies and escapes of cod (Paper 3). Producers of aquaculture equipment, producers of fish feed and professional diver companies were also interviewed as a secondary source of information.

Field experiments

Panels with netting were subjected to cod bite at commercial cod farms (paper 4, preliminary experiments are presented in Paper 3). Both traditional netting materials and various netting concepts that were used or intended for cod aquaculture were tested (involved various structure, polymer materials and surface treatment). The test panels consisted of pieces of netting material attached to a circular steel ring with a diameter of 0.7 – 1 m. The rings were attached to a rope and lowered to about 3 meters below the water surface.

Bite-jig

A test method was developed to simulate damage on traditional netting from cod bite, and a prototype bite-jig was designed and assembled. The bite-jig was built based on a hydraulic tensile test machine usually applied for fatigue testing. A bite mechanism was mounted in the test machine through a load cell, including a teeth blade with two teeth models. The test specimen of netting material was clamped with no pretension in a test frame, which was mounted in a vessel filled with fresh water beneath the bite-mechanism. The test was performed by repeatedly rising and lowering the vessel containing the test frame. When a tooth on the teeth blade made contact with the netting during the vertical movement, the twine was subjected to a bite load. Due to the fixed edges, global structural effects like laddering were limited in these tests. The bite-jig was applied to quantify relative local cod bite resistance. Detailed descriptions with illustrations are given in Paper 4.

Tensile properties of netting damaged by cod bite were investigated through mesh strength tests presented in Appendix C.

Structural analysis

A method for numerical analysis of net cages in constant uniform current was developed and verified for limited solidity, deformations and current velocities (Paper 5). The method was validated by comparing the results to model tests of a cage without bottom (a netting cylinder only, with no bottom panel) performed in a flume tank (Lader & Enerhaug, 2005), then the method was applied to study deformations and global and local forces on full-scale net cages in uniform current.

For simplicity, neither the cage collar nor the mooring system was modelled in these analyses, but assumed to keep their original shape and position. The net cage model was built up of three-dimensional truss-elements and each truss element represented several parallel twines in the netting. Each global truss element was divided into at least two sub-elements, allowing the twines to buckle when subjected to compression.

Morison's equation and the cross-flow principle (Hoerner 1965) were applied to calculate loads on the deformed net cage. An iteration scheme was performed, calculating loads acting on the deformed model, until the difference in drag and lift was less then 2% between the last iterations.

The net cages were modelled in the FEA (Finite Element Analysis) program ABAQUS/Explicit (Dessault Systèmes, 2007). The loads were static, but a dynamic explicit analysis was applied in order to avoid numerical problems due to slack part of the net cage (a standard FEA solver could have problems inverting the stiffness matrix). ABAQUS/Explicit uses a central difference rule to integrate the equation of motion explicitly through time (Dessault Systèmes, 2007). Strain is calculated by integration of the strain rate, which is found for each element as the relationship between velocity at both nodes and the element length. The method for structural analysis is described in detail in Paper 5 and Paper 6.

Summary of results and conclusions

The results are presented through 6 papers and 3 appendices:

Paper 1: In Moe et al., 2007b, *Tensile properties for netting materials used in aquaculture net cages*, a new method for testing was established in order to determine the tensile properties of knotless netting materials. The method was applied on a variety of netting materials and stress-strain relations were developed.

Paper 2: In Moe et al., 2008a, *Temporary creep and post creep properties of aquaculture netting materials*, data on temporary creep properties, recovery of strain post creep and post creep tensile properties of a selection of wet Raschel knitted netting materials were presented.

Paper 3: In Moe et al., 2007a, *Technological solutions and operational measures to prevent escapes of Atlantic cod (Gadus morhua) from sea cages*, how and why cultured cod escape were investigated and fundamental ways to prevent escape were suggested.

Paper 4: In Moe et al., 2008b, *Resistance of aquaculture net cage materials to biting by Atlantic Cod (Gadus morhua)*, damages found on various netting materials subjected to cod bite through field experiments at commercial cod farms were described. Further, a method to test local cod bite resistance of traditional netting structures was suggested and initial results from a test-jig prototype were given.

Paper 5: In Moe et al., 2008c, *Structural analysis of aquaculture net cages in current*, a method for structural analysis of aquaculture net cages was developed and verified by comparing numerical results to tests in a flume tank.

Paper 6: In Moe et al., 2005, *New net cage designs to prevent tearing during handling*, several new designs were compared to a traditional net cage with regard to stresses in the netting material and deformation of the net cage.

Appendix A compares results from uniaxial tensile tests with mesh strength tests (ISO, 2002). Appendix B discusses nominal dimensions of netting materials. Appendix C presents tensile properties of netting materials with cod bite damage.

A new test method was established to determine the tensile properties of knotless netting materials (Paper 1). It was applied on a variety of netting materials and stress-strain relations were developed. The stiffness was expressed as a constant value for relatively small strains, while for large strains the stress-strain relation was defined by a 3rd degree polynomial. The average value of the constant stiffness for the tested wet netting materials was $81\,\mathrm{Nmm^{-2}}$ with a standard deviation of $9\,\mathrm{Nmm^{-2}}$ for strains less than 10%. For netting materials treated with anti-fouling paint, the average constant stiffness value was $131\,\mathrm{Nmm^{-2}}$ with a standard deviation of $13\,\mathrm{Nmm^{-2}}$ for strains less than 30%. The results are valid for uniaxial static loading of netting.

The uniaxial tensile test gave a force at break corresponding to half the mesh strength, which validates the developed test method (Appendix A). Comparing the stress-strain relations from the uniaxial tensile tests and the mesh strength test revealed significant differences in stiffness properties.

Traditional knotless netting materials for aquaculture (Raschel knitted Polyamide multifilaments) have a very low stiffness for small tensile loads. In fact, they are so flexible it is hard to define a precise initial length. Wetting the netting and applying pretension resulted in an average strain of 15±4 % for the 23 materials, approximately 8 % due to wetting (Paper 1). The mentioned large flexibility for small loads can be challenging to handle in a structural analysis (Appendix B).

Data on temporary creep properties, recovery of strain post creep and post creep tensile properties of a selection of Raschel knitted netting materials was presented (Paper 2). Relative creep strain in wet netting materials subjected to a creep target load of 10 – 90 % of average force at break for 30 minutes varied from 1.6 – 3.5 %. The rate of creep decreased with time and decreased target load. The recovery of strain post creep was relatively fast; approximately half of the creep strain was elastic and after 5 minutes of relaxation another considerable amount of strain was recovered. Post creep tensile testing showed that the length and force at break were not significantly affected by the creep load history. However, due to permanent deformations of the specimens from the creep test, the nominal breaking strain decreased and the stiffness increased with increased creep target load.

It was estimated that 0 – 6 % of cod held in sea-cage farms in Norway were reported to have escaped each year from 2000 to 2005, which is a high

proportion compared to salmon (Paper 3). Five working hypotheses that may explain why a greater proportion of cod than salmon escaped was described: 1) cod are more willing to escape than salmon; 2) cod bite the net cage and create wear and tear; 3) net cages have insufficient technical standards for cod culture; 4) cod are placed in sea-cages at considerably smaller sizes than salmon; and 5) cod are more popular feed for predators. The validity of the 5th hypothesis was questioned in Moe et al. (2006).

The nature of the cod bite attack on traditional, multifilament netting materials was described based on studies of cod interaction with traditional knotless netting and resulting fracture damage on netting fibres (Paper 4). The cod bite attack was described as follows: The cod bit into the netting and filaments were caught behind its teeth. The cod made powerful movements with head and body, and the filaments were subjected to shear and tensile forces. In this process filaments were pulled out of the netting and torn. After several bite attacks in one area, the netting was visibly frayed and in time holes could be created. Studies of fractured filaments due to natural and simulated cod bite, revealed fractures with signs of tension and shear overloading and very little abrasion damage on the fibres. Mesh strength tests of netting with cod bite damage showed that bite damage reduced the nominal mesh opening and mesh opening at break, reduced the tensile stiffness and reduced the mesh strength by 35-47% (Appendix C).

Results from field experiments indicated that cod may have been attracted by types of netting that made it possible to draw filaments out of the twine, while stiff, coated netting structures and thick filaments showed no sign of bite damage during the 3 months test period. It was concluded that netting materials for cod aquaculture must be resistant to cod bite or be repellent or uninteresting for cod. Based on the present findings, the better choice among the traditional netting materials seemed to be hard-laid netting materials, preferably with a primer that glues the filaments together.

A method for structural analysis of aquaculture net cages has been developed and verified for a netting solidity of 0.23, water current velocities from 0.1-0.5 m/s and relatively large deformations (volume reduction up to 70 %) by comparing the numerical results to tests in a flume tank (Paper 5). Resulting drag loads and cage volume were shown to be dependent on the net cage size and weight system. Drag loads increased almost proportional to the current velocity for velocities in the range of 0.2-0.5 m/s, while the cage volume was reduced proportional to the current velocity. The

calculated forces in ropes and netting of full-size net cages were well below the design capacity for current velocities up to 0.5 m/s. However, netting seams in the bottom panel of the net cage were identified as a potential problem area as the forces could reach the design capacity. Finite Element (FE)-plots of tensile stress distribution and net cage deformations are given in Figure 7 and Figure 8.

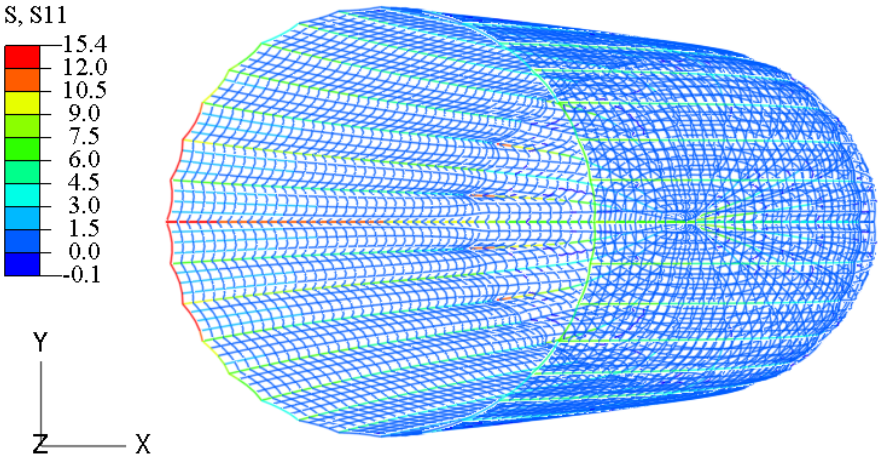

Figure 7: Distribution of tensile stress [MPa] in deformed FE-model of net cage with 160 m circumference, 40 m depth and 32 weights of 1000 N subjected to a current with a velocity of 0.5 m/s in x-direction. Cage is seen from above (the xy-plane is horizontal).

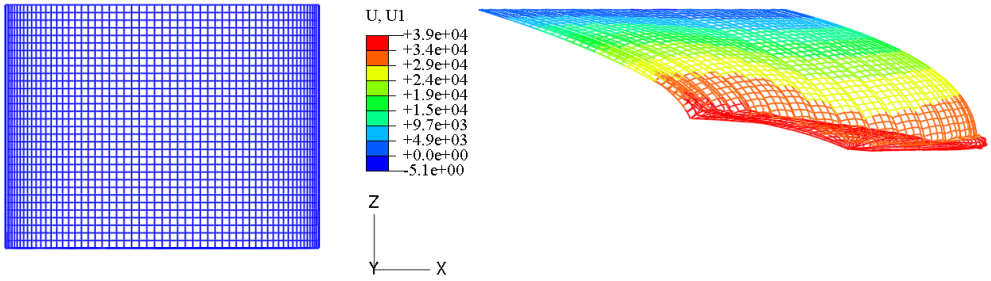

Figure 8: Vertical profile of net cage in the xz-plane (same cage and loads as in Figure 7). Left picture shows the undeformed net cage, while the right picture shows the deformed shape and gives the displacements in x-direction (U1) [m].

Various new designs for aquaculture net cages were presented and compared to a traditional net cage with regard to stresses in the netting material and deformation of the net cage (Figure 9 and Paper 6). The purpose of the new designs was to reduce the probability of escape of fish during lifting of the net cage. Topics of major interest were the risk of tearing of the net cage netting during handling and the shape of the net cage subjected to current loading. The analyses showed that the net cage with twisted bottom was the most promising new design, while the net cage with inclined ropes probably would have a problematic shape with baggy areas.

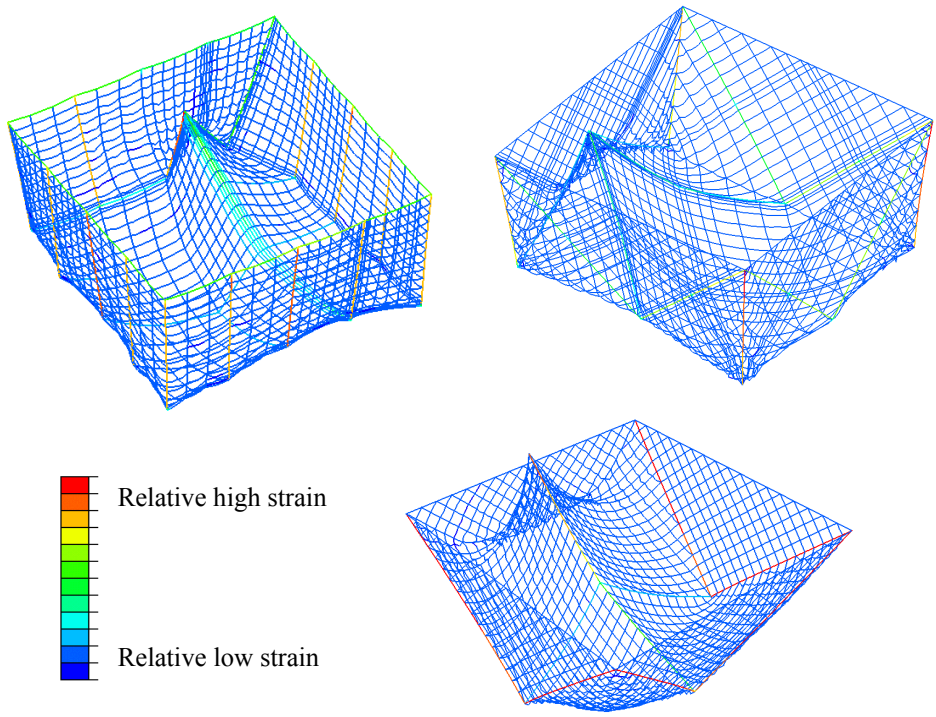

Figure 9: Relative strain plots from analysis of handling of various net cage designs. From upper left: standard net cage, net cage with inclined ropes and net cage with twisted bottom.

Recommendations for further work

Due to the limited knowledge within mechanical properties of netting materials and analysis of net structures, further studies are recommended within all subjects handled in this thesis:

Tensile properties

The mechanical properties of nets and net materials and how they change in time due to damage from wear, UV-radiation, fatigue, abrasion, surface treatments, fish bite etc. are poorly understood. In addition, there exist different types of netting materials of varying raw materials and structure, with unknown tensile properties. Of interest are also the 2D tensile properties of netting materials, i.e. with loading in two directions. Both plasticity and creep are not fully investigated.

Cod bite damage

More knowledge on the interaction between cod and netting is needed to develop net cages for cod culture. Many important and basic questions are still unanswered: What materials do cod prefer to bite at? Do cod attack all materials and what is the nature of the attacks? The behaviour of the cultured cod is far from understood, and future research must include both a technological and biological focus.

Structural analysis

Within structural analysis, the future tasks are many, especially concerning the development and verification of methods and models for various loads and structures. Important keywords are waves, high current velocities and corresponding large deformations, high solidity netting materials and handling situations. To perform a complete strength assessment, extended knowledge on abrasion and fatigue properties is needed.

References

von Brandt, A (1964). Tests on knotless Raschel netting. Modern Fishing Gear of the World 2, p. 88-95. Fishing News Books Ltd., England.

Damiani, M (1964). Knotless Fishing Nets on Raschel Equipment in Italy. Modern Fishing Gear of the World 2, p. 88-95. Fishing News Books Ltd., England.

Dessault Systèmes, 2007. ABAQUS version 6.7 Documentation.

Hoerner, S. F., 1965. Fluid-dynamic drag. Hoerner Fluid Dynamics.

Jensen Ø, 2006. Gjennomgang av tekniske krav til oppdrettsanlegg - basert på rømmingstilfeller i januar. SINTEF Report SFH80 A066056, ISBN 82-14-03953-8.

Klust, Gerhard, 1982. Netting materials for fishing gear. Fishing News Books Ltd., England.

Lader, P., Enerhaug, B., 2005. Experimental Investigation of Forces and Geometry of a Net Cage in Uniform Flow. IEEE Journal of Ocean Engineering, vol. 30, no 1.

Moe H, Pedersen R, Heide M, 2003. Riving og deformasjon av not. Nye rømmingssikre merdkonsept. SINTEF Report STF80 A044019, ISBN 82-14-03310-1(in Norwegian).

Moe H., Gaarder R.H., Sunde L.M., Borthen J. og Olafsen K., 2005. Rømmingssikker not for torsk. SINTEF Report SFH80 A054041, ISBN 82-14-03545-7 (in Norwegian).

Moe H., Olsen A., 2006. Codnet –status report 1. SINTEF Report SFH80 A064067, ISBN 82-14-03960-6 (in Norwegian).

Norwegian Directorate of Fisheries (2008). Rømming. http://www.fiskeridir.no/fiskeridir/kystsone_og_havbruk/r_mming (in Norwegian).

Sala, A., Lucchetti, A., Buglioni, G., 2004. The change in physical properties of some nylon (PA) netting samples before and after use. Fisheries research 69, 181-188.

Standards Norway, 2003. NS 9415 Marine fish farms—Requirements for design dimensioning, production, installation and operation. (In Norwegian).

The International Organization for Standardization, 1976. ISO 3790 Method of test for determination of elongation of netting yarns.

The International Organization for Standardization, 2002. ISO 1806 Fishing nets –Determination of mesh breaking force of netting.

Paper 1

Moe H., Olsen A., Hopperstad O. S., Jensen Ø. and Fredheim A. (2007b). *Tensile properties for netting materials used in aquaculture net cages*. Aquacultural Engineering 37, 252–265.

Available online at www.sciencedirect.com
ScienceDirect
Aquacultural Engineering 37 (2007) 252–265
aquacultural engineering
www.elsevier.com/locate/aqua-online

Tensile properties for netting materials used in aquaculture net cages

Heidi Moe [a,b,*], Anna Olsen [a], Odd Sture Hopperstad [b], Østen Jensen [a], Arne Fredheim [a]

[a] SINTEF Fisheries and Aquaculture, NO-7465 Trondheim, Norway
[b] Norwegian University of Science and Technology (NTNU), Department of Structural Engineering, NO-7491 Trondheim, Norway

Received 3 April 2007; accepted 20 August 2007

Abstract

In order to perform a strength analysis of a net cage, it is crucial to know the tensile stiffness properties of the netting material. A new method for testing was established in order to determine the tensile properties of knotless netting materials. We applied it to a variety of netting materials and developed stress–strain relations. The stiffness was expressed as a constant value for relatively small strains, while for large strains the stress–strain relation was defined by a third degree polynomial. The average value of the constant stiffness for the tested wet netting materials was 81 N mm^{-2} with a standard deviation of 9 N mm^{-2} for strains less than 10%. For netting materials treated with anti-fouling paint, the average constant stiffness value was 131 N mm^{-2} with a standard deviation of 13 N mm^{-2} for strains less than 30%. The results are valid for uniaxial static loading of netting.

Keywords: Aquaculture; Net cages; Nets; Net pens; Netting materials; Material properties; Strength analysis

1. Introduction

Typical fish farms consist of three main components: the net cage, a cage collar and the mooring system (Fig. 1). These different components are equipped with buoyant elements and weights in order to keep the farm floating and to ensure that the net cage maintains its volume.

Net cages are built of a system of ropes and netting (Fig. 1). They are designed to transfer and carry all major forces through the ropes. The netting is attached to the ropes and its intended function is to keep the fish in place. Loads from current, waves and handling induce forces in the netting and it must be dimensioned to withstand this.

The netting used in net cages varies in raw material, size and construction. The netting materials are usually produced of knitted bundles of multifilaments ('knotless' netting) or twines of twisted multifilament bundles that are connected by knots ('knotted' netting). A trade standard exists that defines the number of filaments required to produce netting with a given minimum breaking strength. Most Norwegian net cages are made of square mesh knotless Nylon (Polyamide) netting and Polypropylene/Polyethylene ropes. A variety of other netting materials are available, but knotless Nylon netting is by far the dominating material in aquaculture net cages.

The introduction of the Norwegian standard NS 9415 (Standards Norway, 2003) resulted in legal requirements

* Corresponding author. Tel.: +47 4000 5350; fax: +47 932 70 701.
E-mail address: Heidi.Moe@Sintef.no (H. Moe).

0144-8609/$ – see front matter © 2007 Elsevier B.V. All rights reserved.
doi:10.1016/j.aquaeng.2007.08.001

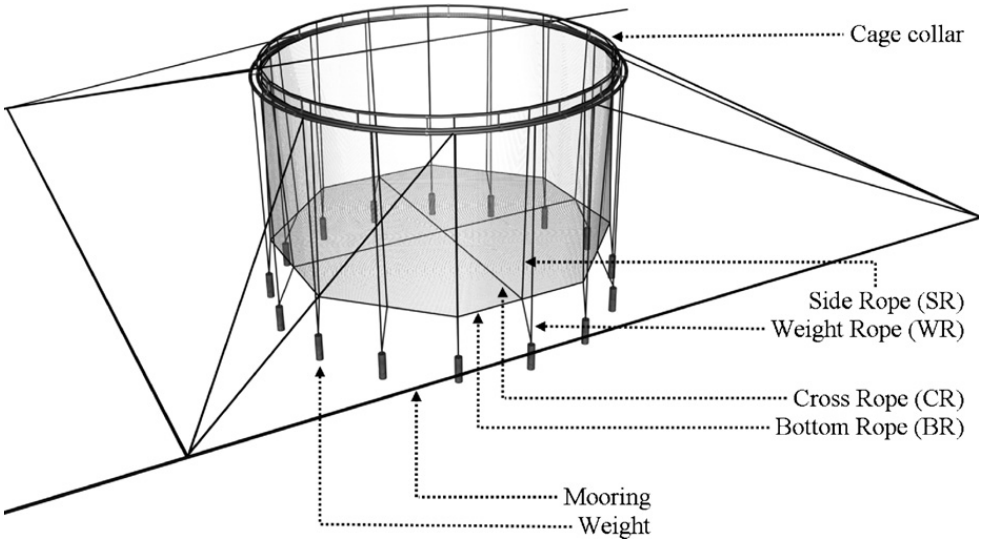

Fig. 1. Illustration of fish farm and net cage components.

for strength analysis of fish farms. Up until then, all net cages had been dimensioned using trade standards based on empirical data. These empirical data were included in NS 9415, but they do not cover all net designs. There is a trend within the Norwegian aquaculture industry that larger net cages and locations with increased exposure to waves and current are used for fish farming (Sunde et al., 2003). The industry has no previous experience with these sizes of nets and environmental conditions, and the new standard requires strength analysis to validate the dimensioning of large net cages and net cages subjected to large environmental loads.

In order to perform a strength analysis of a net cage, it is crucial to know the material properties of the netting material. Traditionally, the material property of major interest for the aquaculture industry has been the tensile breaking strength of netting (mesh) and ropes; comparatively little focus has been on their detailed stiffness properties and general behaviour prior to fracture (Klust, 1982; Sala et al., 2004). There exist established methods for determining the breaking load and elongation of knotted netting materials (knotted twisted yarns), and the netting yarns and knots are tested separately (ISO, 1971; ISO, 2002b; ISO, 1976). Only the mesh breaking force test (ISO, 2002b) is applicable for knotless netting, due to the integrated structure of yarn and knot (Klust, 1982). The resulting stress–strain relation from mesh strength tests does not represent the tensile behaviour of netting materials with loads acting along the twines. Thus, a test new method is needed in order to determine the tensile properties of knotless netting. As a consequence, little information on the stress–strain properties of knotless netting exists. Some information on the mechanical properties for specific dimensions of knotless netting can be found in Slaattelid (1993) and Sala et al. (2004).

Resent research related to aquaculture netting materials focuses mainly on hydrodynamic loading of netting and the resulting response (e.g. Tsukrov et al., 2002; Lader and Fredheim, 2006). Correct material properties will contribute to increasing the accuracy of such analyses.

In this paper, we focus especially on the tensile properties of super-knot Raschel knitted netting. Raschel knitted netting was introduced into the fishing equipment industry in the 1950s. Raschel knitted netting proved to have several qualities superior to the traditionally knotted netting materials, especially due to the lower amount of material in the knot. As a result, Raschel netting is often preferred over knotted netting materials for small mesh widths (Klust, 1982). The mesh widths in netting for traditional Norwegian aquaculture net cages are considered small in this context.

Several different knitting patterns for Raschel netting exist (von Brandt, 1964; Damiani, 1964). The preferred pattern in Norwegian aquaculture netting production is the super-knot pattern, where the knot is strengthened to reduce the risk of laddering of the netting (Fig. 2). Although the netting is called knotless, the connection between twines is still called a knot. The twines are knitted of three strands, each consisting of one to three bundles of very thin filaments (more than 100 filaments in each bundle), as shown in Fig. 2.

The knitted netting has a significant geometric flexibility (Fig. 2); the elongation of the twines and

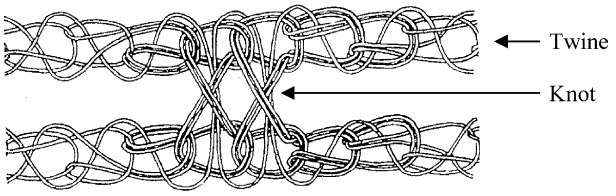

Fig. 2. Illustration of super-knot Raschel knitting pattern (Klust, 1982).

knots will be larger than the elongation of the filaments. This contributes to the fact that netting materials are highly flexible structures with a non-linear stiffness that increases with increased displacement. In addition, the filaments are made of polymers that are known to have large strain at break and non-linear material properties.

Netting materials made of Polyamide 6 multifilaments have a negligible bending stiffness (Klust, 1982; Sala et al., in press) and will in practice take no compression, thus it is the tensile properties of the netting that are needed to be able to perform a strength analysis. In practice this means that we need to know the cross-sectional area of the netting twines and their stiffness properties. The latter can be found from tensile testing, but it is difficult to measure a precise cross-sectional area for knitted netting as it varies along the twines and knots (Fig. 2) and because the netting is very soft (Klust, 1982).

Knowing the tensile properties of the netting material, strength analysis of a net cage structure can be performed using Finite Element Analysis (FEA) software. The netting can be modelled using truss elements that do not take compression. The number of degrees of freedom can be reduced using equivalent truss elements that represent several parallel twines (Moe et al., 2005).

Analysis of net cages can be complex and time consuming due to a high degree of non-linearity in loads, geometry and material properties. Applying a precise material model for netting including non-linear stiffness behaviour will contribute considerably to this complexity. However, it will be beneficial to apply a linear model for small strains when this is feasible, while for large strains and cyclic loading, a more complex material model must be applied.

In this paper we present constant stiffness values for knotless netting materials subjected to small strains, and stress–strain relations expressed as third degree polynomials for large strains. We also give an estimation of the cross-sectional area of the solid material (Nylon-filaments). This is the information needed to model the tensile properties of netting materials in strength analysis.

2. Materials and methods

In order to establish suitable material models for strength analysis involving netting materials, we determined force–displacement curves through uniaxial tensile testing of various Polyamide 6 Raschel knitted netting materials. Presently, no test method exists for determining the tensile properties of knotless netting materials. Therefore, based on existing standards and limitations of the test equipment and laboratory, we established a test method. The BISFA-standard for testing of polyamide filament yarns (BISFA, 2004b) and various ISO-standards were used as a basis (ISO, 2002b; ISO, 1973; ISO, 1976; ISO, 1996; ISO, 1997).

2.1. Tested netting materials

A total of 23 different netting materials from two different producers (P1 and P2) were tested. Test samples were cut from unused netting made of high tenacity Polyamide 6 multifilaments. The various netting materials represent different dimensions given by the producers as half mesh width ($w_{1/2}$, Fig. 3b) and minimum wet

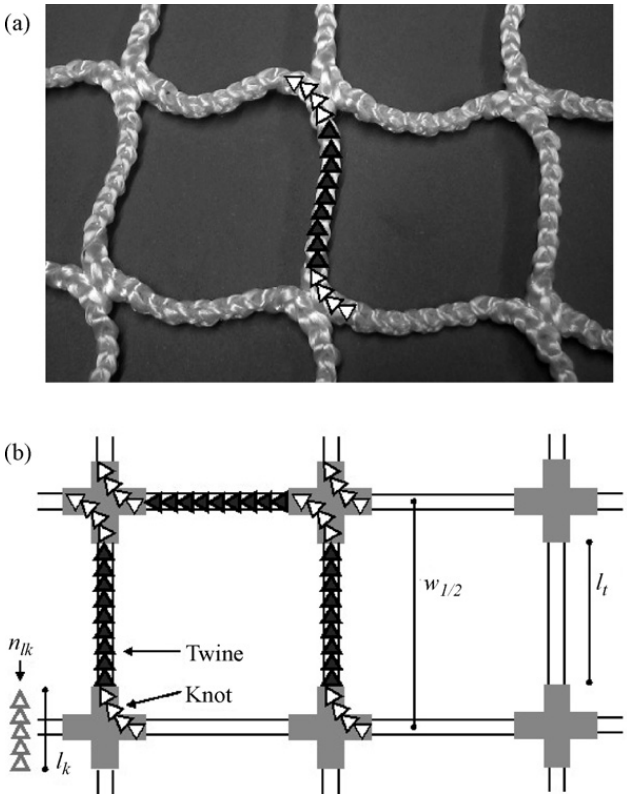

Fig. 3. Two meshes of Raschel knitted netting. (a) Number of loops along the twine (n_l) are indicated with grey triangles and 2 × 4 white triangles represent the knot area. (b) Sketch giving the following measures: length of knot area (l_k), number of loops representing the length of the knot area (n_{lk}), half mesh width ($w_{1/2}$) and length of twine (l_t).

Table 1
Properties of tested netting materials (S_m given by producers)

Netting material number	Prod.	Dry half mesh width $w_{1/2}$ (mm)	Min. wet mesh strength S_m (kg)	Total linear density (dtex)[a]	Loops along the twine, n_l	Hardness, h	Pre-tension P (N)
1	P1	13	55	10320	5	1.12	4.63
2	P1	15.5	63	11280	5	0.98	5.03
3	P1	15.5	79	13920	5	1.07	6.09
4	P1	18	79	13920	5	0.93	6.09
5	P1	18	95	15840	5	0.98	6.78
6	P1	21	95	15840	7	0.99	6.55
7	P1	25.5	95	15840	9	0.92	6.16
8	P1	18	117	18720	5	1.07	8.16
9	P1	22.5	117	18720	7	1.00	7.65
10	P1	25.5	117	18720	9	1.01	7.44
11	P1	25.5	136	21600	7	0.93	8.52
12	P1	20	151	24400	5	1.13	11.12
13	P1	25.5	151	24400	7	0.97	9.42
14	P1	29	151	24400	7	0.87	9.61
15	P1	32	170	27200	9	0.95	10.29
16	P1	29	190	30000	7	0.93	11.06
17	P2	15.3	63	11280	5	1.01	5.27
18	P2	17.5	95	15840	5	0.98	6.45
19	P2	23.7	117	18720	7	0.93	7.49
20	P2	27.5	136	21600	7	0.86	8.49
21	P2	28	151	24400	7	0.91	9.88
22	P2	30.3	151	24400	9	0.96	9.49
23	P2	31	151	24400	9	0.95	9.74

[a] 1 dtex = 10^{-4} g/m.

mesh strength (S_m) (Table 1). The half mesh width (length of mesh side) is defined in ISO 1107 (ISO, 2002a) as 'the distance between two sequential knots or joints, measured from centre to centre when the yarn between those points is fully extended'. The wet mesh strength (S_m) is the traditional measure for the strength of netting materials. The mesh strength test is performed by placing two hooks at the centre of two opposite twines and pulling them apart until the mesh breaks. The test is defined in ISO 1806 (ISO, 2002b): 'A mesh is extended in the dry or wet state until one of the knots or joints reaches the force at rupture'. For the super-knot quality netting used in these tests, the rupture occurs in the twine close to the knot area.

The netting materials were chosen to cover the practical extremities and variety in mesh width and mesh strength (Table 1). Table 1 also gives the number of loops along the twine (n_l) for the materials. This structural property proved to be important during the evaluation of the test results. The number of loops along the twine was found by counting the loops along the twine indicated with grey triangles in Fig. 3. The white triangles represent the knot area, which we defined to include two times four loops for all materials.

Table 2 describes the four different series of tests that were performed. In Series 1, all 23 materials were tested for wet tensile properties. Series 2 included 5 dry materials from producer P1 with wax based anti-fouling treatment. The wax impregnates the material and the properties in dry and wet conditions should be similar. Series 3 and 4 included 2 materials, one from each producer. Series 3 included wet netting and a reduced test velocity of 50 mm/min, while Series 4 included dry netting and the default test velocity (500 mm/min). In all these tests the force and displacement were monitored. Only on-loading of the netting material was tested.

For all materials, at least 10 specimens were tested (ISO, 2002b). Some of the presented tests results represent only 9 test repetitions (Series 1: Material 9 and 17, and Series 2: Material 19). This is due to the removal of single repetitions with obvious errors in the

Table 2
Series of performed tests

	Tested netting materials	Test velocity (mm/min)	Condition of netting material
Series 1	All	500	Wet
Series 2	3, 11, 13, 15, 16	500	Anti-fouling, dry
Series 3	10, 19	50	Wet
Series 4	10, 19	500	Dry

results (for instance from slipping of the extensometer or rupture in the grip area).

2.2. Test set-up

Tests were performed using a single column testing machine with a capacity of 5 kN and a load cell accuracy of ±0.5% of the applied load value from 2 to 100% of the load cell capacity. For loads less than 1% of cell capacity, an accuracy of at least 1% was expected. A travel extensometer was used to measure the elongation of the test specimen. The position accuracy was ±0.01% or 0.001 mm, whichever was greatest, and the speed accuracy was ±0.0005% of set speed.

Single bollard grips were applied to reduce the build up of stress at the clamp point (Fig. 4b). The free ends of the specimen were retained in a screw clamp and the sample was wrapped around the friction bollard at each end.

The test laboratory did not allow for control of temperature and humidity. Temperature during the tests was fairly constant, varying between 20 and 23 °C. The relative humidity varied between 50 and 70%. BISFA (2004b), ISO 1805 (ISO, 1973) and ISO 1806 (ISO, 2002b) have specified an atmosphere for testing of 20 ± 2 °C and a relative humidity of 65 ± 2%. However, ISO 291 (ISO, 1997) states that 'if neither temperature nor humidity has any noticeable influence on the properties being examined, neither the temperature nor the relative humidity has to be controlled'. Testing of wet netting was not significantly influenced by air humidity as the tests were carried out immediately after removal from the water. Moreover, the ISO standards do not give air humidity requirements for testing wet specimens. The results from testing of dry netting may have been influenced by the variation in air humidity. The air temperature was so close to the

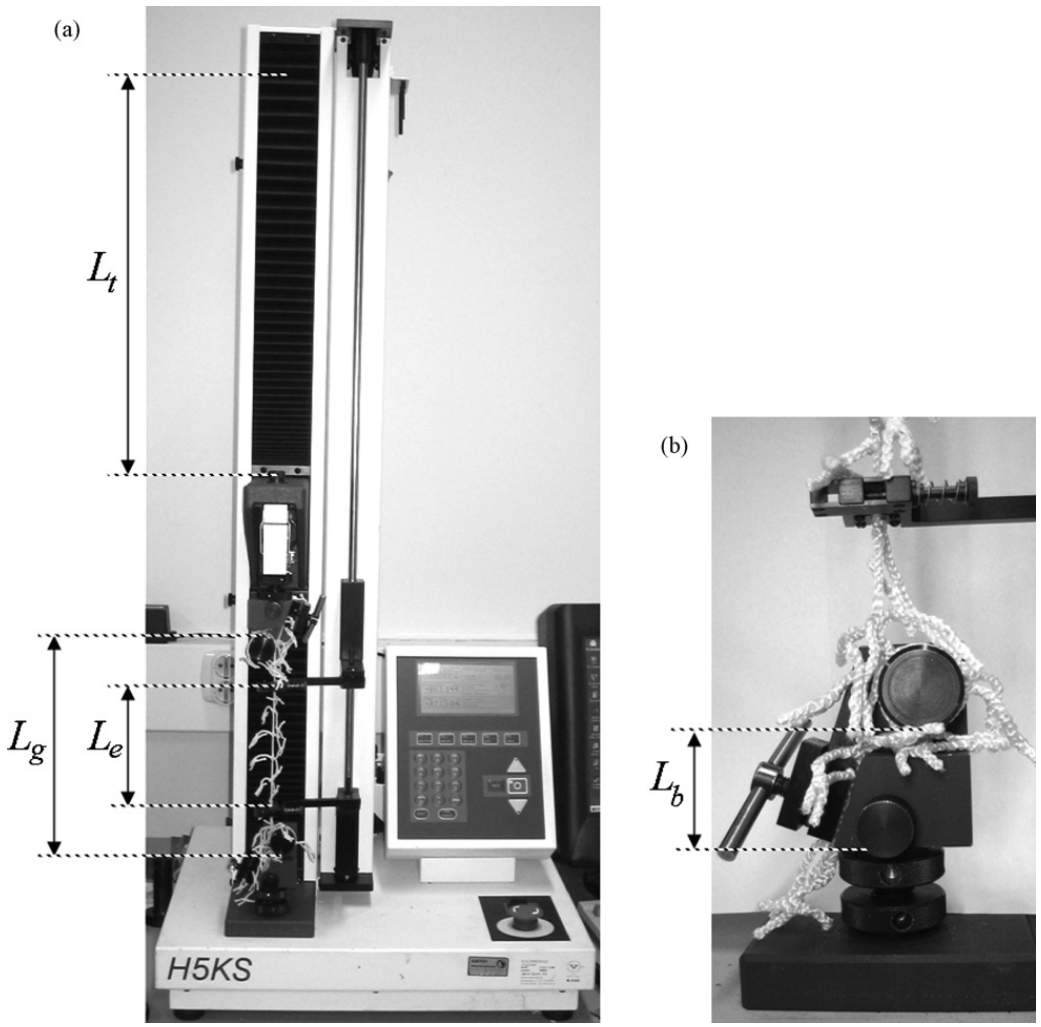

Fig. 4. Test set-up. The following measures are illustrated in picture a: Maximum travel length (L_t), length between grips (L_g), length between extensometer arms (L_e). Picture b shows the lower bollard grip and extensometer and indicates the distance between the bottom of the grip and the bollard (L_b).

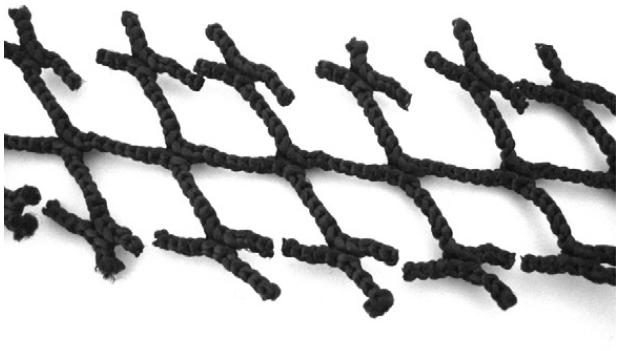

Fig. 5. A section of the test specimen.

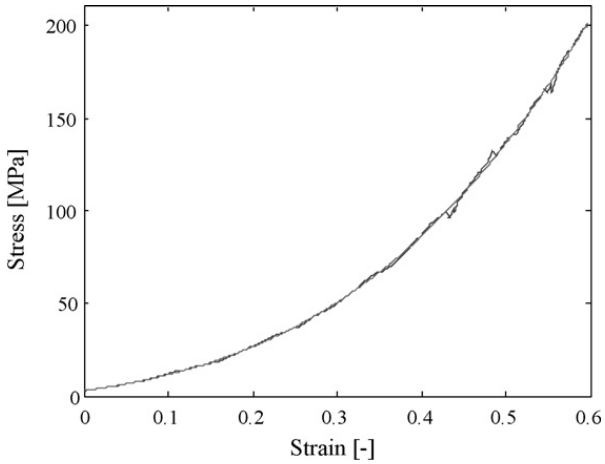

Fig. 6. Example of resulting stress–strain curve from tensile testing of a single wet test specimen (Series 1) and fitted third degree polynomial.

temperature range defined in the standards that it most likely had no significant effect on the test results. In compliance with all previously referred ISO and BISFA standards, specimens were exposed to the previously described atmosphere at least 24 h before testing and the wet specimens were immersed in tap water at least 24 h prior to testing.

The test specimen was a thread consisting of several twines and knots cut out of the netting material (Fig. 5). The symmetry axis along the length of the specimen represents the major load direction in a net cage. The reason for keeping a knot in all cut twines was to prevent slippage of filaments and resulting errors in measured force and displacement.

The maximum travel length for the test (L_t, Fig. 4) was calculated based on the given maximum travel length for test machine excluding grips ($L_{t,max}$ = 750 mm), the nominal length between grips (L_g = 250 mm) and the distance between the bottom of the lower grip and the bollard (L_b = 40 mm): $L_t = L_{t,max} - L_g - 2L_b$ = 420 mm. The length of the applied test specimen (L_s) was 500 mm (except for in total five test specimens of material 15 and 16 with anti-fouling paint, see next paragraph). This allowed for a maximum strain at break of approximately $\varepsilon_{max} = L_t/L_s$ = 84%.

The extensometer arms were attached to the specimen at two separate knots (Fig. 4b). The test specimen was expected to break in the twine close to the knot area, so attaching the extensometer in the strengthened knot area (Fig. 2) should minimize the influence of the minor gripping force caused by the extensometer. The initial distance between the two arms of the extensometer (L_e in Fig. 4a) varied depending on the mesh width of the material, but in general it was not less than 100 mm (4 twines) with two exceptions. Due to the limited size of the received samples of material 15 and 16 with anti-fouling paint, the initial distance between the extensometer for in total five of the test repetitions was smaller (down to 84 mm for 3 twines).

ISO 3790 (1976) requires a pre-tension corresponding to the mass of 250 ± 25 m of the netting yarn to be tested. Based on the mass and dimensions of the netting materials, a complete list of the pretension for the various netting materials is given in Table 1. The actual tests were performed without a specific pretension, starting at a force close to zero. In the post processing of the results, the resulting force–strain curves were adjusted so that the initial force was equal to the calculated pretension (Fig. 6). The required pretension was relatively low and some of the test results showed a minimum load greater than the specified pretension. In these cases, 3 new specimens were stretched and the original 10 test repetitions were adjusted to comply with the three new ones. This was done for Material 9 and Material 10 in Series 1 and Material 10 in Series 3 and Series 4.

The default test velocity was chosen as 500 mm/min, which was the maximum velocity of the test machine. The performed tests were displacement controlled and the test velocity was constant throughout the test. The BISFA-standard suggests a testing speed of 1000 mm/min, while the ISO standards give other recommendations. However, all standards are open for the use of other test velocities. In addition, two materials were tested using a test velocity of 50 mm/min in order to get an indication of the sensitivity of the netting material to test velocity.

3. Results

3.1. Cross-sectional area and hardness

In order to express the tensile stiffness properties of the netting materials, it was necessary to establish the

cross-sectional area for the loaded part of the test specimen. The cross-section varies along the twine and knot area (Figs. 2 and 5); there is no obvious way to directly measure the cross-sectional area.

In a global strength analysis it is not possible to model the local geometry of the netting with twines and knots. A constant average cross-sectional area with the additional mass in the knot smeared along the netting twines is suitable for such analysis, and it is the total area of the solid material (filaments) that is of interest. The average cross-sectional area of the solid material was estimated by weighing samples of the various netting materials and dividing the resulting mass (m) by the number of twines in the sample (n_t), the half mesh width ($w_{1/2}$) and the specific weight of the Polyamide 6 filaments (ρ_{PA6}):

$$A = \frac{m}{n_t w_{1/2} \rho_{PA6}} \tag{1}$$

ρ_{PA6} is equal to 1140 kg/m^3 (Rhodia, 2005). The results (Fig. 8) show that for equal mesh strength, the average cross-sectional area increases for decreased mesh width. This is due to the fact that the size of the knot is approximately constant for a given mesh strength and will thus have a greater influence on the average cross-sectional area for smaller mesh widths.

An expression for the hardness of the knitting was developed during this work to give the relative difference between the width and length of one loop in a twine (for the solid material). As an approximation, the twine cross-sectional area is assumed to be circular with an average diameter (d_{av}). The hardness can be calculated assuming that the length of one loop is equal to the half mesh width ($w_{1/2}$) divided by the number of loops along the half mesh width (n_{lw}):

$$h = \frac{d_{av}}{w_{1/2}/n_{lw}} = \frac{d_{av}(n_l + n_{lk})}{w_{1/2}} = \frac{d_{av}(n_l + 5)}{w_{1/2}} \tag{2}$$

n_{lw} is expressed as the sum of number of loops along the twine (n_l) and number of loops representing the length of the knot area (n_{lk}). n_{lk} was found to be approximately equal to 5 for all materials by measuring the length of the knot area (l_k) and twines (l_t) for the various netting materials (Fig. 3b):

$$n_{lk} = \frac{l_k}{l_t} n_l \simeq 5 \tag{3}$$

When $h > 1$ or $h < 1$, the length of the loop is smaller or larger than the estimated twine diameter (solid material), respectively. A large h-value indicates a 'hard' netting material, while a small h-value indicates a 'soft' material. The hardness of the tested materials is given in Table 1.

3.2. Force and strain at break

The force at break is defined as 'the maximum force applied to a test specimen carried to rupture during a tensile test' (BISFA, 2004a). The force at break was calculated for the different tests and materials as the mean value of the force at break for all valid specimens (ISO, 1980). The resulting force at break for the materials in Series 1 was compared with the given mesh strength for each netting material. The force at break of the tested specimens should be at least 50% of the given mesh strength, since two parallel twines are stretched in the mesh strength test. However, since several meshes were tested implicitly in each specimen (Fig. 5), the resulting breaking strength from these tests was the strength of the weakest of several twines. It was required that the mean force at break of the tested netting materials should not be less than 45% of the given mesh strength. If the breaking strength proved to be smaller, the material was considered to be of inferior quality and the test results were discarded.

Table 3 gives mean values of force at break and nominal strain at break from Series 1 for the various netting materials. The strain was calculated based on the nominal length between the extensometer arms (measured prior to stretching and adjusted to represent length at pretension). The nominal strain at break was on average 62% for wet netting materials. The table also compares the breaking strength to the given mesh strength.

Table 4 gives mean values of force and strain at break from Series 2, Series 3 and Series 4 for the various materials and the relative deviation to force and strain at break from Series 1. The results show that the anti-fouling treatment reduces the breaking strength of a netting material by 13% on average compared to the wet netting. The average strain at break was 74%, which was 17% larger than the average strain at break for wet netting materials. The reduced test velocity in Series 3 does not seem to have a significant effect on the results. The dry netting materials seemed to have a small increase in strain at break compared to wet netting. However, due to the limited number of materials tested and the possible influence of air humidity, it was not possible to make firm conclusions based on the results from Series 4.

The coefficient of variation (CV) was applied to evaluate the variation in the test results. CV equals the

Table 3
Force and strain at break for wet netting materials (Series 1)

Netting material number	Force at break (N)	Nominal strain at break (%)	Force at break/mesh strength (%)
1	288	68	53
2	361	62	58
3	443	70	57
4	448	61	58
5	472	62	51
6	497	63	53
7	497	59	53
8	555	64	48
9	570	64	50
10	570	62	50
11	655	61	49
12	714	71	48
13	698	63	47
14	713	57	48
15	759	61	46
16	881	61	47
17	358	65	58
18	420	61	45
19	532	59	46
20	629	55	47
21	672	58	45
22	709	63	48
23	722	63	49

standard deviation (SD) divided by the mean value (μ) and is given per cent (Walpole et al., 2007):

$$\mathrm{CV} = \frac{100\,\mathrm{SD}}{\mu}(\%) \tag{4}$$

For the results given in Tables 3 and 4, the coefficient of variation between specimens in one test is in average 5% for the force at break and 3% for the strain at break (for all series of tests).

Table 4
Force and strain at break for netting materials with anti-fouling treatment (Series 2), low test velocity (Series 3) and dry netting materials (Series 4)

Series/ material number	Force at break (N)	Nominal strain at break (%)	Force/strain relative to Series 1 (%)
2/3	379	82	−14/+16
2/11	569	74	−13/+20
2/13	620	71	−11/+13
2/15	658	70	−13/+16
2/16	750	72	−15/+18
3/10	552	62	−3/+1
3/19	535	59	+1/+1
4/10	545	66	−4/+6
4/19	523	62	−2/+5

The initial half mesh width for the test specimens varied between Series 1, Series 2 and Series 3. A comparison of the results from Series 1 and Series 2 indicated that the half mesh width for the pre-loaded netting treated with anti-fouling paint was on average 89% of the half mesh width for a pre-loaded wet test specimen. Thus, applying anti-fouling paint reduced the half mesh width, which partly explains the large increase in strain at break. Comparison of Series 1 and Series 4 showed that the half mesh width for the preloaded wet netting was on average 108% of the half mesh width for a pre-loaded dry test specimen. This means that wetting dry netting materials increased the half mesh width with approximately 8%, while the half mesh width of netting materials with anti-fouling paint was on average 4% smaller than for dry netting materials.

3.3. Constant stiffness for relatively small strains

The direct results from the tensile tests were force–displacement curves for all test specimens. However, as an input for strength analysis, for instance using ABAQUS (ABAQUS, 2006), a stress–strain curve for the material is required. Given the tensile test results (Fig. 6), the average cross-sectional area (Fig. 8) and the nominal length between the extensometer arms, the nominal stress versus nominal strain curves were calculated for the various series of tests and netting materials.

The material properties for on-loading of netting materials (given as stress–strain data) can be modelled as linear for relatively small strains. For wet netting materials (Series 1) the stress–strain curve is close to linear up to 10% strain. For netting materials with anti-fouling treatment (Series 3) the curve can be assumed linear up to 30% strain and for dry netting (Series 4) the curve can be assumed to be linear up to 20% strain (Fig. 13). For a linear elastic material model, the constant stiffness value can be directly applied in combination with the average cross-sectional area of the solid material (A). The constant stiffness was calculated using the least squares method and is given in Fig. 7 for the different series of tests and materials. A is found for the 23 different materials in Fig. 8 or can be estimated using Eq. (9).

The coefficient of variation in constant stiffness for the various netting materials tested in Series 1 varied from 2.4 to 17.8% with an average of 6.4% (Eq. (4)). Only material 11 had a CV greater than 7.8% (i.e. 17.8%). CV in constant stiffness for the various netting materials tested in Series 2 varied from 3.0 to 6.9% with

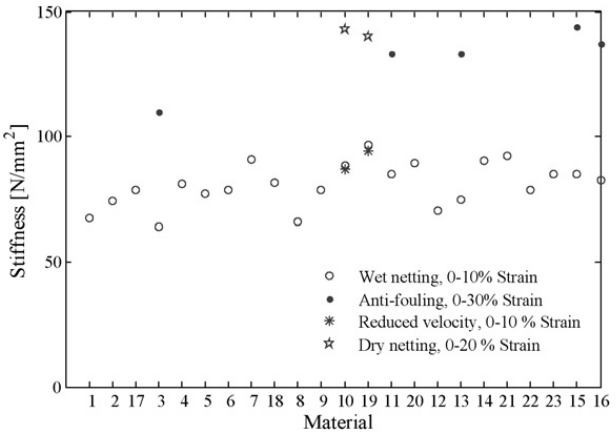

Fig. 7. Constant stiffness for wet netting materials (Series 1), materials with anti-fouling treatment (Series 2), low test velocity (Series 3) and dry netting materials (Series 4) experiencing small strains (materials are sorted with respect to increasing mesh strength and half mesh width).

an average of 4.7%. CV in constant stiffness in Series 3 was 6.8 and 5.9% for material 10 and 19, respectively, for 0–10% strain, while the CV in Series 4 was 3.5% for both materials.

Average values of the constant stiffness for all wet netting materials, netting materials with 5, 7 or 9 loops along the twine and netting materials treated with anti-fouling paint are given in Table 5 for small strains. The constant stiffness of netting with anti-fouling treatment (Series 2) was larger than the stiffness of wet materials (Series 1). This is probably partly due to the dry condition of the impregnated filaments (Fig. 13). In addition, the wax may reduce the geometric flexibility for small strains and affect the internal friction between the filaments.

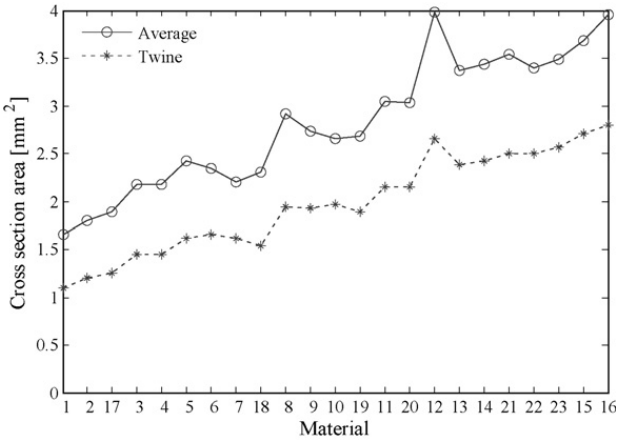

Fig. 8. Estimated average and twine cross-sectional area of solid material for the netting materials (materials are sorted with respect to increasing mesh strength and half mesh width).

Table 5
Average constant stiffness for wet netting materials and netting with anti-fouling paint

Netting materials	Average constant stiffness (N/mm^2)	Valid strain interval	Standard deviation (N/mm^2)/CV (%)
Wet (all)	81	0–0.1	9/11
Wet, $n_l = 5$	73	0–0.1	7/9
Wet, $n_l = 7$	85	0–0.1	7/9
Wet, $n_l = 9$	85	0–0.1	5/5
Anti-fouling paint	131	0–0.3	13/10

Table 6
Stress-strain polynomial constants for wet netting materials (Series 1), materials with anti-fouling treatment (Series 2), low test velocity (Series 3) and dry netting materials (Series 4)

Series/material number	Polynomial constants (MPa)			
	a	*b*	*c*	*d*
1/1	271	118	49	2.8
1/2	673	−2	71	2.8
1/3	219	192	39	2.8
1/4	596	99	62	2.8
1/5	519	102	60	2.8
1/6	695	−5	73	2.8
1/7	809	58	76	2.8
1/8	453	95	48	2.8
1/9	335	250	34	2.8
1/10	343	289	40	2.8
1/11	499	166	62	2.8
1/12	213	133	51	2.8
1/13	504	137	49	2.8
1/14	649	163	67	2.8
1/15	453	191	59	2.8
1/16	606	144	60	2.8
1/17	381	111	64	2.8
1/18	305	184	61	2.8
1/19	473	151	78	2.8
1/20	536	163	68	2.8
1/21	366	271	56	2.8
1/22	160	343	33	2.8
1/23	344	164	73	2.8
1/Av[a]	452	153	58	2.8
2/3	115	58	89	2.8
2/11	195	61	102	2.8
2/13	356	−71	130	2.8
2/15	177	81	112	2.8
2/16	342	−51	127	2.8
2/Av[a]	237	16	112	2.8
3/10	366	260	40	2.8
3/19	464	158	72	2.8
4/10	535	−90	145	2.8
4/19	515	−8	125	2.8

[a] Average polynomial for series of tests.

3.4. Stress–strain polynomial

For relatively large strains, a hyperelastic material model can be applied for on-loading of the tested netting materials. Applying the average cross-sectional area of the solid material (A), the nominal stress as a function of the nominal strain can be expressed as a third degree $\sigma(\varepsilon)$ polynomial for the various tests: $\sigma(\varepsilon) = a\varepsilon^3 + b\varepsilon^2 + c\varepsilon + d$. The polynomial constants a, b, c and d are given in Table 6. The tangent stiffness is obtained by derivation of the stress–strain relation: $K_t = d\sigma/d\varepsilon = 3a\varepsilon^2 + 2b\varepsilon + c$. The polynomial constant d of 2.8 MPa represents the stress due to the pretension in the test specimen.

The polynomials were found using the least squares method and they provide a good fit for all curves (Fig. 6). The validity of each polynomial was evaluated by first assessing the variation in test results (CV between the test repetitions) and then the difference between mean test results and fitted polynomial. The coefficient of variation in stress was calculated for discrete strain values (ε_i) varying from 0 to strain at break (ε_b) with a strain increment of 0.01. CV(ε_i) did not vary significantly with strain. The average value, $\overline{CV}$, was calculated for each test and the total average ($\overline{CV}_{tot}$) was calculated as the sum of $\overline{CV}$ for all tests divided by the total number of tests (equals 32, reference Table 1). $\overline{CV}_{tot}$ was equal to 5% and maximum $\overline{CV}$ was 9% for material 11 in Series 1.

The error in the estimated $\sigma(\varepsilon)$ polynomial for discrete strain values (ε_i) was expressed as the absolute difference between the mean stress-value from the test (μ_i) and the stress-value from the polynomial (f_i):

$$E_i = \left| \frac{f_i - \mu_i}{\mu_i} \right| \tag{5}$$

The average error for a specific strain interval from ε_A to ε_B (ε_A:ε_B) of a test was calculated as:

$$\overline{E}(\varepsilon_A : \varepsilon_B) = \frac{1}{n} \sum_{i=A}^{B} E_i \tag{6}$$

where n is number of strain increments in the interval. The total average error, $\overline{E}_{tot}(\varepsilon_A : \varepsilon_B)$, was calculated as the sum of $\overline{E}(\varepsilon_A : \varepsilon_B)$ for all tests divided by the total number of tests. The total average error for all strains, $\overline{E}_{tot}(0 : \varepsilon_b)$, was equal to 2%. However, the polynomial often had an inferior fit for small strains with $\overline{E}_{tot}(0 : 0.1) = 5\%$ and a maximum average error $\overline{E}(0 : 0.1) = 12\%$ for material 22 in Series 1. Thus, for small strains the constant stiffness is the preferred material model.

4. Discussion

4.1. Average cross-sectional area for a general netting material

The average total cross-sectional area of the solid material for the 23 netting materials was calculated (Fig. 8). Based on these discrete values, a method for calculation of the average cross-sectional area of the solid material for a general netting material was developed. It is assumed that the cross-sectional area of the solid material in the knot area (A_k) is two times the size of the cross-sectional area of the solid material in the twines (A_t) (Figs. 2 and 3):

$$A_k = 2A_t \tag{7}$$

The ratio between the length of the twine (l_t) and the half mesh width ($w_{1/2}$), x, is given as the number of loops along the twine (n_l) divided by the number of loops along the half mesh width (n_{lw}) (Fig. 3, Eqs. (2) and (3)):

$$x = \frac{l_t}{w_{1/2}} = \frac{n_l}{n_{lw}} = \frac{n_l}{5 + n_l} \tag{8}$$

The average cross-sectional area of the solid material can be expressed as follows:

$$A = A_k(1 - x) + A_t x \tag{9}$$

Combining Eqs. (7) and (9) gives the following expression of the average cross-sectional area of solid material in the twines:

$$A_t = \frac{A}{2 - x} \tag{10}$$

The average cross-sectional area of solid material in the twines is given in Fig. 8 for the various netting materials. The results show that A_t is similar for netting materials with similar mesh strength. This is correct considering the trade standard for the production of these netting materials, which requires a specific linear density of filaments (mass per unit length, BISFA, 2004a; Rhodia, 2005) for the production of specific mesh strength (Table 1). Based on the results, average values for A_t for various mesh strengths were calculated (Table 7).

From the estimated cross-sectional area of the twines (Table 7) and knowledge of the local geometry of the netting, the total average cross-sectional area of the solid material was estimated for a general netting material using the following formula:

$$A = A_t(2 - x) = A_t\left(2 - \frac{n_l}{5 + n_l}\right) \tag{11}$$

Table 7
Estimated cross-sectional area of solid material in twine

Minimum mesh strength (kg) S_m	Cross-sectional area of solid material in twine (mm^2) A_t
55	1.10
63	1.23
79	1.45
95	1.61
117	1.93
136	2.15
151	2.50
170	2.71
190	2.79

Eq. (11) is valid in the following range of half mesh width and mesh strength: $13\,\text{mm} \leq w_{1/2} \leq 32\,\text{mm}$, $55\,\text{kg} \leq S_m \leq 190\,\text{kg}$, and the corresponding total linear density of filaments given in Table 1.

4.2. Strain at break for a general netting material

The strain at break for the 23 wet netting materials is given in Table 3. Based on these discrete values, we developed a method to calculate the strain at break for a general netting material. The strain at break depended on both the hardness (h) and the number of meshes per meter of netting material ($N_m = 1000\,\text{mm}/w_{1/2}$). The expected strain at break for a general netting material was calculated as follows:

$$\varepsilon_b(N_m, h) = \frac{h}{N_m}\varepsilon_b^* \tag{12}$$

ε_b^* is the normalized strain at break, and was calculated for the 23 different materials using the discrete values of the strain at break (ε_b), the number of meshes per meter and the hardness:

$$\varepsilon_b^* = \frac{\varepsilon_b N_m}{h} \tag{13}$$

Based on the discrete values of the normalized strain at break, ε_b^*, a continuous expression of ε_b^* as a linear function of N_m was estimated using the least squares method:

$$\varepsilon_b^*(N_m) \approx 0.60 N_m + 1.55 \tag{14}$$

Discrete values of the normalized strain at break, ε_b^*, is plotted for the 23 different materials in Series 1 (Fig. 9). In addition the continuous expression of ε_b^* (Eq. (14)) is plotted. The CV between the discrete values and continuous expression for ε_b^* is 2%. Eq. (12) is valid in the following range of half mesh width and mesh strength: $13\,\text{mm} \leq w_{1/2} \leq 32\,\text{mm}$, $55\,\text{kg} \leq S_m \leq 190\,\text{kg}$ and the corresponding total linear density of filaments given in Table 1.

The strain at break for netting materials treated with anti-fouling paint was on average 17% larger than for wet netting (Table 4). The results from Series 2 indicate that the strain at break for netting materials treated with anti-fouling paint can be estimated using Eq. (12) and multiplying the result by 1.17.

4.3. Stress–strain polynomial for a general netting material

Based on the given nominal stress versus nominal strain polynomials (Table 6), we developed a method to estimate the polynomial of a general netting material. The $\sigma(\varepsilon)$ relationship depends on the following three structural properties: number of loops along the twine, half mesh width and the average diameter of solid material in the netting. The tensile stress in a general netting material can be estimated as follows:

$$\sigma(\varepsilon) \simeq \frac{k_1(n_l)}{h}\bar{\sigma}^*(\varepsilon) = \frac{k_1(n_l)}{n_l + 5}\frac{w_{1/2}}{d_{av}}\bar{\sigma}^*(\varepsilon) = k_2(n_l)\frac{w_{1/2}}{d_{av}}\bar{\sigma}^*(\varepsilon) \tag{15}$$

where $\bar{\sigma}^*$ is the average normalized stress and $k_1(n_l)$ and $k_2(n_l)$ are constants dependent on n_l (given in Table 8). The normalized stress versus strain polynomial was determined for the various materials using the polynomials given in Table 6 and the following expression:

$$\sigma^*(\varepsilon) = \sigma(\varepsilon)\frac{d_{av}}{k_2 w_{1/2}} \tag{16}$$

The average normalized stress versus strain polynomial constants $\bar{a}^*$, $\bar{b}^*$, $\bar{c}^*$ and $\bar{d}^*$ were estimated for

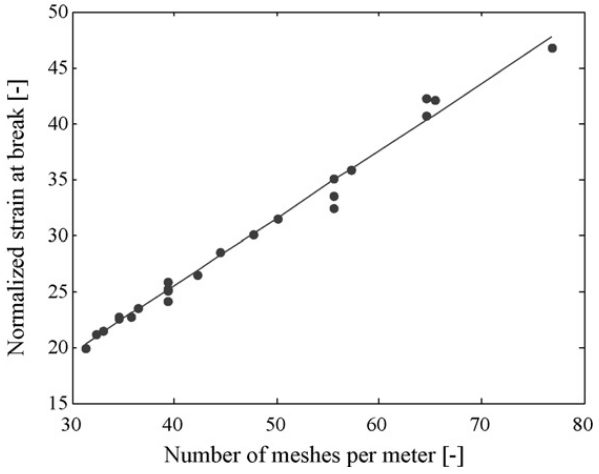

Fig. 9. Normalized strain at break with respect to number of meshes per meter.

Table 8
Normalization constants dependent on number of loops along the twine

n_1	k_1	k_2
5	10.6	1.06
7	12	1
9	12.3	0.88

Table 9
Normalized average stress-strain polynomial constants for wet netting materials (Series 1) and materials with anti-fouling treatment (Series 2)

Condition of netting material	Polynomial constants (MPa)			
	$\bar{a}^*$	$\bar{b}^*$	$\bar{c}^*$	$\bar{d}^*$
Wet	37.0	13.3	4.82	0.23
Anti-fouling	19.1	1.42	9.18	0.23

wet netting materials and materials treated with anti-fouling paint and are given in Table 9.

$$\bar{\sigma}^*(\varepsilon) = \bar{a}^*\varepsilon^3 + \bar{b}^*\varepsilon^2 + \bar{c}^*\varepsilon + \bar{d}^*$$

The constants $k_1(n_1)$ and $k_2(n_1)$ were determined by calculating the average normalized polynomials for n_1 equals 5, 7 and 9 ($\bar{\sigma}^*_{n_1}(\varepsilon)$) with $k_2(n_1)$ set to 1. Then $k_2(n_1)$ were adjusted to make $\bar{\sigma}^*_5(\varepsilon)$ and $\bar{\sigma}^*_9(\varepsilon)$ coincide with $\bar{\sigma}^*_7(\varepsilon)$ using the least squares method, minimizing the total error in the strain interval 0.1–0.5. The CV between the three average polynomials was less than 1% for all strains (dotted line in Fig. 12).

Eq. (15) is valid in the following range of half mesh width and mesh strength: $13\,\text{mm} \leq w_{1/2} \leq 32\,\text{mm}$, $55\,\text{kg} \leq S_m \leq 190\,\text{kg}$, and the corresponding total linear density of filaments given in Table 1.

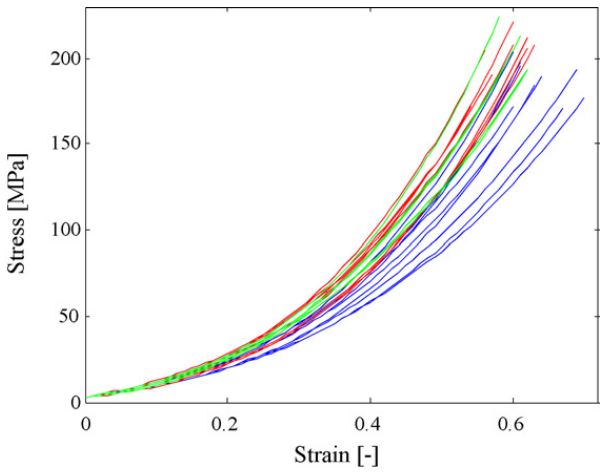

Fig. 10. Stress–strain curves for all wet netting materials (Series 1).

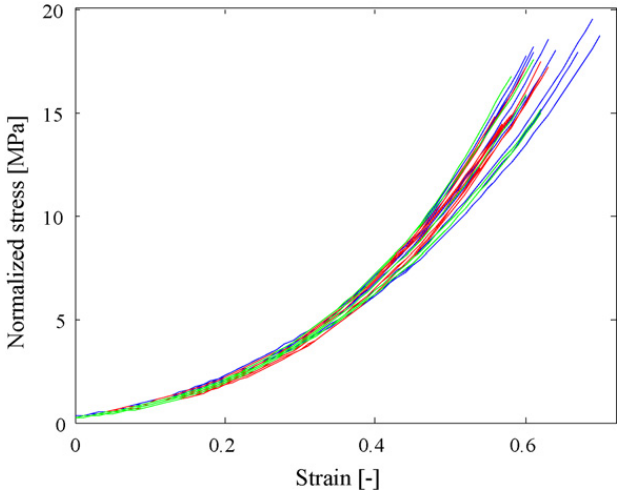

Fig. 11. Normalized stress-strain curves for all wet netting materials (Series 1).

The stress–strain polynomials from Series 1 are plotted in Fig. 10, while Fig. 11 shows the normalized polynomials. The blue curves represent netting materials with 5 loops along the twine, red represent 7 loops and green represent 9 loops along the twine. The total coefficient of variation in stress, $CV_{tot}(\varepsilon_i)$, was calculated as the standard deviation between the fitted $\sigma(\varepsilon)$ polynomials in a series of tests divided by the average polynomial (Table 6) for discrete strain values (ε_i). $CV_{tot}(\varepsilon_i)$ in stress (σ) and normalized stress (σ^*) is plotted for wet netting materials in Fig. 12. The average value, $\overline{CV}_{tot}$, is 12% and 7% for σ and σ^*, respectively. $CV_{tot}(\varepsilon_i)$ for netting materials with anti-fouling paint is similar to $CV_{tot}(\varepsilon_i)$ for wet materials (Fig. 12); stress normalization (Eq. (16)) lead to a reduction in $\overline{CV}_{tot}$ from 12 to 5%. Fig. 13 compares the average normalized stress–strain polynomials from Series 1, Series 2 and Series 4.

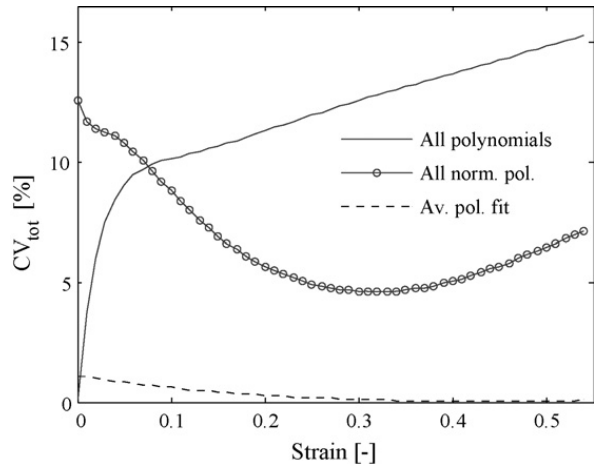

Fig. 12. Total coefficient of variation in stress between all polynomials, all normalized polynomials and average normalized polynomials for n_1 equals 5, 7 and 9 (dotted line).

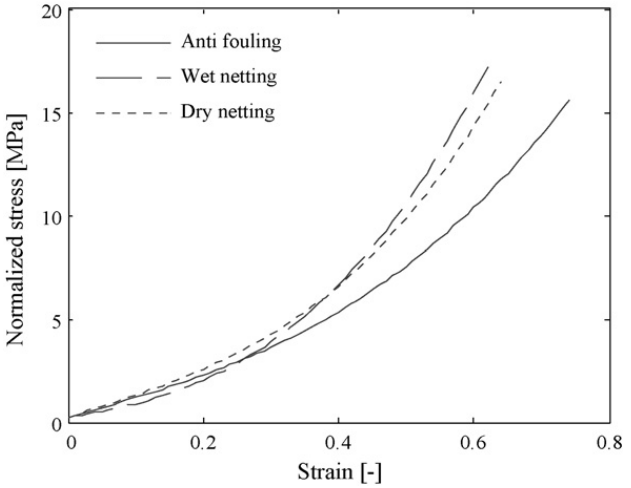

Fig. 13. Comparison of average normalized stress-strain curves from Series 1 (wet netting), Series 2 (anti-fouling) and Series 4 (dry netting).

4.4. Validation and limitations of results

Some of the breaking strength results from Series 1 were confirmed by mesh strength tests. These mesh strength tests were performed at the production site using the same test samples as the test specimens were cut from. The resulting mesh strength was approximately two times the resulting force at break from the tensile tests. This means that the deviation in breaking strength compared to the given mesh strength is not significantly affected by the test set-up. On occasion, slight changes in the properties of the netting material were experienced for unknown causes during the test period.

The difference in number of meshes in the test specimens of the netting materials could be a source of error. Depending on the half mesh width, the number of meshes in the test samples varied from 16 to 38. We expected that the weakest of the meshes in the area between the grips would break during the tests. This could result in a comparatively lower breaking strength for the samples with small mesh width (i.e. high number of meshes). However, a comparison between force at break and the given mesh strength for various half mesh widths (Table 3) indicated that this is not an important source of error for the testing of netting materials.

The results are valid for uniaxial loads in the netting. This is often a good assumption for netting in net cages, as one load direction often dominates over the other for significant stress levels. For biaxial loads it is probable that the tensile behaviour of the knot area will be different from the uniaxial load case.

We developed a method for calculating the cross-sectional area of solid material in the netting twines. In practice the cross-section will be somewhat larger and the average cross-sectional area of the solid filaments is not directly applicable for calculation of loads acting on the netting.

5. Conclusion

Force–displacement curves were found through uniaxial tensile testing of various netting materials. No established test method exists for this kind of test, so we developed a test method. Netting materials from two different producers were tested, and they showed similar properties. Based on the experimental data, relations for the tensile stiffness and stress–strain behaviour of super-knot Raschel knitted Polyamide 6 netting were established. The stiffness was expressed as a constant value for relatively small strains, while for large strains the stress–strain relation was defined by a third degree polynomial. As the behaviour during unloading and cyclic loading has not been investigated, the proposed models are only valid for static analysis.

Netting materials with a specific type of wax based anti-fouling treatment had significantly different tensile properties to wet netting. The tensile strength decreased by 13% on average after application of anti-fouling paint. The strain at break increased by on average 17% and the initial half mesh width was reduced to on average 89% of the half mesh width for wet netting.

Reducing the test velocity by a factor of 10 did not have any noticeable effect on the tensile properties. Thus, the properties of netting materials do not seem to be sensitive to changes in loading velocity when the velocity is in the range of 50–500 mm/min (0.83–8.3 mm/s). Dry netting materials may have somewhat larger strain at break than wet materials. Despite the uncertainties in air humidity, we conclude that dry netting has greater stiffness than wet netting for small strains.

Acknowledgements

The work is sponsored by the Norwegian Research Council through the IntelliSTRUCT programme (Intelligent Structures in Fisheries and Aquaculture) at SINTEF Fisheries and Aquaculture.

References

ABAQUS, 2006. Analysis User's Manual. Hibbitt, Karlsson Sorensen, Inc., USA.

BISFA (The International Bureau for the Standardisation of Man-Made Fibres), 2004a. Terminology of man-made fibres

BISFA (The International Bureau for the Standardisation of Man-Made Fibres), 2004b. Testing methods for polyamide filament yarns.

Damiani, M., 1964. Knotless Fishing Nets on Raschel Equipment in Italy. Modern Fishing Gear of the World 2. Fishing News Books Ltd., England, pp. 88–95.

Klust, G., 1982. Netting Materials for Fishing Gear. Fishing News Books Ltd., England.

Lader, P.F., Fredheim, A., 2006. Dynamic properties of a flexible net sheet in waves and current—A numerical approach. Aquacult. Eng. 35, 228–238.

Moe, H., Fredheim, A., Heide, M., 2005. New Net Cage Designs to Prevent Tearing during Handling, 2005. IMAM, Lisbon, Portugal.

Rhodia P., 2005. Multifilament product information. (http://www.rhodia-iy.com/RIY/download/ebusiness/Multifil_2005.pdf).

Sala, A., Lucchetti, A., Buglioni, G., 2004. The change in physical properties of some nylon (PA) netting samples before and after use. Fish. Res. 69, 181–188.

Sala, A., O'Neill, F.G., Buglioni, G., Lucchetti, A., Palumbo, V., Fryer, R.J. Experimental method for quantifying the resistance to opening of netting panels. ICES J. Marine Sci., in press.

Slaattelid, O.H., 1993. Strekk/forlengelse av notpanel, forsøk (in Norwegian). SINTEF-report MT40 F93-0021.

Standards Norway, 2003. NS 9415 Marine fish farms—Requirements for design dimensioning, production, installation and operation (in Norwegian).

Sunde, L.M., Heide, M.A., Hagen, N., Fredheim, A., Forås, E., Prestvik, Ø., 2003. Review on technology in the Norwegian aquaculture industry. SINTEF Fisheries and Aquaculture Report STF 80 A034002, 32 p.

The International Organization for Standardization, 1973. ISO 1805 Fishing nets—Determination of breaking load and knot breaking load of netting yarns.

The International Organization for Standardization, 1976. ISO 3790 Method of test for determination of elongation of netting yarns.

The International Organization for Standardization, 1980. ISO 2602 Statistical interpretation of test results – Estimation of the mean – Confidence interval.

The International Organization for Standardization, 1996. ISO 527-1 Plastics—Determination of tensile properties.

The International Organization for Standardization, 1997. ISO 291 Plastics—Standard atmospheres for conditioning and testing.

The International Organization for Standardization, 2002a. ISO 1107 Fishing nets—Netting – Basic terms and definitions.

The International Organization for Standardization, 2002b. ISO 1806 Fishing nets—Determination of mesh breaking force of netting.

Tsukrov, I., Eroshkin, O., Fredriksson, D., Robinson Swift, M., Celikkol, B., 2002. Finite element modelling of net panels using a consistent net element. Ocean Eng. 30, 251–270.

von Brandt, A., 1964. Tests on Knotless Raschel Netting. Modern Fishing Gear of the World 2. Fishing News Books Ltd., England, pp. 88–95.

Walpole, R.E., Myers, R.H., Myers, S.L., Ye, K., 2007. Probability and Statistics for Engineers and Scientists, eighth ed. Pearson Education, Inc..

Paper 2

Moe H., Hopperstad O. S., Olsen A., Jensen Ø. and Fredheim A., (2008a). *Temporary creep and post creep properties of aquaculture netting materials.* Submitted for possible journal publication.

Temporary creep and post creep properties of aquaculture netting materials

Authors: Heidi Moe[a,b*], Odd Sture Hopperstad[b], Anna Olsen[a], Østen Jensen[a] and Arne Fredheim[a]

[a] SINTEF Fisheries and Aquaculture, NO-7465 Trondheim
[b] Norwegian University of Science and Technology (NTNU), Department of Structural Engineering, NO-7491 Trondheim
* Corresponding author. Telephone: +47 4000 5350, Fax: + 47 932 70 701, E-mail: Heidi.Moe@Sintef.no

Abstract

Creep in materials and structures may lead to increasing strains, permanent deformations, change in mechanical properties and rupture at loads significantly smaller than the breaking strength. In this paper, we present data on temporary creep properties, recovery of strain post creep and post creep tensile properties of a selection of Raschel knitted netting materials. Relative creep strain in wet netting materials subjected to a creep target load of 10 – 90 % of average force at break for 30 minutes varied from 1.6 – 3.5 %. The rate of creep decreased with time and decreased target load. The recovery of strain post creep was relatively fast and approximately half of the creep strain was elastic. Post creep tensile testing showed that the length and force at break were not significantly affected by the creep load history. However, due to permanent deformations of the specimens from the creep test, the nominal breaking strain decreased and the stiffness increased with increased creep target load.

Keywords: Aquaculture; net cages; nets; net pens; netting materials; creep; material properties; strength analysis; tensile testing

1 Introduction

Creep is the time dependent strain resulting from stress; it occurs gradually with time, as opposed to the strain that occurs instantly upon the application of stress (Ashby & Jones, 1980). Net cages for aquaculture are built of a system of ropes and netting. In Norway, the netting materials are usually produced of Raschel knitted bundles of Nylon 6 (Polyamide 6) multifilaments (Moe et al. 2007). When a net cage is loaded over a period of time, creep may lead to increasing strains, permanent deformations, change in mechanical properties and rupture at loads significantly smaller than the breaking strength. Loads from weights, currents, waves and handling of a net cage will act over periods of time lasting from seconds to several months.

The creep behaviour of aquaculture netting materials has not previously been documented. In general, mechanical properties of netting materials are only known to a limited extent (Moe et al. 2007; Klust, 1982 and Sala et al., 2004). Moe et al. (2007) provided information on the tensile stiffness and stress-strain relations for netting materials, but no information was given on the time dependent properties, the recovery of the netting material after loading and the properties of previously loaded netting materials. Some information on the latter can be found in Sala et. al. (2004). They found that no significant change in breaking strength could be detected for pre-loaded knotless netting materials, while the strain at break was reduced.

Polymers can experience large creep, and creep should be considered in the design of structures made of polymer materials. Large creep strain can occur above the polymers' glass transition temperature, which for Polyamide 6 can be significantly less than $20^{\circ}C$ in air and below $-20^{\circ}C$ in water (Kohan, 1995; Dowling, 2007; Ashby & Jones, 1980; Buchanan & Walters, 1977; Murthy & Bray, 2003). Therefore both dry and wet netting will be expected to creep in a standard atmosphere of 65 % relative humidity and a temperature of $20^{\circ}C$ (ISO 291, 1997). This is confirmed by creep data for Nylon 6 filaments given in Murthy & Bray (2003), which showed that the creep elongation was significant already within seconds of loading. Creep behaviour of polymers is very sensitive to temperature (Ashby & Jones, 1980). In practice, the temperature of the netting will vary with the seawater temperature, i.e. from 0 °C and higher. A reduction in temperature will probably reduce the creep strain of the netting material, and creep tests should be performed at different temperatures.

The creep behaviour of netting materials will probably be the combined effect of friction between filaments and material creep in fibres. Knitted netting has a significant geometric flexibility; the elongation of the twines and knots will be larger than the elongation of the filaments (Moe et al., 2007), and the deformations will be dependent on friction between filaments. In addition, due to the knitting pattern of the netting (Moe et al., 2007), bundles of fibres in one twine will be of varying length and experience different levels of loading and creep reactions. Materials often experience three stages of creep: The primary or transient stage with a relatively high (decreasing) strain rate, followed by a secondary or steady-state phase where the strain rate is approximately constant. In the tertiary stage, the strain rate increases in an unstable manner approaching rupture failure (Ashby & Jones, 1980). For these reasons, it is not trivial to establish the creep properties of netting materials and creep tests are necessary in order to investigate the creep properties. This paper presents the results from creep tests of a selection of Raschel knitted netting materials, and will give insight into the response of a netting material subjected to loads acting over a period of time. We present data on temporary creep properties, recovery of strain post creep and post creep tensile properties.

2 Materials and methods

Three different unused netting materials were subjected to creep testing and the following recovery and post creep properties were investigated. Beforehand, breaking strength tests were performed for all materials in order to establish stress-strain relations and find the average breaking strength for unused netting materials. The netting materials represent common dimensions given as dry half mesh width in ISO 1107 (ISO, 2002a) and wet mesh strength in ISO 1806 (ISO, 2002b) in Table 1. Table 1 also gives cross-sectional area of solid material in a twine, total linear density of the fibres in a twine, number of loops along the twine (n_l), hardness (h) and pretension for the netting materials. n_l and h describe the local netting structure, and the pretension is calculated in accordance with ISO 3790 (ISO, 1976). Thorough explanation of the material properties is given in Moe et al. (2007).

Tests were performed using a single column testing machine. A travel extensometer was used to measure the elongation of the test specimen. Single bollard grips were applied to reduce the build up of stress at the clamp point. The test set-up is the same as described in detail in Moe et al. (2007).

Test specimens were cut from unused wet netting made of high tenacity Polyamide 6 multifilaments (Figure 1). Room temperature was fairly constant during the tests period, varying between 20 and 23 °C. All specimens were immersed in tap water at least 24 hours prior to testing, except for four specimens of netting material 1 which were tested in dry condition (at a relative humidity, RH, of 33%).

Table 1: Properties of tested netting materials (S_m given by producers).

Netting material number	Dry half mesh width $w_{1/2}$ [mm]	Min. wet mesh strength S_m [kg]	Cross sectional area [a] A [mm^2]	Total linear density [dtex] [b]	Loops along the twine n_l	Hard-ness h [-]	Pre-tension P [N]
1	15.0	95	2.60	15840	5	1.21	7.3
2	27.0	95	2.21	15840	9	0.87	6.2
3	26.5	136	3.30	21600	7	0.93	9.2

[a] of solid material
[b] 1 dtex = 10^{-4} g/m.

Figure 1: Section of a test specimen.

Specimens were tested using the following procedure:

Creep test

1. The test specimen was mounted in the testing machine and the initial gauge length (length between the extensometer arms, L_e) was measured manually with a slide calliper.
2. The specimen was stretched with a constant velocity of 50 mm/min (between grips) until the creep target load was reached. The low rate of loading eliminated effects of kinetic energy as the creep target load was reached.
3. The target load was kept for a time period of 30 minutes, during which the length was recorded as a function of time, $L_e(t)$. Data was logged at 200 time steps with a logarithmic distribution.

Recovery

4. Immediately after the creep test, the specimen was unloaded with a velocity of 500 mm/min until a load level of approximately 7.3 N was reached (pretension for netting material 1). At this point, the length between the extensometer arms was measured manually.
5. The specimen was unloaded and left to relax for 5 minutes, then the specimen was reloaded to a level of approximately 7.3 N and the length between the extensometer arms was measured manually.
6. The specimen was removed from the testing machine and was put in water where it was left to relax for 24 +/- 2 hours or 144 +/- 4 hours (6 days). At this point the specimen was mounted in the testing machine and the gauge length was measured.

Post creep properties (tensile breaking strength test)

7. The specimen was stretched to rupture with a velocity of 500 mm/min.

All three netting materials were tested using four different creep target loads, represented as four series of tests (C10, C30, C60 and C90) as described in Table 2. Target loads were chosen in order to represent the different areas in the stress-strain curve of the netting materials as shown in Figure 2. F_b is force at break, which was found in the initial breaking strength tests of Series B0 (Table 2). Series B0 (break of unused netting) and Series BP (break post creep) were performed in accordance with stage 7 in the procedure description above. Initially four specimens of each netting material were tested in each creep series. Due to a relatively high variability in the results of series C60 and C90, additional four to seven specimens of each netting material were tested in these series.

Table 2: Series of performed tests.

Series	Type of test	Load level	Number of specimens [a]
B0	Break (unused)	F_b	5 / 10 / 10
C10	Creep	$0.1F_b$	4 / 4 / 4
C30	Creep	$0.3F_b$	4 / 4 / 4
C60	Creep	$0.6F_b$	8 (4 [b]) / 8 / 8
C90	Creep	$0.9F_b$	10 / 8 / 11
BP	Break (post creep)	F_b	26 / 24 / 27

[a] Material 1 / 2 / 3
[b] 4 specimens of netting material 1 were tested in dry condition.

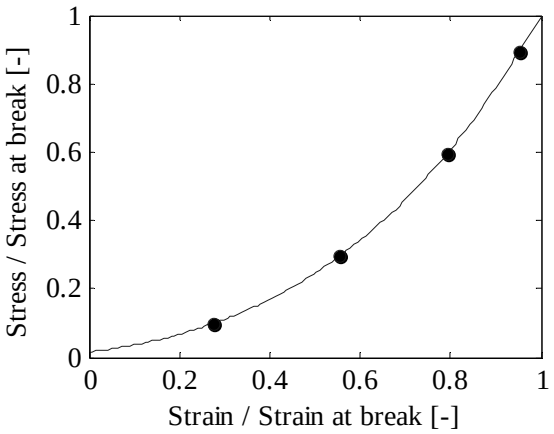

Figure 2: Load levels chosen for creep tests.

The tests were performed in air due to limitations of the test equipment. The duration of the creep test was limited to 30 minutes to avoid a significant reduction in water content in the specimens during the test period. This is considered a short term creep test, yielding the temporary creep properties. We believe that drying of the netting was not significant during this period of time, as the specimens were dripping wet when mounted and still felt wet after the creep test. To further investigate this, tests of dry specimens of netting material 1 (at 33% RH) were also included in Series C60. The

results indicate that the wet netting did not experience a significant reduction in water content during the test period (as discussed in results and discussion chapter).

3 Results and discussion

3.1 Stress-strain relations for unused netting

Prior to creep testing a series of breaking strength tests were performed in order to establish the tensile stress-strain relations of the unused netting materials (Series B0, Table 2). The mean and standard deviation in nominal strain and force at break was calculated for the unused netting materials (ISO 2602, 1980) and is given in Table 3. The nominal strain at break was calculated as the length between the extensometer arms at break (L_{eb}) divided by the length at pretension (L_{e0}): $\varepsilon_b = L_{eb}/L_{e0}$. The resulting stress-strain relations for Series B0 are given in Figure 9 (unused netting materials). Normalized elongation is equal to the engineering (nominal) strain for all unused netting materials.

Table 3: Percentage increase in half mesh width ($w_{1/2}$) for wet netting at pretension compared with dry, unloaded netting. Nominal strain and force at break; mean values with standard deviation.

Netting material number	Increase in $w_{1/2}$ at pretension [%]	Nominal strain at break [%]	Force at break [N]
1	15	68.3 ± 1.3	448 ± 11
2	12	55.3 ± 1.3	438 ± 15
3	13	60.6 ± 1.0	605 ± 18

The half mesh width for wet netting at pretension is given in Table 3 as percentage increase in half mesh width compared with dry, unloaded netting. 5-7 % of the increase in half mesh width was directly caused by

wetting of the netting; the additional 7-8 % was due to application of pretension.

3.2 Temporary creep strain

Creep strains are presented as the sum of initial creep strain, ε_{c_i}, and relative creep strain, $\varepsilon_{c\_rel}(t)$:

$$\varepsilon_c(t) = \varepsilon_{c\_i} + \varepsilon_{c\_rel}(t) = \frac{L_{e\_i} - L_{e0}}{L_{e0}} + \frac{L_e(t) - L_{e\_i}}{L_{e0}} = \frac{L_e(t) - L_{e0}}{L_{e0}} \quad (1)$$

$L_e(t)$ is the measured length between the extensometer arms at time t, while $L_{e\_i} = L_e(t=0)$ is the length at the beginning of the creep test. L_{e0} is the length between extensometer arms at pretension (from series B0). The relative creep strain is strictly speaking not a nominal strain, but a normalized elongation (with respect to L_{e0}).

The relative creep strain was calculated for 20 discrete values of $L_e(t)$ for each test repetition (equally distributed on a logarithmic time scale). Mean values of the relative creep strain are given for Series C10, C30, C60 and C90 in Figure 3. The average standard deviation ($\overline{SD}$) and standard deviation at end of creep tests ($SD(t=1800s)$) are given in Table 4. Table 4 also gives the initial creep strain with standard deviation and relative creep strain at end of creep tests for the different series and netting materials.

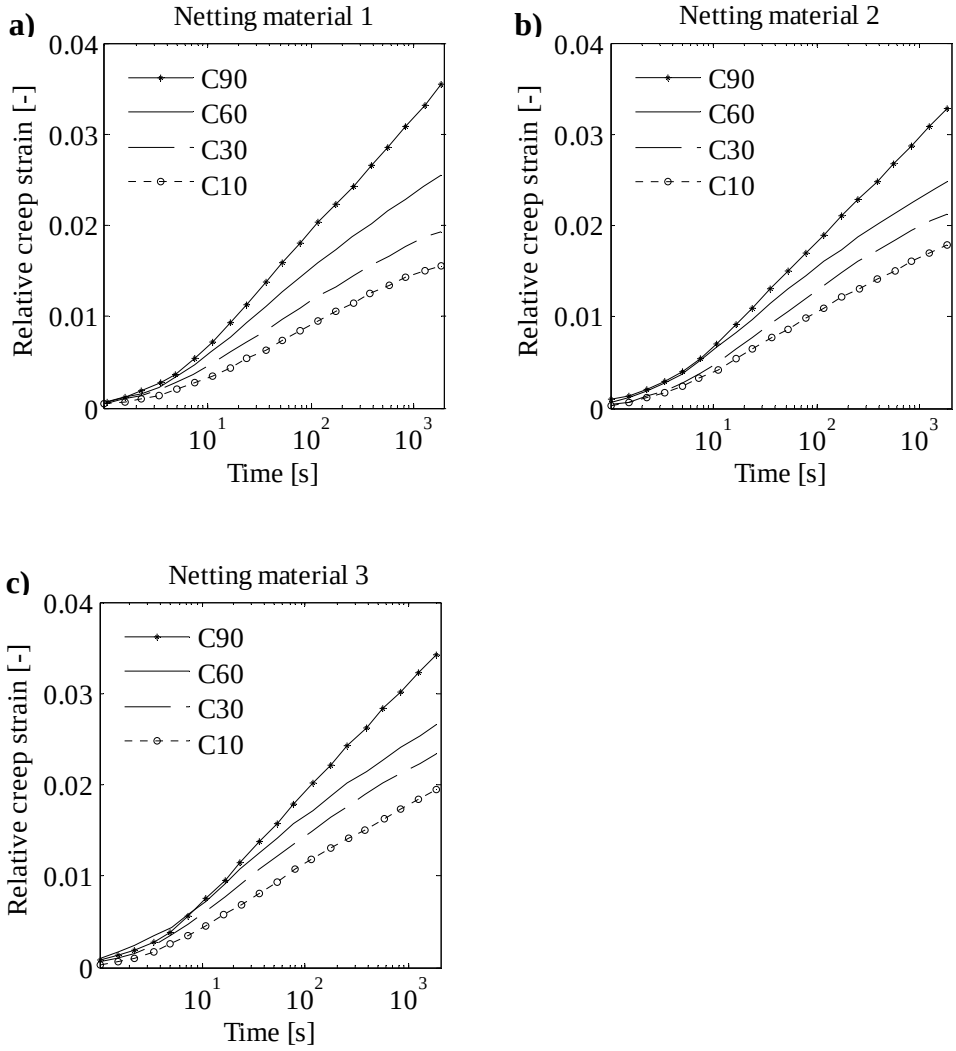

Figure 3: Relative creep strain versus time, $\varepsilon_{c\_rel}(t)$, for series of creep tests. a) Netting material 1. b) Netting material 2. c) Netting material 3.

Table 4: Initial creep strain (ε_{c_i}), relative creep strain at end of creep test (mean value and standard deviation) and average standard deviation of $\varepsilon_{c\_rel}(t)$. All values are given in [%].

Series / Netting material	Initial creep strain ε_{c_i}	Relative creep strain at end $\varepsilon_{c\_rel}(1800s)$	$\overline{SD}$ of $\varepsilon_{c\_rel}(t)$
C10 / 1	16.7 ± 0.7	1.6 ± 0.0	0.0
C10 / 2	13.2 ± 0.8	1.8 ± 0.0	0.0
C10 / 3	16.2 ± 1.0	1.9 ± 0.0	0.0
C30 / 1	37.0 ± 0.3	1.9 ± 0.1	0.1
C30 / 2	29.0 ± 0.3	2.1 ± 0.1	0.0
C30 / 3	33.7 ± 0.6	2.3 ± 0.1	0.1
C60 / 1	48.7 ± 1.1	2.6 ± 0.3	0.2
C60 / 2	41.5 ± 1.3	2.5 ± 0.3	0.2
C60 / 3	46.9 ± 1.0	2.7 ± 0.3	0.2
C90 / 1	59.8 ± 1.2	3.5 ± 0.4	0.3
C90 / 2	49.6 ± 1.0	3.3 ± 0.2	0.2
C90 / 3	54.6 ± 3.2	3.4 ± 0.4	0.3

The variation in relative creep strain within the tested specimens of a netting material was relatively high for series C60 and C90 with a coefficient of variation up to 11 % at the end of the creep test (Table 4). The coefficient of variation (CV) equals the standard deviation (SD) divided by the mean value (μ) and is given per cent (Walpole et. al 2007). This variation within a test was probably due to a variation in properties between the specimens, depending on the location of the specimens on the piece of netting material (especially noticed for netting material 3) and release of geometric flexibility. When subjected to a tensile force of $0.6F_b$, it seems like the netting material reacts in an unstable manner. It has reached an area of the stress-strain curve involving relatively high loads and significant geometric flexibility (Figure 2). During the testing it was observed distinct tightening of the knots at this level of loading. SD was fairly constant during time, indicating that the major differences in creep behaviour occurred shortly after the target load was reached at the beginning of the creep test.

Two of the tested specimens of series C90 (netting material 1 and 3) broke within the 30 minutes creep test period. These results are excluded from the calculation of the creep strain (Figure 3 and Table 4). Comparison of the creep strain of specimens that broke during the creep test period with the creep strain of specimens that did not break, does not indicate that these results stand out. Their influence if included in the results would not be significant. The creep lifetime will not be assessed in this work, but it is obvious that twines in the netting materials subjected to a constant load of 90 % of the average breaking force can rupture within minutes.

For most of the test repetitions the target load was reached at a strain level lower than the expected value, which is the strain value corresponding to the target load in the stress-strain polynomial from Series B0 (Table 4 and Figure 9). The major cause is probably the smoothing of the results through the polynomial estimation. The original force-displacement curves were often uneven, especially for high loads due to uneven release of geometric flexibility (Figure 9d). The difference in stretching velocity between the creep test and breaking test (50 and 500 mm/min respectively) should not affect the stress-strain relation significantly, as shown in Moe et al. (2007).

The total relative creep during the 30 minutes of testing did not vary much between the different netting materials (Figure 3 and Table 4). Significant creep was experienced already at low loads (10% of F_b), and increased load led to increased creep. The creep strain was not proportional to the creep load: Increasing the target load with a factor of 9 (from 10% to 90% of F_b), increased the relative creep with a factor of approximately 2 from a nominal strain of in average 1.8% to 3.4%.

In series C60 a test of netting material 1 was also performed for dry specimens. Resulting relative creep strains and half mesh width are given in Figure 4 as a function of time for wet and dry specimens of netting material 1. L_{e0} for dry specimens was assumed to be 8 % less than for wet specimens (Moe et. al. 2007), meaning that the half mesh width at pretension was on average 16.3 mm for dry and 17.5 for wet specimens. The initial creep strain of the dry specimens was on average 51.6 % (relative to length of dry specimens at pretension), while for wet specimens it was 48.7 % (Table 4). This means that the half mesh width increased by 8.4 mm and 8.5 mm for dry and wet materials respectively during on-loading from pretension to creep target load. Comparing the creep test results for wet and dry netting shows that the creep rates were different and that the difference in rate was

fairly constant throughout the test period. The increase in length with time, i.e. the rate of elongation; $\dot{L}_e(t) = \Delta L_e(t)/\Delta t$ was on average 1.8 times larger for dry netting specimens than wet, and the difference in wet and dry half mesh width was reduced by 20 % during the creep test.

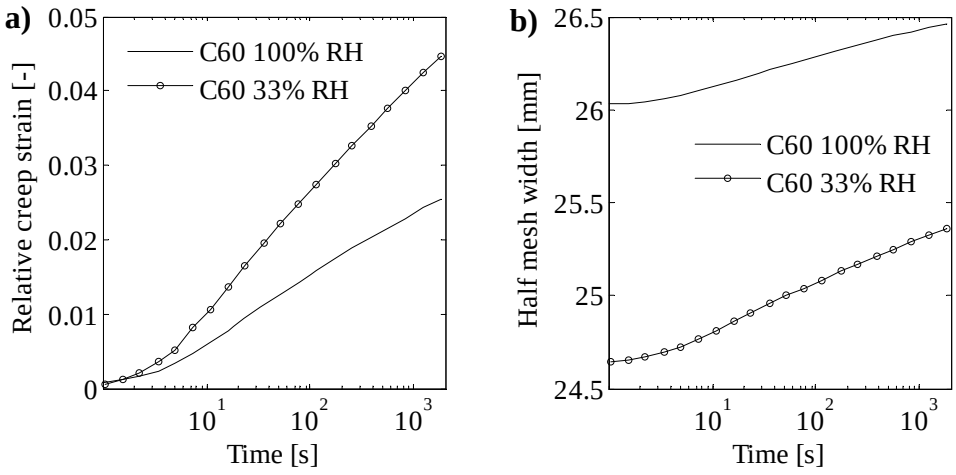

Figure 4: Comparing creep in wet (100% RH) and dry (33% RH) specimens of netting material 1 in Series C60. a) Relative creep strain versus time, $\varepsilon_{c\_rel}(t)$. b) Half mesh width versus time, $w_{1/2}(t)$.

3.3 Creep rate

The creep rate was calculated for 15 time intervals as change in creep strain, $\Delta\varepsilon_c$, divided by length of the interval in seconds, Δt:

$$\dot{\varepsilon}_c = \frac{\Delta\varepsilon_c}{\Delta t} \tag{2}$$

The 15 time intervals were calculated based on the same 20 discrete points in time as in the creep strain calculations (Figure 3). The three first intervals include several of the time values in order to achieve a smooth curve for the creep rate. The time intervals varied in size from 2 – 550 seconds. The mean

creep rate for Series C10, C30, C60 and C90, $\bar{\dot{\varepsilon}}_c$, is plotted against average value of the corresponding time interval in Figure 5 (all three netting materials combined). The creep rate for the various series of tests did not vary significantly between the three netting materials (Figure 3). The creep rate increased with increased target load and the initial creep strain varied from approximately $4 \cdot 10^{-4} s^{-1}$ to $8 \cdot 10^{-4} s^{-1}$, which was reduced with a factor of 230 to 440 during the creep test. The decrease in creep rate was approximately linear on a double logarithmic scale from 8 seconds after start of creep until the end: $\log \dot{\varepsilon}_c = a - b \log t$, where the constants a and b can be found from Figure 5. The difference in creep rate between the series of tests was fairly constant with time, except for C90. The creep rate of Series C60 and C30 was on average 1.4 and 1.2 times larger than the creep rate of C10. Series C90 experienced a smaller reduction in creep rate with time. The creep rate was on average 2.0 larger than the creep rate of C10 for the 10 first minutes, increasing up to 2.9 during the last 20 minutes.

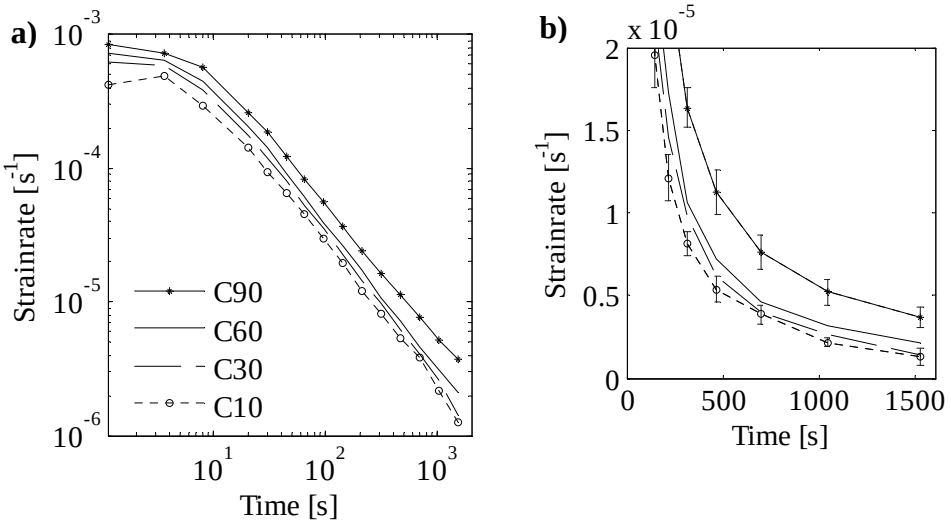

Figure 5: Mean strain rate ($\bar{\dot{\varepsilon}}_c$) as function of time for Series 1 to 4. a) Both axes with logarithmic scale, b) Detail, time from approx. 200 – 1800 seconds, both axes are linear.

Figure 5b gives the average creep rate on normal scales at time 200 s and onwards, including the standard deviation for Series C10 and Series C90 (standard deviation was similar for series C30 and C60). The test results represent a part of a primary creep stage with decreasing strain rate. A steady state with constant creep rate was not observed during the test period, but Figure 5b shows that the netting materials could have been approaching constant strain rate and secondary creep. The creep rates versus time for the specimens that fractured were similar; the material broke without experiencing a noticeable secondary or a tertiary creep phase.

The coefficient of variation in strain rate was high at the beginning of the creep test and was reduced between 8 and 20 seconds after the start of the creep test. For all netting materials combined, the mean coefficient of variation was $\overline{CV} = 26\%$ for the first 8 seconds (first three points in Figure 5), with a maximum value $CV_{\max} = 43\%$. For the time period lasting from 20 to 1800 seconds, $\overline{CV} = 12\%$ and $CV_{\max} = 39\%$ (for the last strain interval of Series C10). The variation in strain rate was similar for the three different netting materials separately as for the combined results presented in Figure 5.

Average creep rates have been calculated based on data on creep properties of Nylon 6 filaments given in Murthy & Bray (2003) and the results from the presented creep tests of netting for time intervals of approximately 10-100 s and 100-1000 s. The results are presented in Figure 6 for Nylon 6 filament in an atmosphere of 43% and 84% RH, wet and dry (33% RH) netting from series C60 and wet netting from series C10 (netting material number 1, Table 1). Murthy & Bray did not give the target load for their creep tests, but the initial creep was approximately 2%, meaning that the creep load was relatively low, probably 5-10% of the force at break of the fibres (personal communication, Polyamide High Performance). It is not possible to directly compare the data in Figure 6, but they may give us an idea of the importance of friction between filaments for creep behaviour of netting. Except for dry netting materials, all creep rates are similar for fibres and wet netting. Creep rate of dry netting is 1.8 times larger than for wet netting and dry (43% RH) and humid (84% RH) filaments. Morton & Hearle (1975) state that increased water content of nylon usually increases the coefficient of friction, which can explain why dry netting experience higher creep rate than wet materials, as a larger portion of the creep due to

geometric flexibility in the knitted netting material will be released during temporary creep.

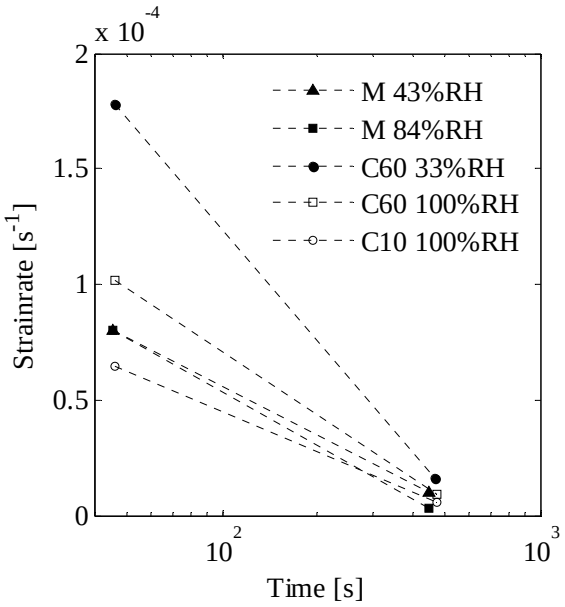

Figure 6: Comparing strain rate data for Nylon filaments at various relative humidity (M: Murthy & Bray, 2003) with data for netting material 1 (series C60 and C10).

3.4 Recovery post creep

In the recovery part of the test procedure, the gauge length was measured four times: At the end of the creep test, immediately after unloading, after 5 minutes of relaxation and finally after 24 hours or 6 days. In general all specimens were measured 24 hours after creep, except for approximately half of the specimens in series C60 and C90 that were measured after 6 days instead. The resulting strains (mean values with standard deviation) were calculated based on the length of each specimen at pretension and are given for the various netting materials as a function of breaking strain ($\varepsilon/\varepsilon_b$) in Figure 7. All strains except the final creep strain (at end of creep test) are given for a load level of approximately 7.3 N (pretension for netting material 1, Table 1).

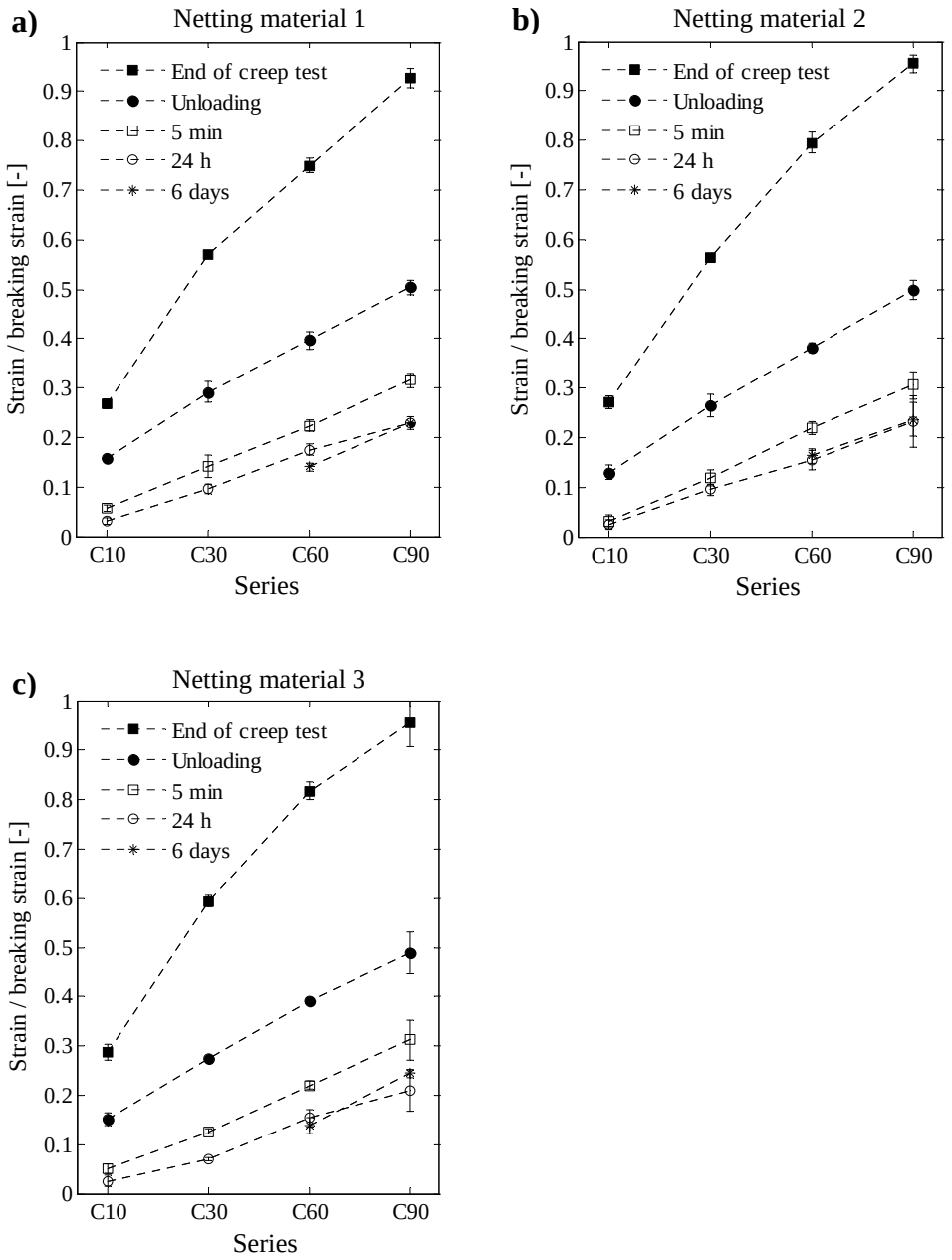

Figure 7: Recovery post creep given as relative strain, $\varepsilon/\varepsilon_b$, for the various series of tests. Strain /breaking strain was calculated at the end of the creep test, immediately after unloading the specimen, 5 minutes after unloading and 24 hour or 6 days after unloading. a) Netting material 1. b) Netting material 2. c) Netting material 3.

The variation in strain results was small for most netting materials and series of tests (standard deviation is given in Figure 7). Exceptions are found for Series C90, which in our opinion is a result of the already mentioned variation in material properties (especially release of geometric flexibility). Figure 7 shows that the relative strain for the various series of tests is similar for all tested netting materials. The combined results for all netting materials are given in Figure 8a and c. The standard deviation was small for most results, except at the end of creep test series C60 and for some of the results of series C90. It was previously discussed that the netting behaviour can be unstable at these load levels, which combined with variations in material properties was reflected in relatively high deviations in results.

Fractions of the creep strain can be of elastic, viscoelastic and permanent nature. The recovery procedure allows us to distinguish between various types of strains as shown in Figure 8b: Elastic strain was calculated as the difference between the strain at the end of the creep test and the strain immediately after unloading. The difference between the strain immediately after unloading and 5 minutes later represents a viscoelastic strain called VE1, VE2 is viscoelastic strain recovered between 5 minutes and 24 hours or 6 days after the creep test. R24h and R6d represent residual strains after 24 hours and 6 days respectively.

The recovery of strain post creep was relatively fast; approximately half of the creep strain was elastic and after 5 minutes of relaxation another considerable amount of strain was recovered (VE1). 24 hours or 6 days thereafter a smaller portion of strain was recovered (VE2). The viscoelastic strains seemed to be less dependent of the creep target load than the elastic and residual strains.

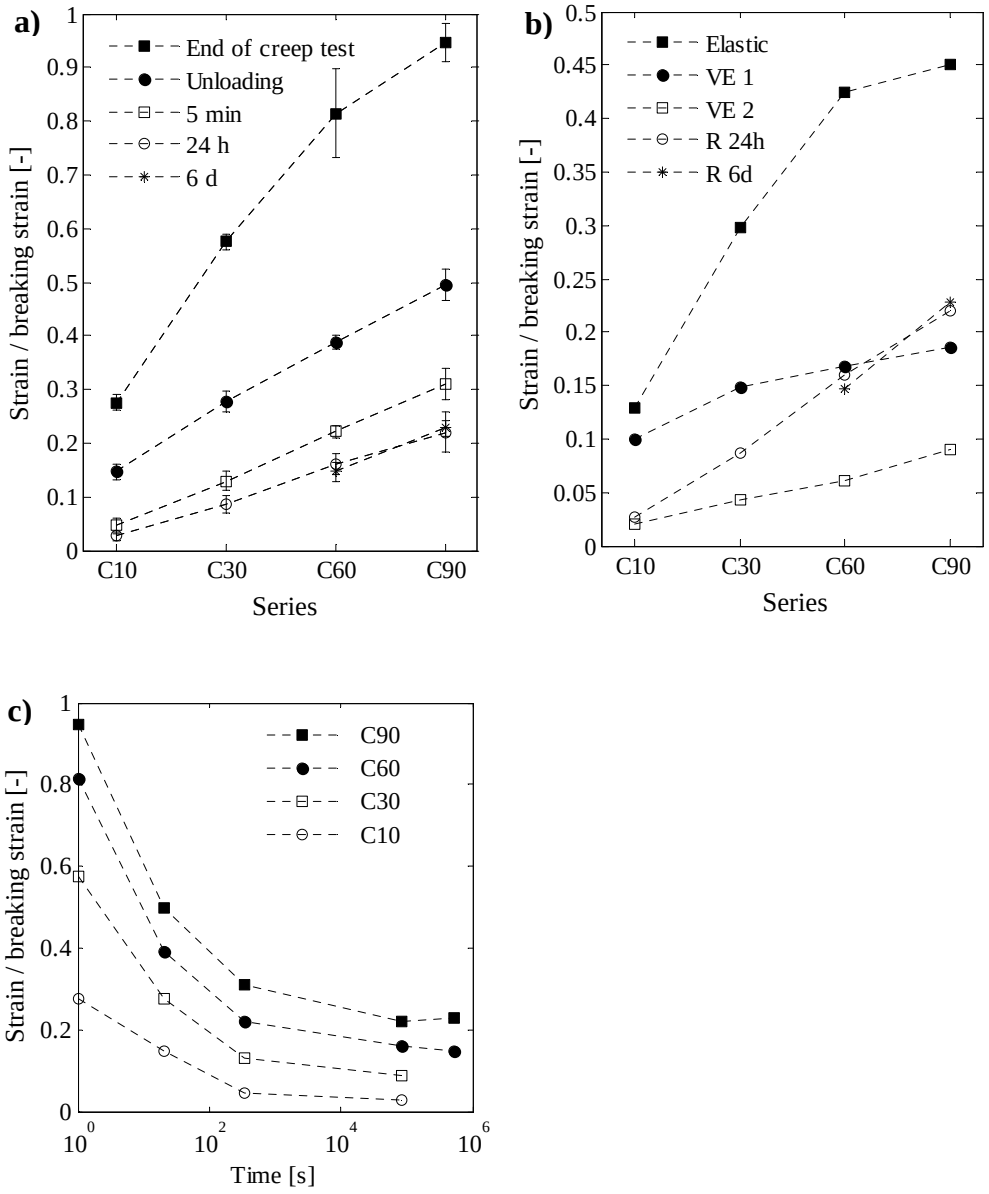

Figure 8: a) Recovery post creep for all netting materials combined given as relative strain, $\varepsilon/\varepsilon_b$, for the various series of tests. b) Various types of strain. c) Recovery post creep for all netting materials combined given as relative strain as a function of time for the various series of tests.

Figure 7 and Figure 8 show that there were small, irregular differences in the measured strain after 6 days and 24 hours. These differences were probably mainly due to a natural variation in material properties. Previous experiments with Nylon filaments showed that the rate of recovery was greater than the rate of creep (Morton & Hearle, 1975). If this is a valid assumption for the netting materials, it supports the hypothesis that variations in length of test specimens measured at 24 hours and 6 days after the creep test represented variations in material properties and that the test specimens most likely were fully recovered within 24 hours after the creep tests. This implies that the measured residual strain was a permanent elongation of the netting material, and that netting materials should have the same properties 24 hours and 6 days after creep.

3.5 Post creep properties

After the recovery period of 24 hours or 6 days, the specimens were stretched to break in Series BP. Figure 9a to c gives average results for the various test series represented by 3rd to 7th order stress versus normalized elongation ($\sigma - L^*$) polynomials. The polynomials were found using the least squares method and they provide a good fit for all curves. The stress equals the stretching force divided by the cross-sectional area of solid material (Table 1 and Moe et al, 2007). The normalized elongation is the measured relative elongation $\Delta L_e(t)$ divided by the length at pretension from Series B0:

$$L^*(t) = \frac{\Delta L_e(t)}{L_{e0}} = \frac{L_e(t) - L_{e0}}{L_{e0}} \tag{3}$$

For unused netting materials, the normalized elongation is equal to the nominal strain (engineering strain).

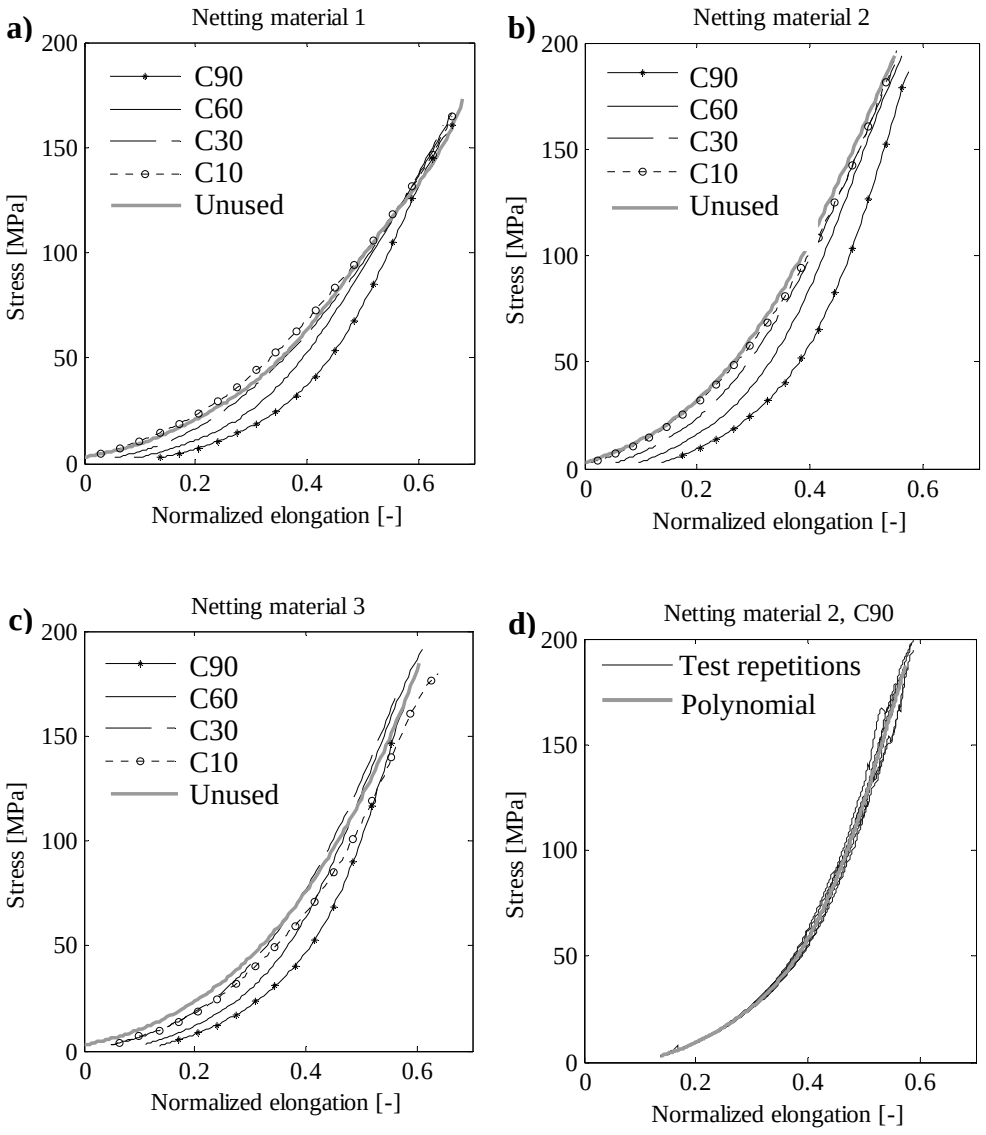

Figure 9: Stress versus normalized elongation, L^*, for specimens previously subjected to creep tests and unused netting materials. a) Netting material 1. b) Netting material 2. c) Netting material 3. d) Example of test result for netting material 2 in Series C90.

The results from the test repetitions performed 24 hours and 6 days after creep showed in general no differences other than what could be expected as a natural variation in material properties of a netting material. The initial normalized elongation (permanent elongation due to creep test) increased with increasing creep target load. However, the normalized elongation and stress at break (i.e. total elongation and force at break) were not significantly affected by the previous load history. The difference in tensile properties between unused netting materials and netting subjected to a creep load of 10% of force at break was negligible.

The validity of each polynomial in Figure 9 was evaluated by assessing the difference between mean test results and fitted polynomial (error), and the variation in test results (*CV* between test repetitions). The error and coefficient of variation was calculated for intervals of 10 % relative normalized elongation. The relative normalized elongation was calculated as $L^*_{rel} = L^* - L^*_P$, where L^*_P is normalized elongation due to initial permanent deformation from creep test (given in Figure 9). *CV* in test results was on average 3 % for all series of tests, with a maximum value of 8 % for netting material number 3 in series C60 and relative normalized elongation interval of 30 – 40 %.

The error in the estimated $\sigma\left(L^*\right)$ polynomial for discrete values of normalized elongation (L^*_i) was expressed as the absolute difference between the mean stress-value from the test (μ_i) and the stress-value from the polynomial (f_i):

$$\mathrm{E}_i = \left|\left(f_i - \mu_i\right)/\mu_i\right| \qquad [\%] \tag{4}$$

The average error for a specific interval of relative normalized elongation from L^*_{relA} to L^*_{relB} ($L^*_{relA} : L^*_{relB}$) of a test was calculated as:

$$\overline{\mathrm{E}}\left(L^*_{relA} : L^*_{relB}\right) = \frac{1}{n} \cdot \sum_{i=A}^{B} \mathrm{E}_i \tag{5}$$

where n is number of normalized elongation increments in the interval. The total average error, $\overline{\mathrm{E}}_{tot}\left(L^*_{relA} : L^*_{relB}\right)$, was calculated as the sum of $\overline{\mathrm{E}}\left(L^*_{relA} : L^*_{relB}\right)$ for all tests divided by the total number of tests. The total

average error for all relative elongations, $\overline{\mathrm{E}}_{tot}\left(0:L^{*}_{rel\_b}\right)$, was equal to 1 % ($L^{*}_{rel\_b}$ is relative normalized elongation at break). The maximum average error was $\overline{\mathrm{E}}\left(0:0.1\right)=3\%$ for netting material 1 in Series C30.

Figure 9d shows the test result for netting material 2 in Series C90 and the estimated polynomial representation. This polynomial has an average error of $\overline{\mathrm{E}}\left(0:L^{*}_{rel\_b}\right)=0.5\%$ compared to the mean test results and $CV=3.6\%$.

To better assess the change in stiffness properties post creep, average stepwise constant stiffness values were calculated for intervals of normalized elongation of 10 % using the least squares method. Mean values with standard deviation are given in Figure 10 for 10 % intervals of relative normalized elongation.

The stiffness post creep did not vary much for relative normalized elongations less than 20%. For relative normalized elongations L^{*}_{rel} greater than 20%, the stiffness tended to increase with increased creep target load. This is a natural consequence of the findings that neither force nor length at break was influenced by the material's creep history. At high relative elongations, the variation in stiffness between the different specimens in a test was significant as shown in Figure 10.

The tangent stiffness was obtained by derivation of the stress-relative elongation polynomials; $K_t = d\sigma / dL^{*}$ and is plotted as a function of relative normalized elongation in Figure 11. The tangent stiffness was independent on creep history for relative elongations than 20%, which agrees with previous conclusions. For some of the series, especially C60 and C90, a drop in tangent stiffness can be observed towards the point of break. However, it is difficult to conclude in this manner due to the large variation in stiffness between the test specimens at large elongations (Figure 10).

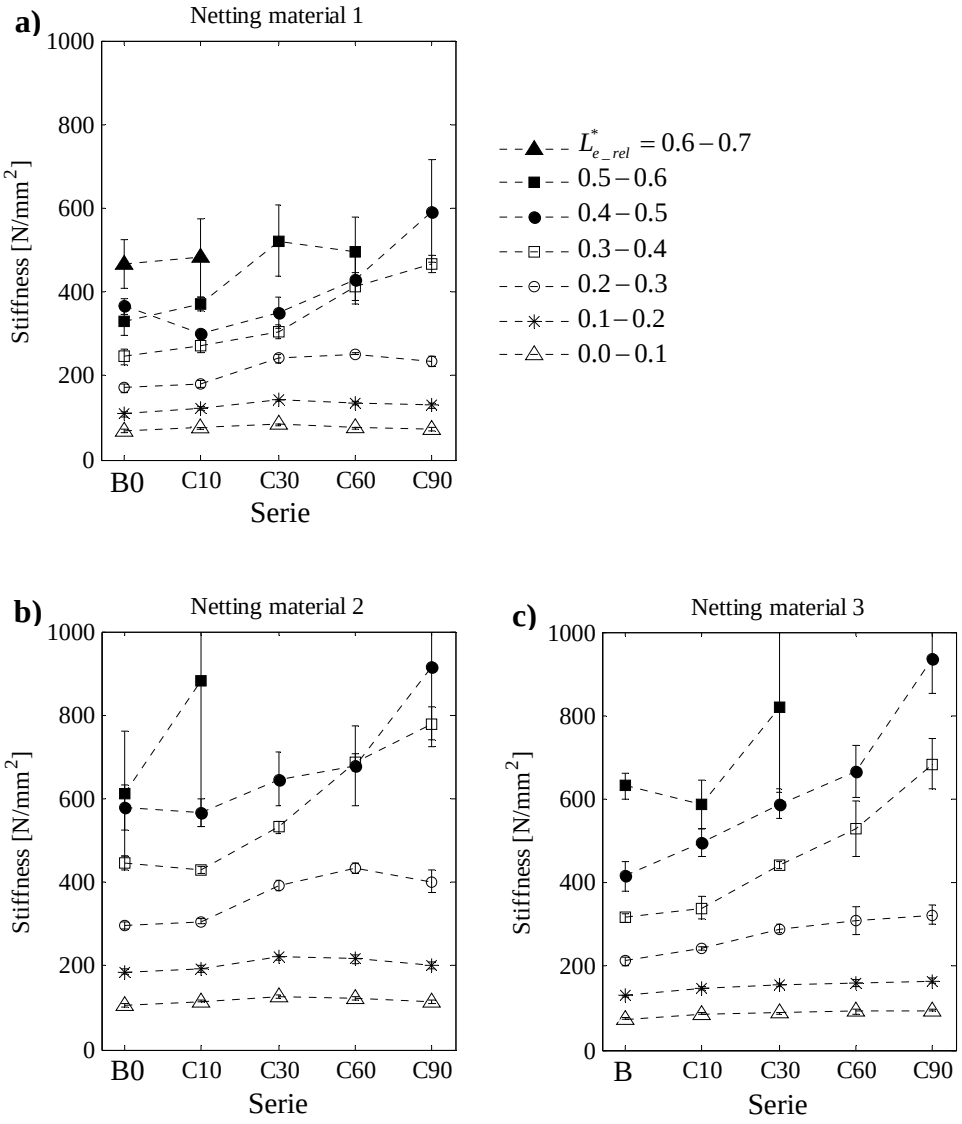

Figure 10: Stepwise constant stiffness values for various intervals of relative normalized elongation given for Series B0 and Series BP for specimens previously subjected to Series C10, C30, C60 and C90.

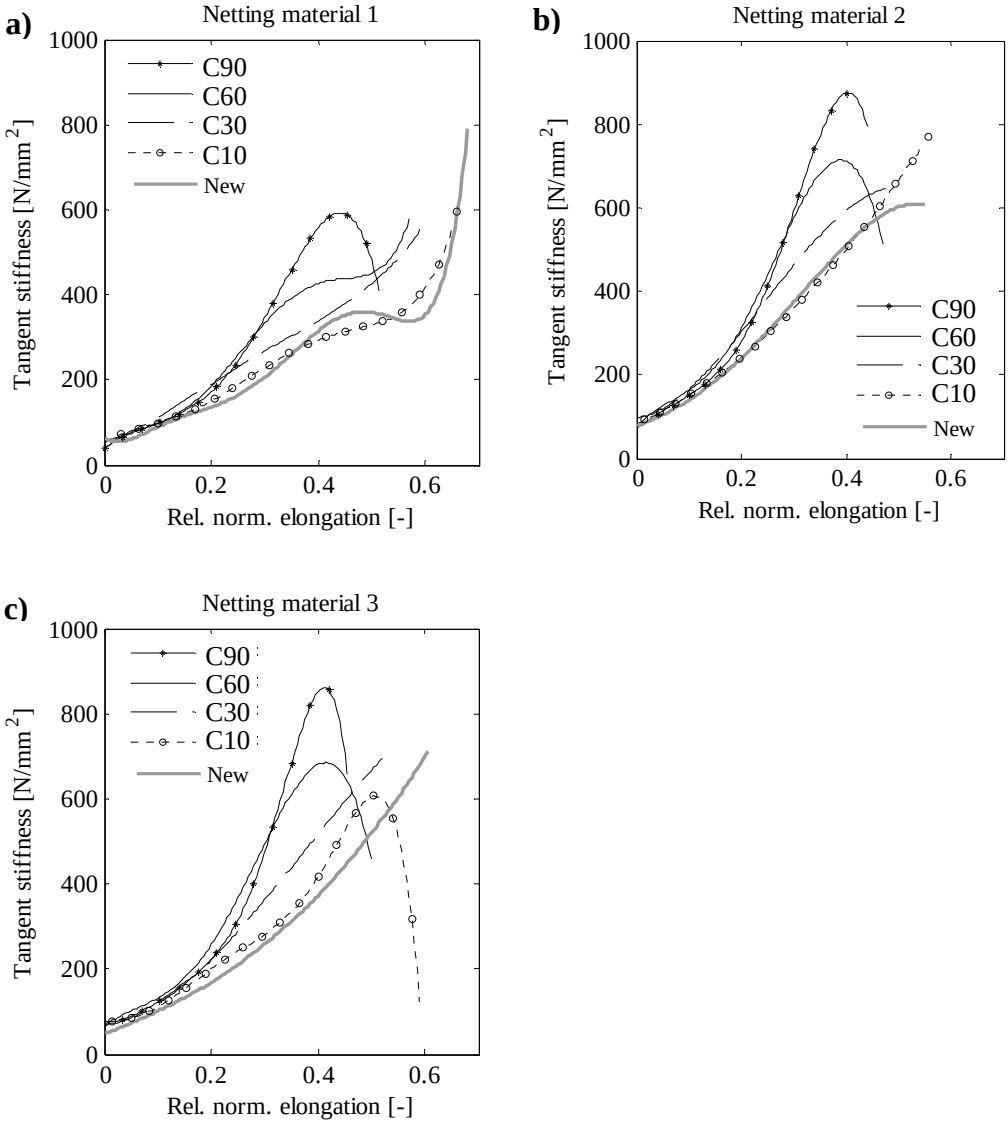

Figure 11: Tangent stiffness as a function of relative normalized elongation.

4 Conclusions

Relative creep strain in wet netting materials during 30 minutes varied from 1.6 – 3.5 % for a creep target load of 10 to 90% of average force at break. Significant variation in creep strain was observed within a test, probably due to a physical variation in properties between the specimens, depending on the location of the specimens on the piece of netting material and release of geometric flexibility. 2 of the 29 test specimens subjected to a creep target load of 90 % of the average breaking force ruptured within a few minutes.

The rate of creep was similar for the three netting materials and it decreased with time with a linear trend on a double logarithmic scale. The strain rate increased slightly with increased target load.

The recovery of strain post creep was relatively fast; approximately half of the creep strain was elastic and after 5 minutes of relaxation another considerable amount of strain was recovered. The results from the test repetitions performed 24 hours and 6 days after creep showed in general no differences other than what could be expected as a natural variation in material properties of a netting material. It is probable that the netting materials were fully recovered within 24 hours and that the residual strain at this point was a permanent elongation of the netting material.

The difference in tensile properties between unused netting materials and netting subjected to a creep load of 10% of force at break was negligible. The initial (permanent) elongation of specimens previously subjected to creep increased with increasing creep target load. However, the total elongation and force at break were not significantly affected by the creep target load.

The stiffness was independent on creep history for relative elongations less than 20%. For relative normalized elongations greater than 20%, the stiffness tended to increase with increased creep target load.

5 Acknowledgements

This work was sponsored by the Norwegian Research Council through the IntelliSTRUCT programme (Intelligent Structures in Fisheries and Aquaculture) at SINTEF Fisheries and Aquaculture.

6 References

Ashby, Michael F. & Jones, David R H, 1980. Engineering Materials 1. Pergamont Press, England.

Buchanan, D. R. & Walters, J. P., 1977. Glass-Transition Temperatures of Polyamide Textile Fibers, Part I: The effects of Molecular Structure, Water, Fibre Structure, and Experimental Technique. Textile research journal 47, 398-406.

Dowling, Norman E., 2007. Mechanical behaviour of materials. Pearson Education, Inc. United States of America.

Klust, Gerhard, 1982. Netting materials for fishing gear. Fishing News Books Ltd., England.

Kohan, Melvin I., 1995. Nylon Plastics Handbook. Carl Hanser Verlag, Germany.

Moe, H., Fredheim, A., Heide, M., 2005. New net cage designs to prevent tearing during handling. IMAM 2005, Lisbon, Portugal, 26 – 30 September 2005.

Moe, H., Olsen, A., Hopperstad, O. S., Jensen, Ø., Fredheim, A., 2007. Tensile properties for netting materials used in aquaculture net cages. Aquacultural Engineering 37, 252–265.

Morton, W. E., Hearle, J. W. S., 1975. Physical properties of textile fibres. The textile institute, Great Britain.

Murthy, N. S. & Bray, R. G., 2003. Structure and properties of polyamide 6 and 4-aminomethylcyclohexane carboxylic acid copolymers with an unusually short helical pitch for nylons. Polymer 44, 5387-5396.

Sala, A., Lucchetti, A., Buglioni, G., 2004. The change in physical properties of some nylon (PA) netting samples before and after use. Fisheries research 69, 181-188.

The International Organization for Standardization, 1976. ISO 3790 Method of test for determination of elongation of netting yarns.

The International Organization for Standardization, 1980. ISO 2602 Statistical interpretation of test results – Estimation of the mean – Confidence interval.

The International Organization for Standardization, 1997. ISO 291 Plastics – Standard atmospheres for conditioning and testing.

The International Organization for Standardization, 2002a. ISO 1107 Fishing nets –Netting – Basic terms and definitions.

The International Organization for Standardization, 2002b. ISO 1806 Fishing nets –Determination of mesh breaking force of netting.

Walpole, R.E., R. H. Myers, S. L. Myers and K. Ye. (2007). Probability and Statistics for Engineers and Scientists (8th Edition). Pearson Education, Inc.

Paper 3

Moe H., Dempster T., Sunde L.M., Winther U. and Fredheim A. (2007a). *Technological solutions and operational measures to prevent escapes of Atlantic cod (*Gadus morhua*) from sea cages.* Aquaculture Research 38, 91-99.

Aquaculture Research, 2007, **38,** 91–99 doi: 10.1111/j.1365-2109.2006.01638.x

Technological solutions and operational measures to prevent escapes of Atlantic cod (*Gadus morhua*) from sea cages

Heidi Moe, Tim Dempster, Leif Magne Sunde, Ulf Winther & Arne Fredheim
SINTEF Fisheries and Aquaculture, Trondheim, Norway

Correspondence: H Moe, SINTEF Fisheries and Aquaculture, 7465 Trondheim, Norway. E-mail: Heidi.Moe@sintef.no

Abstract

Escapes of cod (*Gadus morhua*) from sea cages represent an economic problem for farmers and a potential environmental problem. We estimate that 0–6% of cod held in sea-cage farms in Norway were reported to have escaped each year from 2000 to 2005, which is a high proportion compared with salmon. We interviewed employees at 19 coastal sea-cage cod farms in Norway to investigate both how and why cultured cod escape and to document cage handling and management strategies that were effective in minimizing escapes. Based on the interviews, we describe five working hypotheses that may explain why a greater proportion of cod than salmon escape: (1) cod are more willing to escape than salmon; (2) cod bite the net cage and create wear and tear; (3) net cages have insufficient technical standards for cod culture; (4) cod are placed in sea cages at considerably smaller sizes than salmon; and (5) cod are more popular feed for predators. Preliminary testing of the hypothesis that cod bite netting and create holes was done by placing pre-damaged net panels with cut twines and control panels inside sea cages. Holes in the pre-damaged net panels increased in size over a period of 3 months. The type of damage indicated that biting of netting twines was the likely cause.

Keywords: Atlantic cod (*Gadus morhua*), aquaculture, escape, sea cages, technology

Introduction

Escapes are widely acknowledged as an environmental problem in the grow-out phase of sea-based salmon aquaculture (Soto, Jara & Moreno 2001; Naylor, Hindar, Fleming, Goldburg, Williams, Volpe, Whoriskey, Eagle, Kelso & Mangel 2005). Documented escapes of salmon (*Salmo salar*) in Norway numbered 2 00 000–10 00 000 per year for the period from 1995 to 2005 (Norwegian Fisheries Directorate 2005). Escapes of salmon are largely due to structural failures of cage systems in storms and net damage from collisions, propeller strikes and predators (Norwegian Fisheries Directorate 2006a). Escapes of other marine species from on-growing sea cages have been documented occasionally [e.g. sea bream (*Sparus auratus*) and sea bass (*Dicentrarchus labrax*): Dempster, Sanchez-Jerez, Bayle-Sempere, Giménez-Casalduero & Valle 2002; kingfish (*Seriola lalandi*): Gillanders & Joyce 2005], although comparatively little is known of the causes of escape and their environmental consequences.

Aquaculture of Atlantic cod (*Gadus morhua*) is a growing industry in Norway; 3000 tonnes of cod were produced by 200 farms in 2004, and the production increased to 5000 tonnes in 2005 (Moe, Gaarder, Sunde, Borthen & Olafsen 2005). Cod aquaculture is also a developing industry in Scotland, Ireland and Canada. Cod aquaculture in Norway began in the 1980s, but development of the industry was slow due to the difficulties and expense of juvenile production. In the late 1990s, juvenile production techniques improved and cod aquaculture moved into a phase of increasing industrialization. Cage technologies and farming systems to on-grow cod have been largely inherited from salmon production, which has lead to new and unexpected problems. Escapes of cod from sea cages are one such problem; they have occurred frequently in Norway and are regarded as a critical bottle-neck to future growth and industrialization of cod aquaculture.

The Norwegian Directorate of Fisheries (2005) has estimated that cod are 10–20 times more likely than salmon to escape from a sea-based fish farm. Cod

escape is largely regarded by fish farmers as an economic problem, but interactions of escaped cod with wild cod populations are possible (P.A. Bjørn & I. Uglem unpubl. data). Currently, information regarding the extent of cod escape is relatively limited and insufficient to identify the most important causes. Thirty-six cases of escape of cod have been reported to the Norwegian Directorate of Fisheries since registration started in 2001 to February 2006. However, the Directorate states that many cases of escape remain unreported.

Development of new species in aquaculture creates new challenges in developing suitable technologies for their culture. Problems may arise when technologies developed for culturing one species are used, with little modification, to culture a new species. For instance, wear and tear on the netting may differ greatly due to different behavioural characteristics of the fish themselves or different behaviour exhibited towards them by predators. In this study, we generated baseline information on the range of possible causes of escape of cod at commercial farms in coastal Norway through surveys of cod farmers. Further, we tested whether cultured cod were capable of causing damage to nets by placing experimental net panels in a commercial cod farm.

Material and methods

Estimating the percentage of cod escapees in Norway

Numbers of reported escaped cod, the causes of escape, numbers of juveniles produced and the total number of cod in sea cages in Norway for 2000–2005 were obtained from the Norwegian Directorate of Fisheries. We defined the percentage of cod that escaped relative to the number of cod in sea cages in any given year, expressed by the following formula:

$$N = (E/S) \times 100$$

where E is the number of reported escaped fish and S is the number of cod held in Norwegian sea cages for the specific year.

Surveys of cod farmers to determine causes of escape

We surveyed employees at 19 cod farming companies throughout Norway to collect information on their experiences with net culture technologies and escapes of cod. The companies represented the full geographic spread of fish farms for on-growing of cod in Norway (Fig. 1), and together produced approximately 50% of the biomass of cod in Norwegian sea-based farms in 2004. Producers of aquaculture equipment, producers of fish feed and professional diver companies were also interviewed as a secondary source of information.

Interviews were performed through telephone calls, e-mail and visits to specific farms. Responses were obtained from all 19 farms, although the level of detail of responses varied among farms. The main topics in the interviews were

1. What equipment and technology was used by the farm and what was their condition? Particular emphasis was placed on the type, condition and age of the net cages.
2. What attempts had been made to reduce escapes of cod? What is effective?
3. What were the standard operating procedures at the farm and what was their possible effect on escape? For example, details of feeding strategies and handling of the net cage were obtained.
4. What damage had occurred to net cages that hold cod and what was the cause? Information was obtained on the type, location, number and frequency of net damage and whether the damage represented an escape hazard.
5. Does cod behaviour within cages differ to salmon? Do cod interact with the cage net (e.g. do cod bite the net)? Does the behaviour of cod depend on fish age, size and density, water quality, the net cage environment or the feeding regime?
6. What are the reasons for unregistered (unknown) losses of cod? What is the importance of escape, cannibalism, predation and loss of dead fish in this context?
7. What are the reasons for escape of cod?

Experimental testing of cod interactions with netting

Most cod farmers reported that cod interact with the cage netting through biting and thereby create wear and tear. The majority of farmers considered this as a direct reason for the creation of holes in the net and escapes of cod on several occasions. Therefore, we performed a field test to try to provoke biting from cod at net panels placed in full-scale commercial cages. The main goals of the study were to investigate if cultured cod would bite the net and create wear and tear, and to determine if the cod were more attracted to damaged areas of the net rather than normal undamaged netting.

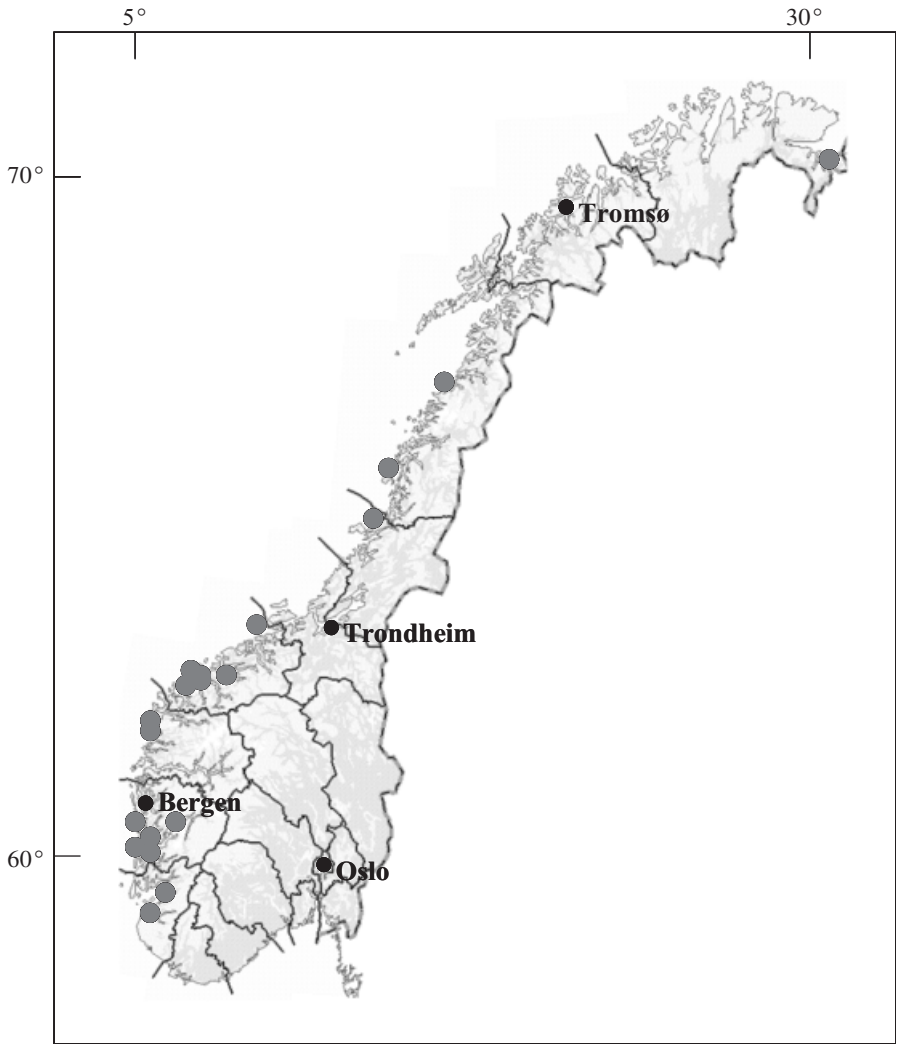

Figure 1 Locations of the 19 cod farms in Norway included in the survey.

Four wooden frames with Raschel knitted Nylon netting and pieces of rope were launched in cages with cod on 1 June 2005 (Fig. 2). The frames measured 0.8 × 1.2 m. Two of the frames had netting with three different types of damage: one cut twine, two adjacent cut twines and a tear of three cut twines that had been mended using a grey thread (Fig. 3). The other two frames had undamaged netting and acted as controls.

The field study was performed in two different cages (with circumference of 60 and 70 m and 15 m deep) at a fjord-based cod farm in mid-Norway (Fig. 1). Cage 1 contained cod with an average weight of 0.3 kg, while the cod in Cage 2 had an average weight of 2 kg. Relatively, large variations in weight among fish existed in both cages. In Cage 2, fish weights ranged between 1 and 3 kg. One frame with undamaged netting and one with damaged netting were launched in each of the two fish cages.

Results

Extent and causes of cod escapes in Norway

Figure 4 indicates that the total number of cod that escaped from sea cages in Norway has increased steadily from 2000 to 2005 following the increase in overall production. We estimate that 0–6% of the cultured cod was reported to have escaped each year from 2000 to 2005 (Fig. 4a). These should be regarded as minimum estimates, as it is probable that not all escape episodes were detected or reported

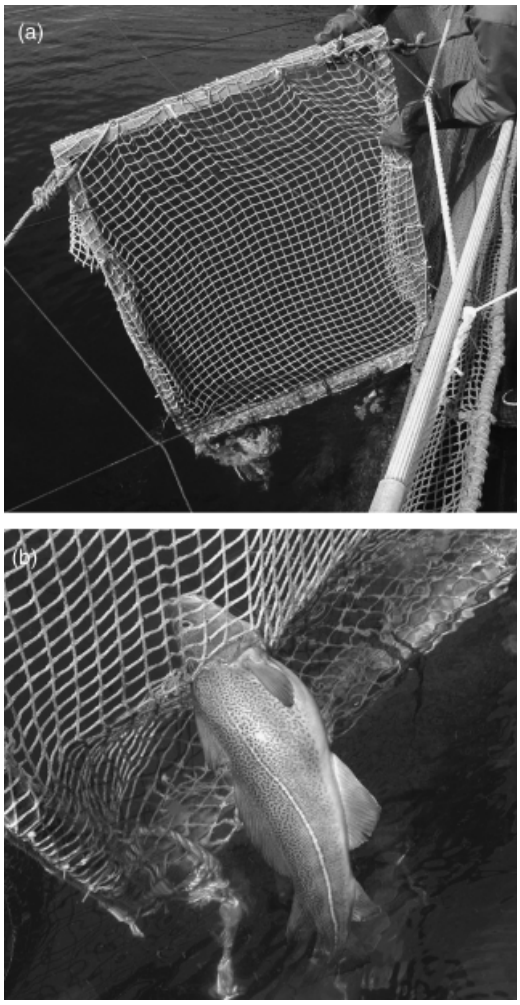

Figure 2 (a) Launch of a test net panel in a commercial cod sea cage and (b) an escape attempt through a pre-damaged hole (one-twine cut) in a test net panel by a 1 kg fish. The panel had been in the cage for 1 month.

as is believed to be the case for salmon (Fiske, Lund & Hansen 2006).

Overall, damage to the net cage by storms was the greatest cause of escapes by number, although this was largely due to a single mass escape of 160 000 cod from a farm in January 2006 (Fig. 4a). Holes to the nets from other causes (cod/predator biting, handling, unknown causes) were responsible for the greatest number of escape incidents, and more than 50% of escapee numbers were due to these causes in 2003–2005.

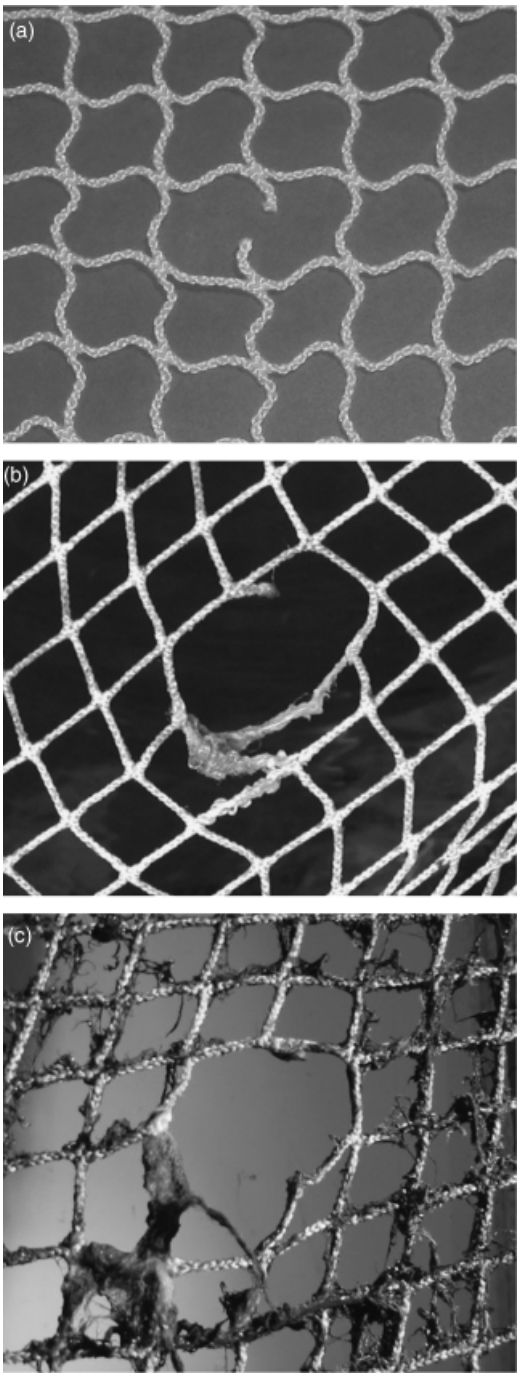

Figure 3 (a) Test panel netting with one cut twine, (b) extent of net damage after 1 month, (c) extent of damage after 3 months. After 3 months, an adjacent twine had also been cut, doubling the initial hole size.

Experience with escape and fish bite

Eight out of the 19 cod farmers responded as to whether their farm had experienced an escape, and all eight indicated that they had. These farmers confirmed that they had found bite damage on the net cages. Five of the eight farmers believed that wear and tear from fish bite was the direct cause of escape.

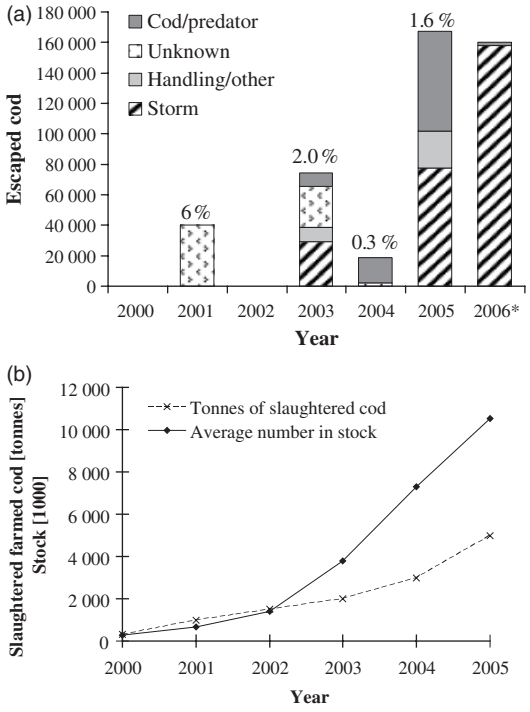

Figure 4 (a) Number and estimated percentage of reported escaped cod and their cause. *The 2006 figures are for January and February only. Cod/predators refers to escapes due to holes in the net caused by either cod from inside the cage or predators from outside the cage. (b) Numbers of juveniles produced and tonnes of production in sea cages in Norway from 2001 to 2005.

The other three farmers gave net handling procedures and storms as the cause of net damage, which led to escape. Several fish farmers described the net biting behaviour as a series of violent pulling and tearing movements where the cod flung its entire body from side to side.

Cod farming technology

Most cod farmers reported that common salmon net cages were unsuitable for cod aquaculture. Most farmers have applied stronger netting, double net cages, various types of net impregnation (used to glue net fibres together) and anti-biofouling treatments. However, several farmers were unsatisfied with the available net cage products, and indicated that the present net cage technology did not make it possible to avoid escape of cultured cod in a cost-effective manner. Sixteen of the 19 fish farmers provided the age of their net cages. Over 85% of nets in use were 2 years old or less, while 8% of nets were 6 or 7 years old (Fig. 5).

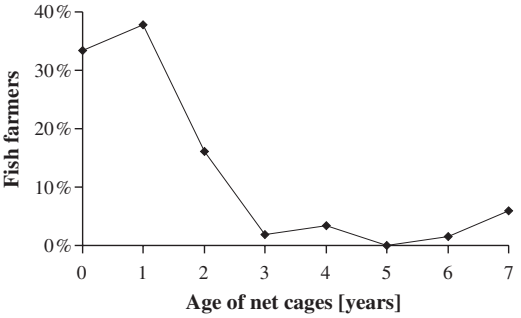

Figure 5 Proportion of net cages of various ages used in 17 of the Norwegian cod farms surveyed.

Creation of working hypotheses of why more cod escape than salmon

As the same basic technology is used, it is sensible to assume that the reasons for escape of salmon also lead to escape of cod. These include the structural breakdown of farms and the formation of holes in the netting through abrasion of weights on the net cage, predator damage (seal, otter, wild fish and birds), inferior net cage quality and construction and propeller damage from boats (Norwegian Fisheries Directorate 2006a). However, as cod escape more frequently than salmon, additional reasons for escape may exist. Based on the survey responses, we describe five working hypotheses that may explain why a greater proportion of cod than salmon have escaped in recent years:

1. *Cod are more willing to escape than salmon.* Cod have a greater ability and motivation to swim through small holes in net cages than salmon (Aas 2005). Cod search the net cage wall and will find holes in the netting if they exist. A small hole, just big enough for the cod to squeeze through, can quickly lead to escape of many cod (see Fig. 2).
2. *Cod bite the net cage and create wear and tear.* Several of the fish farmers had observed that cod vigorously bite at netting and ropes and those areas subjected to fish bite showed distinct signs of wear and tear. This resulted in round holes that are different to typical abrasion damage and cut twines due to mechanical damages to net cages. Cod may be attracted to irregularities in the net cage, such as existing mechanical damages, loose sewing threads or areas of slack netting.
3. *Salmon net cages have an insufficient technical standard for cod.* Cod farmers have previously used old net cages from salmon farms. Most fish farmers are aware of this problem and have invested in

new net cages (see Fig. 5), but the common understanding is that none of the solutions that exist today give adequate protection against escape of cod. The survey results also indicate that net cages that have sufficient strength for salmon are unable to withstand cod biting.

4. *When cod are placed in sea cages they are considerably smaller than salmon.* Cod can be put into cages at 10 g, while salmon usually are at least 50 g when transferred to sea. If farmers use traditional salmon smolt net cages for small cod juveniles, one broken twine can form a large enough hole for cod to escape. In the worst case scenario, juvenile cod could be so small compared with the mesh size that they swim directly through an undamaged mesh, as is also suspected for salmon (Hansen 2006).
5. *Cod are popular feed for predators.* Several cod farmers indicated that some predators prefer cod over salmon, while others reported no such difference. Predators such as seals are known to distinguish between different species and sizes of fish (Sepulveda & Oliva 2005).

All of these hypotheses require experimental testing to determine their validity and significance. However, they form a good platform for future research.

Net panel tests

The test panels of netting were removed from the cages after 1 month in the sea due to net changes. The fish farmer observed that one cod was caught in the panel with pre-damaged netting in Cage 2 (cage containing 2 kg fish). Two days later, the frames were brought up again for inspection and a different cod was now caught in the same part of the netting (Fig. 2). The cod had been caught in the netting where we had initially cut a single twine (Fig. 3). The area close to the cut was worn; the netting material had frayed considerably and the hole had increased in size. During the interviews before the net panel testing, the fish farmer at this site had reported that cod often bit at both netting and ropes within cages, so it is likely that biting of the loose twine end created the hole.

Frames were removed from the cages after 3 months in the sea. All pre-damaged areas showed signs of further damage. For instance, the hole formed by an initially single cut twine had increased in size as a second, adjacent twine had been cut (Fig. 3). The other test damages in both panels also showed signs of considerable wear and tear, with frayed twines consistent to all. Filaments had been drawn out of the twines and all cut twines had frizzy ends. There were no obvious differences between the frames in the two different cages, indicating that both small cod of 0.3 kg and large cod of 2 kg were capable of causing this damage.

A thorough inspection of the net revealed that areas of the initially undamaged netting on both the control panels and panels with pre-damaged areas also showed signs of wear and tear. Although no new holes appeared in the undamaged sections of netting, areas where wear and tear was observed were free from biofouling and filaments in the netting were drawn out. One twine in one of the pieces of undamaged netting was partly cut, but we could not definitively attribute this damage to fish bite.

Discussion

Extent and causes of cod escape

Although it is likely that escapes from storms will be reported, as damage is noticeable and escapes from storms are typically large, escapes through holes in the net are less likely to be noticed and reported. Moreover, farmers may have little idea how many fish have escaped if a hole in the netting is discovered, which may lead to under-reporting of numbers of escaped fish. Therefore, it is likely that holes in the netting contribute a greater proportion of escaped cod than is reflected by officially reported numbers. Our estimate of cod escapes between 2000 and 2005 (Fig. 4) should therefore be regarded as a minimum as escapes are likely under-reported.

Cod aquaculture currently operates with large quantities of lost fish with no known or given cause. It is not uncommon that unregistered losses reach more than 5% of total production (Norwegian Fisheries Directorate 2005), which is significantly greater than the typical level of unregistered losses for salmon of $< 1\%$. Causes of unregistered loss are numerous, and include cannibalism, loss of dead fish and predation. For cod, it is possible that frequent loss of small numbers of fish occurs through small holes in the netting. Some proportion of the gap between the 1% unregistered loss of salmon and the 5% loss of cod is therefore likely to be due to additional escape.

The level of escape entails a considerable economic cost and is considered to be environmentally unacceptable by the authorities (Norwegian Fisheries Directorate 2006b), especially as the production of cod expands. Development of technology and operating procedures to minimize escapes of cod is clearly

required to reduce the economic and environmental impacts of escapes.

Damage caused by storms was the most significant reported cause of escapes of cod in terms of absolute numbers of escaped cod, which corresponds to similar statistics for salmon (Norwegian Fisheries Directorate 2006a). The second most significant reported cause of escapes of cod by number and the most significant cause in terms of number of escape episodes was damage to the net cage by either the cod themselves and/or the predators. Technological development to reduce escapes should therefore focus on two areas: (1) cages that avoid or better respond to the physical forcing of storms and (2) improving the net cage to minimize the formation of holes.

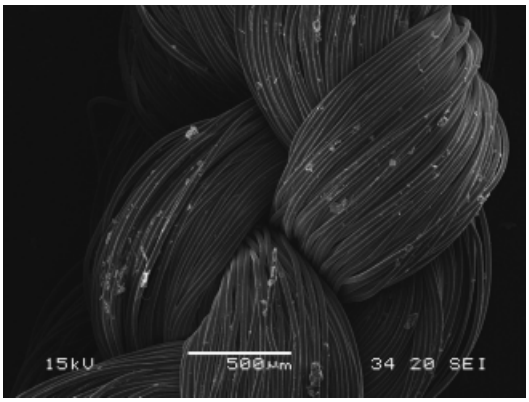

Figure 6 Electron microscope image of a netting twine of approximately 2 mm in diameter showing the many fine filaments. Photo: Jens Anton Horst, SINTEF.

Interactions of cod with the netting

Damage to the test net panels indicates that cod are capable of directly damaging netting material. Cod are equipped with groups of sharp teeth in both the mouth and the throat (Harder 1976; Morrison 1987; Kryvi & Totland 1997), which they use to catch and hold prey. Their teeth are bent backwards and hinged so that the prey can be pulled backwards towards the throat. In practice, this means that prey can be easily pulled into the mouth, while the direction of the teeth prevent it from escaping. Owing to the shape and properties of the teeth, it is probable that the cod bite at the netting rather than gnawing at it. Although we do not have direct, detailed visual evidence of this behaviour, we hypothesize that cod bite the net, catch a few twine filaments in their teeth and pull at them until they break. If a section of the netting is particularly attractive, repeated biting at the same piece of netting by different cod may create holes. Direct video of cod repeatedly biting netting is needed to confirm this process of hole formation.

A twine is built up of several hundred nylon filaments (Fig. 6), each with an initial breaking strength of approximately 50 g (calculated based on data given on www.polyamide-hp.com). Thus, larger cod could break one or more twines with a single bite. Smaller fish may also be able to tear filaments that have decreased strength due to existing wear and tear (including pre-existing damage from fish bite).

Wild Atlantic cod are physically adapted to bottom feeding; they have an overbite and a 'beard', which functions as a smell organ used to locate food. Within a sea cage, the net wall and bottom will thus be interesting structures, and it is likely that cod will search them for food. Biting of the net may be a behaviour related to cod checking if the net contains feed.

Cod are exploratory by nature and exhibit markedly different behaviour to the typical circular swimming and schooling behaviour exhibited by salmon in sea cages (e.g. Juell & Westerberg 1993). While salmon typically avoid the net cage boundary and remain approximately 1 m from the net cage wall (Fernö, Huse, Juell & Bjordal 1995), cod explore the netting, regularly make contact with the net cage and can locate and swim through small holes (Aas 2005). It is likely that this behaviour predisposes cod to escape at a greater rate than salmon.

Operational measures to prevent escape of cod

The results of the survey of fish farmers presented in this paper indicated that particular farm operation procedures reduce the likelihood of escapes. Based on these results, we propose the following set of farm operational measures to prevent escapes:

Use good quality net cages. Worn and damaged net cages may attract cod and result in increased occurrence of fish bite. Netting with low residual strength has less resistance against wear and tear.

Avoid small damages to nets from handling and abrasion. Small damages that do not represent an escape hazard for salmon can result in several cod escaping in a relatively short time.

Inspect the net cage frequently for holes. Most net cages will be damaged from time to time, and it is especially important to discover these damages as early as possible when culturing cod. The most

common way to inspect the net cage is using divers, and cod farmers have inspections up to once a week. Inspections at certain critical periods, such as after events that can lead to damages, for instance, after bad weather or handling of the net cage, and before stocking, are particularly important.

Make demands for good quality repairs. Repairs may attract cod, especially if the thread is of a different colour than the netting and if loose ends point out from the netting.

Keep the net cage clean. Biofouling may attract cod. Fish farmers indicated that cod eat feed that becomes caught in the biofouling organisms that grow on the net cage wall. Cod may tear at the netting with their teeth during this behaviour.

Make sure that the netting is taut. Slack netting may invoke biting by cod and should be avoided, particularly where the bottom and side panels are connected. Several fish farmers reported problems with fish gathering in this area and biting the slack netting. Taut netting can be achieved through correct and sufficient weighing of nets and impregnation of nets to increase stiffness.

Check that the mesh width is suitable for the fish size. As a minimum requirement for a suitable mesh size, one broken twine should not lead to a hole large enough to represent an escape hazard.

Make sure that the cod is fully fed at all times. Biting behaviour is most likely linked to the search for food and may thus decrease when the fish is full. Several fish farmers reported that cod were generally calmer when fully fed.

Sort the fish by size frequently. Several fish farmers reported that cod behaviour changed with variation in size between the individuals within a cage. When fish within cages are of equal size, most fish will manage to eat enough to be satisfied. In contrast, farmers reported that if smaller fish were present, they tended to be forced towards the upper part of the net near the cage boundary where access to feed was poorest. These insatiated smaller fish may have greater motivation to bite the net cage during periods of hunger.

Developing an 'escape-free' net cage

Based on the information received from the surveys and our present knowledge of the circumstances of cod escape, we believe that the solution for an escape-free net cage lies within the following three areas or their combination:

1. *Using stronger net cage constructions.* Cod seem to require a net cage that can resist wear and tear of all sorts. Different coatings can increase the resistance to abrasion and fish bite, but will most likely have a limited effect on the breaking strength of the netting. Unidirectional fibres will increase the tensile breaking strength, but will reduce the resistance against abrasion and maybe fish bite. A combination of these structural changes may increase the general strength of the netting. Thicker filaments and monofilaments may increase abrasion resistance, but twines would have to be thicker in order to provide the required breaking strength. Thicker twines are problematic as they will increase drag in currents, the total loading of the fish farm and the mooring system and decrease the flow of fresh water through the net cage. The general strength of the netting can also be increased by choosing filament materials that are stronger than the traditional nylon.
2. *Developing an uninteresting or 'repulsive' net cage wall.* This may be obtained by providing a stiff or taut net cage with a smooth surface. Cod have strong senses, and it may be possible to use taste, smell, sound, colour and shape to prevent biting at the net cage.
3. *Providing a stimulating cage environment*. A sea-cage environment that is modified to encourage the natural behaviour of cod may increase fish welfare, distract the fish from biting at the netting and thereby reduce escape. Present day sea cages are stimulant-poor and it is likely that small changes will significantly improve the culture environment for cod (Norwegian Research Council 2005). For many other species of cultured animals, creating a stimulating environment has involved satisfying the need for challenges and adventure and preventing boredom (Young 2003).

As a measure to reduce the large number of escapes in the short term, use of stronger net cage constructions is the obvious choice. Developing an uninteresting or repelling net cage wall and providing a stimulating net cage environment will require more knowledge on cod behaviour and further experimental testing.

Acknowledgments

This study forms part of the project 'Escape-free net cages for cultured cod' funded by Innovation Norway. We wish to thank Rune Gaarder and Kjell Olafsen from SINTEF Materials and Chemistry, and the Norwegian cod farmer's network 'Go for cod' represented by Jørgen Borthen for their assistance throughout the work.

References

Aas K. (2005) Houdini of the sea. *Outlook on Aquaculture* **2005**, 2.

Dempster T., Sanchez-Jerez P., Bayle-Sempere J.T., Giménez-Casalduero F. & Valle C. (2002) Attraction of wild fish to sea-cage fish farms in the south-western Mediterranean Sea: spatial and short-term temporal variability. *Marine Ecology Progress Series* **242**, 237–252.

Fernö A., Huse I., Juell J.-E. & Bjordal Å. (1995) Vertical distribution of Atlantic salmon (*Salmo salar* L.) in net pens: trade-off between surface light avoidance and feed attraction. *Aquaculture* **132**, 285–296.

Fiske P., Lund R.A. & Hansen L.P. (2006) Relationships between the frequency of farmed Atlantic salmon, *Salmo salar* L., in wild salmon populations and fish farming activity in Norway, 1989–2004. *ICES Journal of Marine Science* **63**, 1182–1189.

Gillanders B.M. & Joyce T.C. (2005) Distinguishing aquaculture and wild yellowtail kingfish via natural elemental signatures in otoliths. *Marine and Freshwater Research* **56**, 693–704.

Hansen T (2006). *Rømning av laks fra nøter med ulik maske.* Institute of Marine Research report. http://www.imr.no/_data/page/6719/romning_maskevidde_2006.pdf (in Norwegian).

Harder W. (1976) *Anatomy of Fishes*. Schweizerbart'sche Verlagsbuchhandlung, Stuttgart, 744pp.

Juell J-E. & Westerberg H. (1993) An ultrasonic telemetric system for auto-positioning of individual fish used to track salmon (*Salmo salar* L.) in a sea cage. *Aquaculture Engineering* **12**, 1–18.

Kryvi H. & Totland G.K. (1997) *Fiskeanatomi*. Norwegian Academic Press, Oslo, 332pp (in Norwegian).

Moe H., Gaarder R., Sunde L.M., Borthen J. & Olafsen K. (2005) *Escape-free nets for cod*. SINTEF Fisheries and Aquaculture Report SFH A 054041, Trondheim, Norway (in Norwegian).

Morrison C.M. (1987) Histology of the Atlantic Cod, *Gadus morhua*: an atlas. Part one. Digestive tract and associated organs. *Canadian Journal of Fisheries and Aquatic Science Special Publication* **98**, 219.

Naylor R., Hindar K., Fleming I.A., Goldburg R., Williams S., Volpe J., Whoriskey F., Eagle J., Kelso D. & Mangel M. (2005) Fugitive salmon: assessing the risks of escaped fish from net-pen aquaculture. *Bioscience* **55**, 427–437.

Norwegian Fisheries Directorate. (2005) *Statistics for Aquaculture 2005*. www.fiskeridir.no/fiskeridir/kystsone_og_havbruk/statistikk

Norwegian Fisheries Directorate. (2006a) *Escaping of salmonids from fish farms*. www.fisheries.no/aquaculture/environment/escape_of_fish/

Norwegian Fisheries Directorate. (2006b) *Visjon nullflukt*. http://www.fiskeridir.no/fiskeridir/kystsone_og_havbruk/kontrolloffensiv(in Norwegian).

Norwegian Research Council. (2005) *Research needs within animal welfare in Norway*. www.forskningsradet.no/publikasjoner(in Norwegian).

Sepulveda M. & Oliva D. (2005) Interactions between South American sea lions *Otaria flavescens* (Shaw) and salmon farms in southern Chile. *Aquaculture Research* **36**, 1062–1068.

Soto D., Jara F. & Moreno C. (2001) Escaped salmon in the inner seas, southern Chile: facing ecological and social conflicts. *Ecological Applications* **11**, 1750–1762.

Young R.J. (2003) *Environmental Enrichment for Captive Animals*. Blackwell Science, Oxford, UK, 228pp.

Paper 4

Moe H., Gaarder R. H., Olsen A. and Hopperstad O. S. (2008b). *Resistance of aquaculture net cage materials to biting by Atlantic Cod (*Gadus morhua*).* Aquacultural Engineering (in press).

Resistance of aquaculture net cage materials to biting by Atlantic Cod (*Gadus morhua*)

Heidi Moe [a,b]*, Rune Harald Gaarder [c], Anna Olsen [a] and Odd Sture Hopperstad [b]

[a] SINTEF Fisheries and Aquaculture, NO-7465 Trondheim
[b] Norwegian University of Science and Technology (NTNU), Department of Structural Engineering, NO-7491 Trondheim
[c] SINTEF Materials and Chemistry, P.O.Box 124 Blindern, NO-0314 Oslo
* Telephone: +47 4000 5350, Fax: + 47 932 70 701, E-mail: Heidi.Moe@Sintef.no

Abstract

Cod bite on aquaculture net cages has resulted in damages like frayed netting and holes, which in part can explain why cultured cod have escaped more frequently than salmon over the last years. We describe damages found on various netting materials subjected to cod bite through field experiments at commercial cod farms. Further, a method to test local cod bite resistance of traditional netting structures is suggested and initial results from a test jig prototype are given. Results from field experiments indicated that cod may have been attracted by types of netting that made it possible to draw filaments out of the twine, while stiff, coated netting structures and thick filaments showed no sign of bite damage during the test period. We concluded that netting materials for cod aquaculture must be resistant to cod bite or be repellent or uninteresting for cod. Based on the present findings, the better choice among the traditional netting materials seemed to be hard-laid netting materials, preferably with a primer that glues the filaments together.

Keywords: Atlantic cod (*Gadus morhua*), fish bite, aquaculture, net cages, nets, net pens, netting materials, material properties.

1 Introduction

Aquaculture of Atlantic Cod (*Gadus morhua*) is a new and growing industry in Norway. Sea-based cage technologies and farming systems for cod aquaculture have been largely inherited from Atlantic salmon (*Salmo salar*) production, but differences between cod and salmon have led to new and unexpected problems. Cod farmers have reported that cod interact with the cage netting through biting and thereby create wear and tear (Moe et al. 2007a). Filming of cod interaction with traditional netting at a commercial cod farm showed that fish of all sizes bit at the netting (Moe et al. 2008a). Cod bite resulted in damages like frayed netting and holes, which in part can explain why cod have escaped more frequently than salmon over the last years (Moe et al. 2007a).

Not much literature has been published on cod interaction with structural elements at fish farms or cod bite in general. Several farmed species (including salmonids and Atlantic cod) can bite at each other, resulting in fin damage (Hatlen et al., 2006). Fish bite, especially from sharks, is a known problem for mooring lines (Flory et al., 1982). ICES (2006) states that sea bream nibble the nets to feed on bio-fouling, which leads to damage and holes in the cages. The same report states that the experience of Scottish Executive Working Group on Escapes is that nibbling of nets does not appear to be an important factor with cod, particularly with use of double nets. However, in Norway double nets are not considered to be a good or even possible alternative for all farms. Double nets may have a negative impact on fish farming through reduced water quality, increased loads on the farm and heavier operations involving higher risks of damage and escapes (Moe et al., 2005).

Moe et al. (2008a) performed surveys of net cages used in cod aquaculture in order to map holes and damages. Damages with signs of cod bite were relatively common on cod net cages in Norway, but the number of holes varied significantly in time and between fish farms. It was estimated that diver inspections on average revealed one hole in each net cage per month, while during inspections of used cod nets at net workshops on average 30 damages were found. These damages often showed signs of cod bite. Areas with frayed netting due to cod bite were shown to have a reduction in strength greater than the accepted values given in NS9415 (Standards Norway, 2003). In addition the nominal length of the frayed netting twines was reduced, as well as their tensile stiffness and twine length at break.

Design rules for net cages given in NS9415 (Standards Norway, 2003) are based on empirical data. The rules give requirements for mesh strength of netting (ISO, 2002) and strain at break for the applied filaments. Until recent years, little more of the mechanical properties of aquaculture netting materials have been general knowledge (Moe et al., 2007b). The mechanical properties of the netting will change during use (Klust, 1982; Sala et al., 2004; Moe et al., 2008b), but there are no specific requirements for documentation of effects of external loading like abrasion and cod bite. Standard methods for testing of abrasion resistance of textiles exist and may be applied with some modifications (e.g. ASTM, 2001; ISO, 1998). However, cod bite damage to netting materials has neither been documented nor described before (Moe et al., 2007a), and consequently methods for testing of cod bite resistance do not exist.

In this paper we describe damages found on various netting materials subjected to cod bite through field experiments at commercial fish farms. Further, a method to test local cod bite resistance of traditional netting structures is suggested and initial results from a test jig prototype are given. Finally conclusions are given based on a discussion of the combined results.

2 Materials and methods

2.1 Physical properties of cod bite

Before developing a method to test cod bite resistance of aquaculture netting, the properties of cod bite had to be known; e.g. the nature of cod bite, bite load and the shape of cod teeth. In the following we present results from a preliminary study of the cod bite attack and cod teeth.

The nature of the cod bite attack on traditional netting materials was described based on studies of cod interaction with traditional knotless netting and resulting fracture damage on netting fibres. In this context, traditional netting meant materials with hundreds of available filaments (multifilaments) in the twine; typically Raschel knitted knotless netting and knotted netting with twines of twisted multifilaments (Figure 1). The cod bite attack was described as follows: The cod bit into the netting and filaments were caught behind the teeth (Figure 2b). The cod made powerful movements with head and body, and the filaments were subjected to shear and tensile forces. In this process filaments were pulled out of the netting

and eventually some of them would slip out of the mouth unbroken, while others would break. After several bite attacks in one area, the netting was visibly frayed and in time holes could be created. Studies of fractured filaments due to natural and simulated cod bite, revealed fractures with signs of tension and shear overloading and very little abrasion damage on the fibres (Figure 2d). The fact that cod teeth are sharp (Figure 2a-c) with a hard and smooth surface supports this.

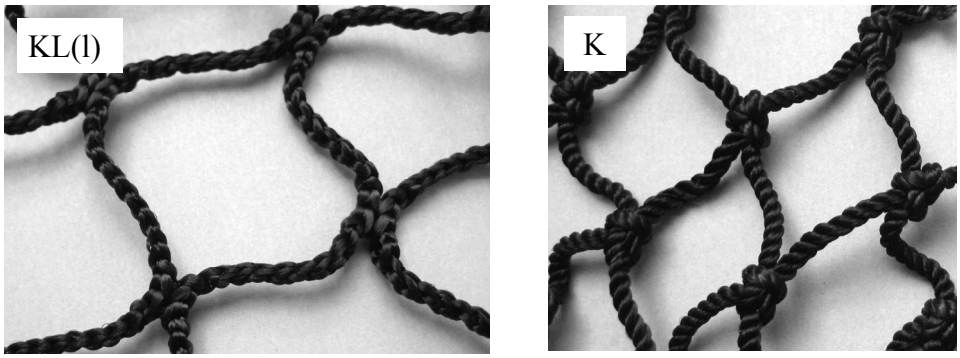

Figure 1: Examples of traditional types of netting. KL(l): Loosely laid knotless netting. K: Knotted netting.

Studies of twelve cultured cod of 1.5 to 4.5 kg showed that the upper jaw had several tight rows of small teeth, while the bottom jaw had one row of larger teeth (Figure 2a and b). On average, the teeth in the bottom jaw were 1.8 mm long with an average separation distance of 3 mm. The teeth were approximately 1 mm thick at the base and 10 μm at the tip, which is 1/3 of the diameter of a typical nylon filament used in aquaculture netting (Figure 2). In the upper jaw, the teeth were on average 0.8 mm long with a separation distance of 1 mm between teeth. The thickness was not measured, but it was smaller than for the lower jaw teeth. Simple manual tests pulling pieces of netting over jaws from cultured cod showed that the teeth were easily caught in the netting (Figure 2b). Using relatively little energy, filaments were pulled out of the twine and broken. As data on the biting and pulling forces of cod were unavailable, we assumed that cod pulled with a force corresponding to its weight in air, as occurs in other fish species (Steinberg, 1963).

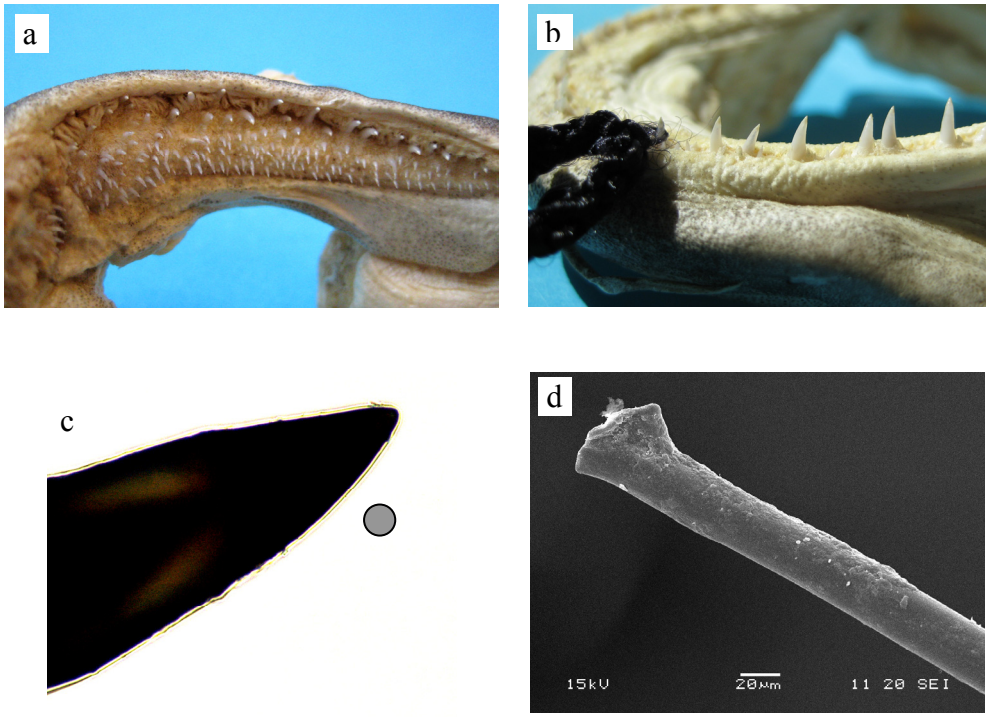

Figure 2: a) Upper cod jaw with several rows of small, sharp teeth. b) Bottom cod jaw with one row of larger, sharp teeth. Cod teeth are easily caught in uncoated, traditional netting. c) Photo of cod tooth from bottom jaw magnified through a microscope. Cross-section of one filament is indicated (approximately 30µm in diameter). d) Example of filament fracture due to cod bite. The fractures showed signs of over-loading in tension and shear and little or no signs of abrasion damage.

2.2 Field experiments of cod interaction with various types of netting

Panels with netting were subjected to cod bite at commercial cod farms in two different experiments. Experiment 06 was performed summer/fall 2006 and Experiment 07 was performed summer/fall 2007. The practical test set-up was similar for the two experiments, but types of applied netting materials and number of cages involved was different.

In both experiments the test panels consisted of pieces of netting material attached to a circular steel ring with a diameter of 0.7 – 1 m. The edges of the netting were connected to the metal ring at points along the circumference, between these points the netting edges were free (Figure 3). The rings were attached to a rope and lowered to about 3 meters below the water surface. Each netting panel was given an initial damage of one cut twine.

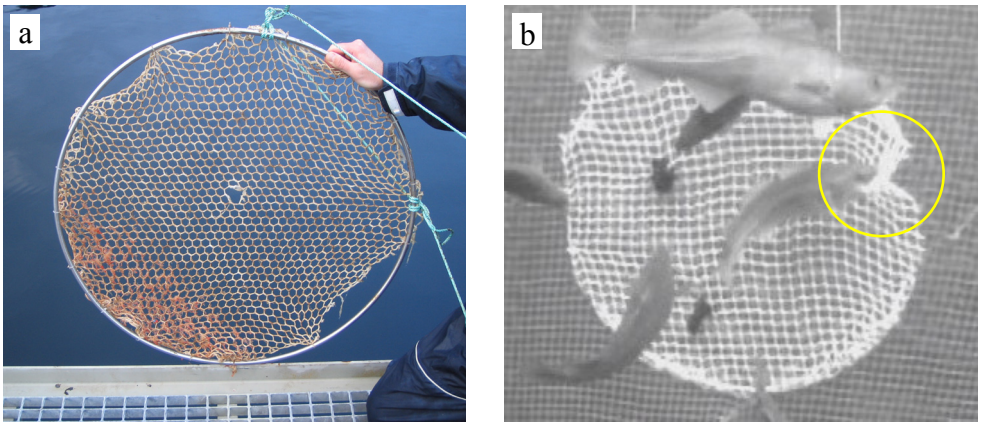

Figure 3: Test panel. a) Netting panel after approximately 3 months in a commercial cod farm. b) Picture from filming of cod bite at a commercial cod farm.

Various types of netting structures with various specifications, listed in Table 1 and Table 2, were tested in the field experiments. This included Raschel knitted knotless netting materials. The traditional version consisted of Nylon (PA6) multifilaments (KL, Figure 1) with square mesh and 'super-knot' to prevent laddering. Other variations of knotless netting were also tested, including a hard-laid hexagonial mesh netting (KL6), and loosely laid netting with 70 % UHMWPE ("Ultra-High-Molecular-Weight-Polyethylene", known as 'Dyneema') and 30 % Polyester (PES) multifilaments (KL_{UPE}). Both KL6 and KL_{UPE} had a knitting pattern without 'super-knot'. The knotted netting materials (K, Figure 1) consisted of twines with twisted bundles of Nylon multifilaments, knotted to form a square mesh. The fibre thickness was approximately 0.03 mm for all applied multifilaments. Knotted netting with twines consisting of braided

Polyethylene (PE) monofilaments (K_{PE}) was also tested. Each twine consisted of 40 filaments with a thickness of approximately 0.2 mm. The PVC-netting consisted of bundles of unidirectional Polyester multifilaments arranged in a mesh and dipped in PVC.

Table 1: Tested types of netting structures and filaments.

KL	Knotless netting with square mesh and PA6 multifilaments
KL6	Knotless netting with hexagonal mesh and PA6 multifilaments
KL_{UPE}	Knotless netting with UHMWPE and PES multifilaments
K	Knotted netting with PA6 multifilaments
K_{PE}	Knotted netting with PE monofilaments
PVC	Netting of PES fibre reinforced PVC

Table 2: Netting specifications (colour, surface treatment, hardness and thickness).

b	Black colour
w	White colour
p	Covered in a cured copolymer primer
af	Treated with water soluble anti-fouling paint
wax	Covered in wax
h	Hard-laid netting
l	Loosely laid netting
t	Netting with thick twines

In Experiment 06, four different types of traditional Nylon multifilament netting materials without surface treatment were tested. The goal was to see whether cod bite damage would vary between knotted and knotless netting, and netting with black and white colour. The tested netting materials were black and white, knotless netting (KL(b) and KL(w), Table 1 and Table 2),

black, knotted netting (K(b)) and white knotless netting with hexagonal mesh (KL6(w)). KL6(w) was hard laid, while the firmness of the knitting was not known for KL(b) and KL(w).

In Experiment 07 we studied various netting concepts that were used in or intended for cod aquaculture, involving various structures, polymer materials and surface treatment. A hard-laid, white knotless netting material, KL(h) was included in all cages as control panel for comparing results between farms. Experiment 07 included hard-laid netting with hexagonal mesh treated with either a cured copolymer primer (KL6(p)), a water soluble anti-fouling paint (KL6(af)) or both (KL6(p+af)). Knotted Polyethylene (K_{PE}), PVC and knotless Dyneema netting (KL_{UPE}), including a few samples covered in wax (KL_{UPE}(wax)) were also tested.

The tests were performed and supervised by the fish farmers at the various farms. Experiment 06 was performed in 2 cages at 4 fish farms (Cage A and Cage B) and in 1 cage at 1 farm (Cage A). 3 netting panels were tested in each cage. In Experiment 07, 6 panels were tested in one cage at each farm, and 4 fish farms returned test results. Fish size varied between 0.2 – 2.7 kg, the density (fish per undeformed cage volume unit) was low to moderate and varied between 2-14 kg/m^3.

All panels were removed from the cages after approximately 3 months. The initially undamaged netting, edges and pre-cut hole were investigated for cod bite damage. The degree of damage was visually assessed and classified using a scale from 1 to 3. The value 1 was given for no visible or unimportant cod bite damage. Cod bite damage appearing to have a considerable impact on the properties of the netting material was given a value of 2. A value of 3 was given for major damages like new holes or areas with an apparently seriously reduced breaking strength. Examples of damages are shown in Figure 4. The damage values were given based on subjective assessments, as it was not possible to make a more quantitative assessment for instance by mesh strength tests.

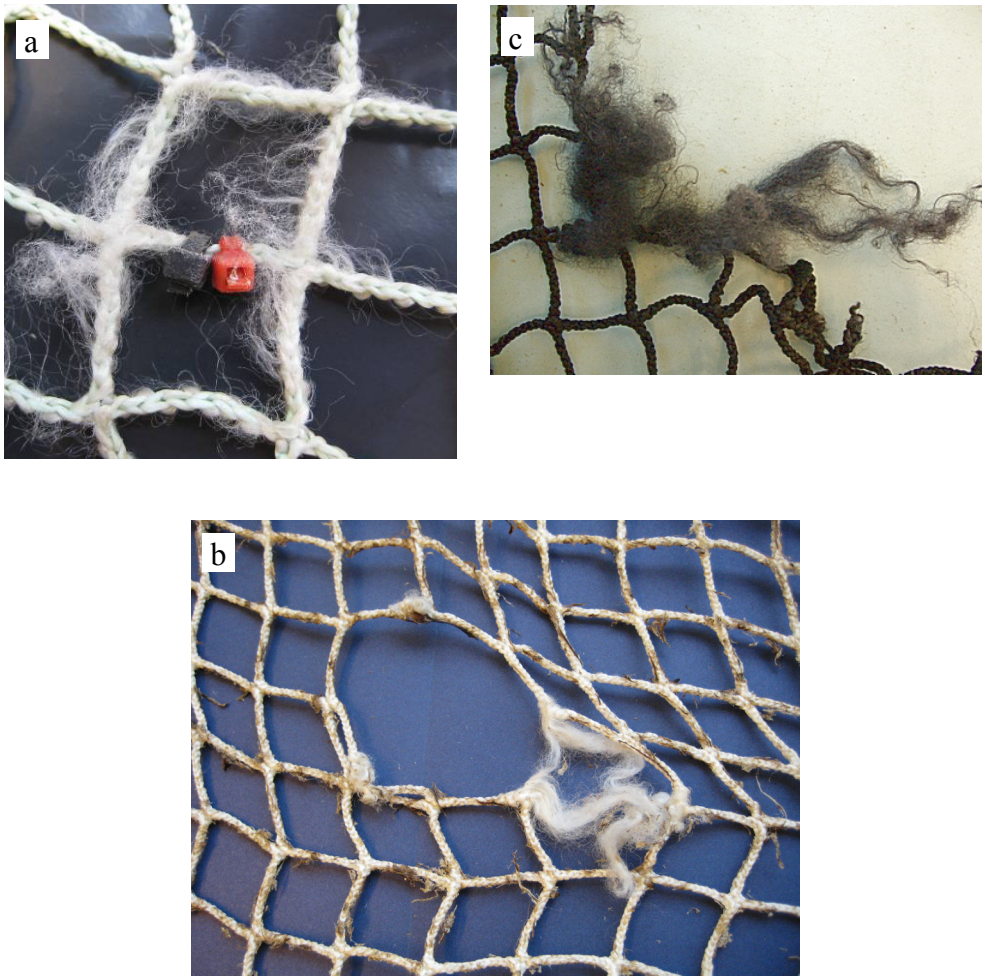

Figure 4: Damages to test panels due to cod bite. a) Frayed netting (considerable damage). b) Hole with frayed netting (major damage). c) Considerable damage on edge of black, knotless netting.

2.3 Laboratory testing of cod bite resistance of various netting materials

2.3.1 Bite-jig

Based on the previous findings, a test method for cod bite resistance of traditional multifilament netting materials was proposed and a corresponding test jig was built based on a hydraulic tensile test machine usually applied for fatigue testing. The bite-jig was applied to quantify relative local cod bite resistance.

A bite mechanism was mounted in the test machine through a load cell (Figure 5a). The bite mechanism consisted of a part fixed to the load cell and a moveable part including the teeth blade. A single bolt was used to connect the two parts, allowing for almost friction-free rotation of the moveable part. An O-ring was used to control the contact pressure between teeth blade and test specimen. The test specimen of netting material was clamped with no pretension in the aluminium test frame with an inner width of 150 mm (Figure 5b), which was mounted in a vessel filled with fresh water beneath the bite-mechanism. The water vessel was fixed to the test machine, and was not allowed to move horizontally. Both test specimen and water had a temperature of 20 °C (BISFA, 2004; ISO, 1973 and ISO, 2002). The relative air humidity was not relevant as the test specimen was submerged in water (ISO, 1997).

The test was performed by repeatedly rising and lowering the vessel containing the test frame. The movement followed a sinusoidal displacement-time curve with maximum possible amplitude of approximately 50 mm (limited by the apparatus) and a frequency of 0.2 Hz. This set-up yielded the relative local cod bite resistance of a point on the test specimen twine. Due to the fixed edges, global structural effects like laddering were limited in these tests.

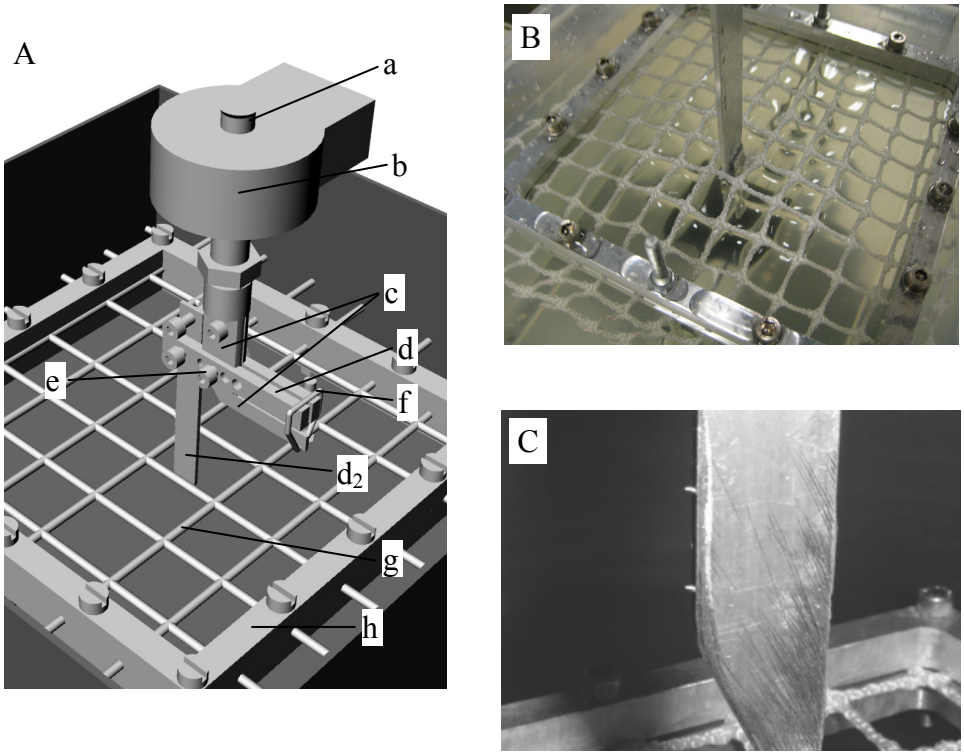

Figure 5: A) Illustration of bite-jig with test specimen: a) connection to test machine, b) load cell, c) fixed part of bite mechanism, d) moveable part of bite mechanism (including teeth blade, d_2), e) bolt connecting fixed and moveable part of bite mechanism, f) O-ring, g) netting material (test specimen), h) test frame. B) Testing of local cod bite resistance of netting in bite-jig. The netting was clamped in an aluminium frame. When a tooth on the teeth blade made contact with the netting, the twine was subjected to a simulated bite-load. C) Detail of teeth blade showing the two teeth.

The teeth blade had two teeth-models of 0.9 and 1.1 mm length, applied with an angle of inclination of 10 degrees (Figure 5c). The chosen material was ordinary sewing needles made of hardened steel. Initially the steel teeth were almost as sharp as the measured cod teeth (Figure 2c). When a tooth on the teeth blade made contact with the netting during the vertical movement, the twine was subjected to a bite load (Figure 5b). This

happened both during up- and downward movement of the vessel, and either one or both teeth made contact.

Horizontal position of the teeth blade and dimensions of the O-ring were chosen to ensure correct contact force between teeth blade and netting. The contact force was the same at the beginning of all tests, adjusted by requiring a defined angle between fixed and free part of bite mechanism prior to attaching the O-ring (contact force was never measured). It was required that the maximum bite load should be less than 30 N (for some tests the bite load was occasionally slightly larger without having any considerable effect on the results). If filaments caught in the teeth did not break within this load level, the teeth blade would rotate and release the netting (corresponding to the cod releasing the netting from its grip). Even though the teeth segment was made out of hardened steel, it was blunted during the tests through abrasion, probably by a type of hardened polymer primer.

2.3.2 Netting materials

Different netting materials were tested for local cod bite resistance in the bite jig. Only untreated netting materials with a traditional, multifilament structure gave good and valid results from the tests, as the bite jig was built to simulate damage to such materials. Three different versions of KL (Table 1) were included to study the possible effect of variations in knitting firmness and twine thickness. Hard-laid (KL(h), Table 2) and loosely laid (KL(l)) netting materials with a mesh strength of 95 kg, and a medium hard laid netting material with a relatively thick twine (mesh strength of 170 kg, KL(t)) were tested. In addition, K and KL_{UPE} with mesh strength of 71 kg and 118 kg, respectively, were subjected to the bite jig.

All previously mentioned netting materials had 5-7 valid test repetitions, except KL_{UPE}. Due to abrasion of the teeth segment, there were only two valid test repetitions of KL_{UPE}. Material KL6(af), KL6(p), KL6(p+af), K_{PE} and KL_{UPE}(wax) were also tested in the bite-jig, but due to the mentioned tooth abrasion, only K_{PE} gave valid results for several specimens. For these materials, the results from the bite-jig may not be a valid assessment of cod bite resistance due to the untraditional structure that may affect the cod bite and behaviour.

3 Results and discussions

3.1 Field experiments

Experiment 06 resulted in 27 panels that had been subjected to cultured cod, and possibly cod bite, at 5 different commercial fish farms. An overview of the tested netting materials and their damage classification of edges, initially undamaged netting and pre-cut hole are given in Table 3. All panels had signs of cod bite damage like frayed netting and holes (Figure 4). 12 out of 27 panels had unimportant damages only, while 8 had major damages. In 4 panels biting had led to increased size of the pre-cut hole. The overall impression was that netting panels from fish farmer #3 and #4 had very little cod bite damage, while netting from farmer #1 and #5 had several and in part major damages.

Table 3: Assessment of damages on net panels from Experiment 06 with traditional netting materials (edges / netting / hole). The extent of damage is described using a scale from 1 to 3: 1 - unimportant, 2 - considerable, 3 – major damage.

Fish farmer	Cage A				Cage B			
	K(b)	KL(b)	KL(w)	KL6(w)	K(b)	KL(b)	KL(w)	KL6(w)
#1	2/1/1 2/1/1*			3/1/3	1/1/1 2/1/3*			2/1/3
#2	1/1/1	2/1/1	1/1/1		2/1/1	2/1/1	2/1/1	
#3	1/1/1	1/1/1	1/1/1					
#4	1/1/1	1/1/1	1/1/1		1/1/1	1/1/1	1/1/1	
#5	3/2/1	3/2/1	2/2/1		3/2/3	3/2/1	3/2/2	

*Two equal panels were tested.

All bite damages found on initially undamaged netting of test panels from fish farmer #5 were found near identification marks (most panels had plastic marks for identification, Figure 4a). The netting from fish farmer #1 was not marked and had no considerable damage of initially undamaged netting. Panels of all types of traditional netting experienced unimportant,

considerable and major damages from cod bite. Cod bit at both black and white netting and netting with and without knots, resulting in damages on the netting. For example knotless netting with hexagonal mesh was laddered and knots in knotless netting were bit open. It was not possible to express any variation in cod bite resistance between various materials based on the evaluation of this experiment (Table 3).

Major damages to the hole (pre-cut twine) was observed by fish farmer #1 after only two weeks, indicating that also net cages can experience major cod bite damage during a few weeks of operation.

Experiment 07 resulted in 24 panels that had been subjected to cultured cod, and possibly cod bite. The bite damages on different areas of the netting material were assessed for each of the panels and given a value from 1 to 3 as shown in Table 4. All netting materials, except all repetitions of K_{PE} and PVC, and KL6(af) for fish farmer #1, had plastic markings for identification.

Table 4: Assessment of damages on net panels from Experiment 07 of various netting concepts (edges / netting / hole). The extent of damage is described using a scale from 1 to 3: 1 - unimportant, 2 - considerable, 3 – major damage.

Fish farmer	KL(h)	KL6(af)	KL6(p)	KL6(p+af)	K_{PE}	PVC	KL_{UPE}	KL_{UPE}(wax)
#1	2/1/1	2/1/3	1/1/1			1/1/1	3/2/1	3/2/1
#2	3/3/3	2/1/3	1/1/1	1/1/1	1/1/1		3/3/1	
#4	1/1/1	1/1/3	1/1/1	1/1/1		1/1/1	2/2/1	
#5	1/1/1	1/1/1	1/1/1	1/1/1	1/1/1	1/1/1		

Netting with primer (KL6(p) and KL6(p+af)), netting of PE (K_{PE}) and netting with PVC coating (PVC) showed no or unimportant signs of cod bite damage in the field experiments. However, only two repetitions of panels with K_{PE} were not a good enough base for firm conclusions. For material KL6(p+af) the anti-fouling treatment was missing at the edges and near the marking, however no considerable damages to the netting material were

found. It seemed like the cod had nibbled at the panel without causing damage to the netting material. The PVC-coating had cracked in one of the panels of PVC, revealing the PES filaments. No signs of bite damage were observed on the PES filaments or PVC coating in either of the panels of PVC.

The panels with traditional netting (KL) from fish farmer #1 and #2 had extensive and major damages from cod bite. On the latter, a hole was created on initially undamaged netting, the edges had major damages and the pre-cut hole had increased in size (Figure 4b). The very hard-laid netting with anti-fouling treatment (KL6(af)) showed no signs of damage on initially undamaged netting. The edges were frayed in two of the panels, while the pre-cut hole had increased in size at 3 of 4 fish farms. All panels of loosely laid netting with UHMWPE-fibres (KL_{UPE} and KL_{UPE}(wax)) had extensive and major damages from cod bite. 3 of 4 panels (including the one of KL_{UPE}(wax)) had considerable damage at the mark (Figure 4a) and major damages of the edges. Two of the panels with KL_{UPE} had considerable fraying of initially undamaged or unmarked areas of netting. In one of the panels the netting was laddered.

Cod bite damage varied greatly between cages (Table 3 and Table 4). Average cod bite damage was calculated for each cage based on the damage assessment of traditional netting with and without anti-fouling treatment. The average damage of a single panel was found by adding the three damage values for edges, netting and hole and dividing the result by 3. The average cod bite damage data was compared to fish size and density within the cages. However, cod bite might also be dependent on other factors such as feeding regimes, variation in fish size, environmental conditions (temperature, current and oxygen), genetics and stiffness of the net cage (Moe & Olsen, 2006).

There was no obvious correlation between fish bite damage and fish density in these experiments. A possible correlation was found between average fish bite damage and weight of fish at launch of panels. In Figure 6 the resulting average damage for traditional netting in Experiments 06 and 07 is given as points, while the dotted line suggests a possible trend in the results.

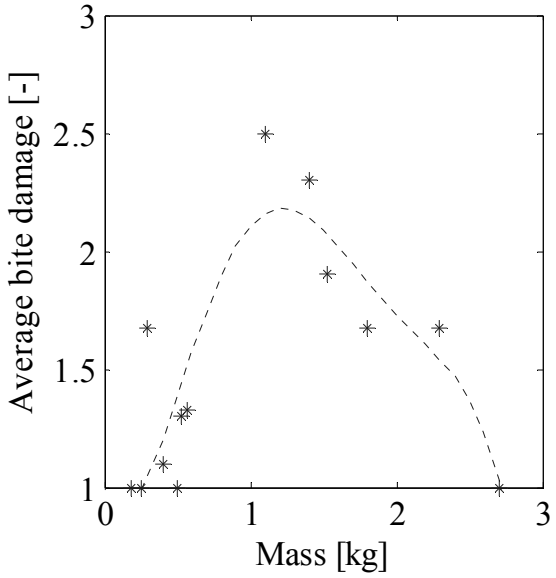

Figure 6: Average bite damage on panels with traditional netting as a function of average cod weight at launch of panels.

Small fish less than 500 g created unimportant damage of the netting (Figure 6), with one exception: in one cage, cod of 300 g at launch of panels created a considerable average damage of 1.7. These cod were on average 1 kg when the panels were retrieved. Figure 6 indicates that cod of approximately 1 kg caused the greatest damage to netting panels, which coincides with the practical experience of cod farmers (Moe et al. 2008a). Video recordings of cultured cod indicated that small fish of approximately 100 g attacked the netting more frequently than fish of 1 kg, which again seemed more willing to bite than 3.5 kg cod. Both field experiments, filming and practical experience indicated that at 1 kg, the cod was both relatively aggressive and strong and subjected the netting to most damage, while relatively large cod subjected the netting to little bite damage, probably due to a reduced number of attacks (Moe et al., 2008a).

The field experiments indicated that fish of only a few hundred grams can damage the netting. The breaking force of a single filament is approximately 0.5 N (50g) (Rhodia Polyamide, 2005). Assuming that cod can exercise a force corresponding to its own weight in air (as found for perch and roach

by Steinberg, 1963), it is probable that small cod can also damage the netting, but the damage per bite would be relatively small.

Several factors may have affected the results from the cod bite field experiments. Bio-fouling levels on the panels varied, and may have affected the wear and tear of cod bite on the netting. The cod seem to be attracted by the edges of the panel, and such edges will normally not be found in net cages. Studying films of cultured cod near a cage wall with and without the presence of a netting panel, clearly shows that the cod was attracted by the panels and that the panels provoked cod bite. During filming with and without the presence of a net panel, no cod bites were observed on the net cage wall, while approximately 100 bites were documented on the panel during 4 hours of filming. In addition, the cod may have found some test panels more attractive than others, influencing the resulting difference in bite damage between the panels.

Fish farmers claim that cod behaviour is strongly dependent on water temperatures, and that the cod is much calmer at high water temperatures (Moe et al., 2008a). The water temperatures varied in time and between farms, which may have affected the fish behaviour and cod bite damage. Other factors that vary between the fish farms and in time (feeding regimes, environmental conditions, genetics etc.) may also have affected the results in an unknown manner.

3.2 Testing in bite-jig

The results from the bite-jig test were used to assess the relative local resistance towards cod bite for different materials. The bite-jig did not predict the lifetime of a netting material, but gave relative values of cod bite resistance for comparison between various types of netting. Interesting findings were time to break, number of simulated bites to break, work to break and the development of bite load during time. The latter indicated the development of damage as time progressed; the larger bite load the more damage was done to the netting.

A summary of the results from the bite-jig tests are given in Figure 7 as time, number of simulated bites and work to break for netting with traditional structure. The three plots in Figure 7 have the same trends; the relative difference in time, bites and work to break are on the whole similar

between the various materials. Netting specimens that lasted for a relatively long time in the bite-jig also endured a relatively high number of simulated bites and work, and vice versa. The plots all show that loosely laid and medium hard laid netting with thick twines were the netting materials with lowest resistance against simulated cod bite. Increasing the mesh strength did not increase the local cod bite resistance. This can be explained by the fact that the knitting pattern was the same, making the filaments more available for cod bite damage in the relatively thick twine. Hard-laid netting lasted approximately twice as long as loosely laid netting in the bite-jig, and experienced on average 40% more work before break. The filaments in hard-laid netting and especially knotted netting were probably less available, increasing the bite life-time. Knotted netting and netting with UHMWPE- and PES-fibres (KL_{UPE}) endured 2.5 and 4 times more simulated local cod bite than ordinary loosely laid knotless netting respectively. The latter is due to the high strength of the applied UHMWPE-fibres, which typically have 3 times the tensile strength of the commonly used nylon quality (DMS Dyneema, 2009).

Tests of netting with thick PE-filaments (K_{PE}) yielded 6 valid test repetitions. The time to break was at the same level as for KL(t) given in Figure 7, but K_{PE} only endured half of the work to break compared to KL(t).

Figure 8 gives examples of the average bite-load versus time for single test repetitions of knotted netting, K, and loosely laid knotless netting, KL(l). Negative bite force occurred when the netting twine was pushed down by the teeth and the teeth functioned like a barb on a fish hook, while positive forces occurred when the test frame moved downwards (Figure 5b and c). The knotted netting was hard-laid with a twine constructed of three bundles of twisted multifilaments (Figure 1). The hard twist probably made it hard for the tooth to capture filaments, and tests of hard-laid knotted netting initially yielded relatively low forces (Figure 8). In time, the teeth got hold of more filaments, increasing the "bite load" until the twine finally broke. In knotless netting the bundles consisted of unidirectional multifilaments, making the filaments more available to cod teeth. During tests of loosely laid knotless netting the initial bite-load was larger, and the increase in load started sooner and at a higher rate than for knotted netting. This indicated that the loosely laid netting underwent more damage per simulated bite than knotted netting, which is confirmed by the considerably shorter time to break.

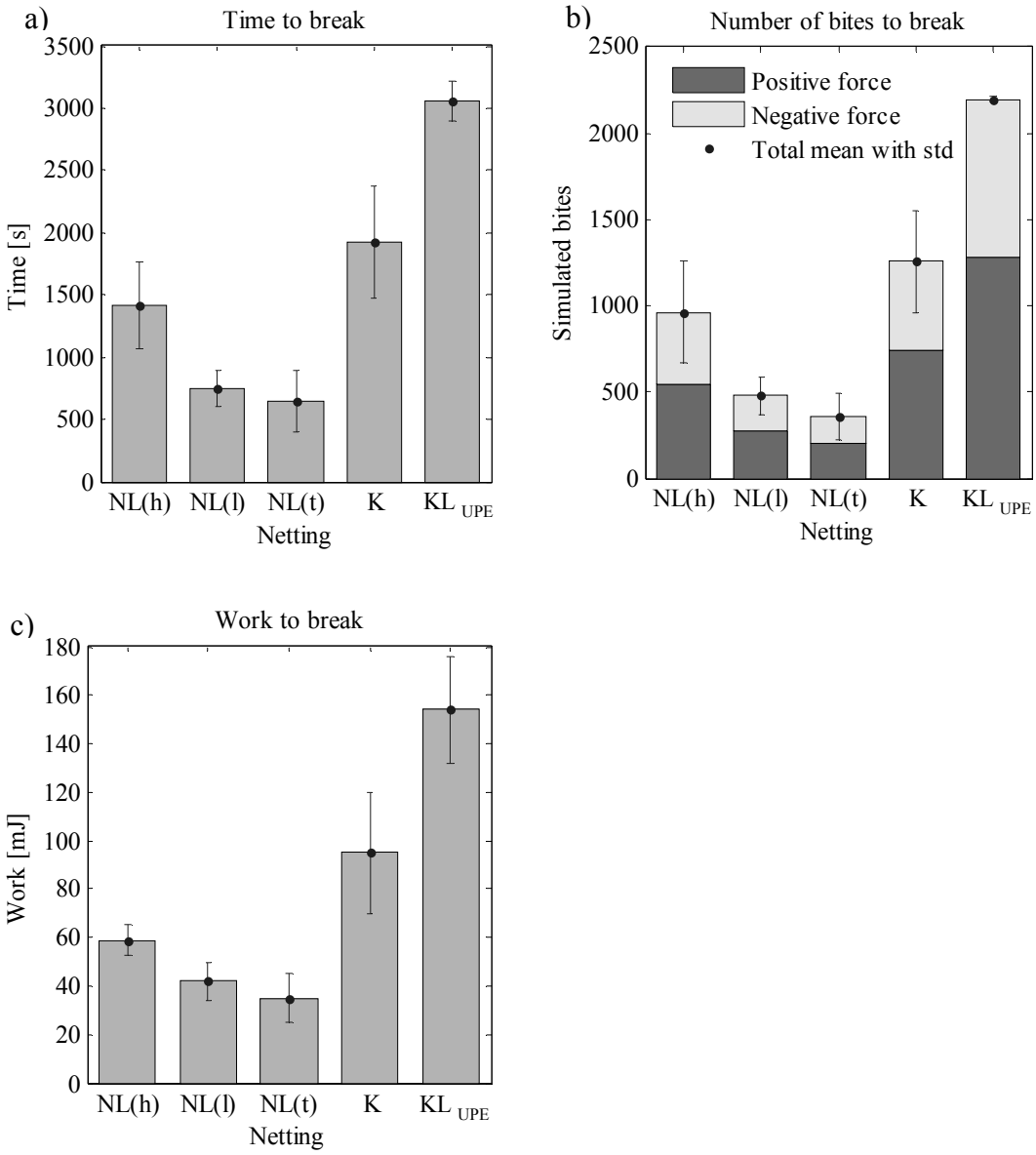

Figure 7: a) Time to break, b) number of simulated bites to break, and c) work to break for various netting materials tested in the bite-jig (mean values with standard deviation). KL is traditional knotless Nylon netting, where h stands for hard-laid, l loosely laid and t stands for netting with thick twines. K is knotted netting and KL_{UPE} is netting with UHMWPE- and PES-fibres.

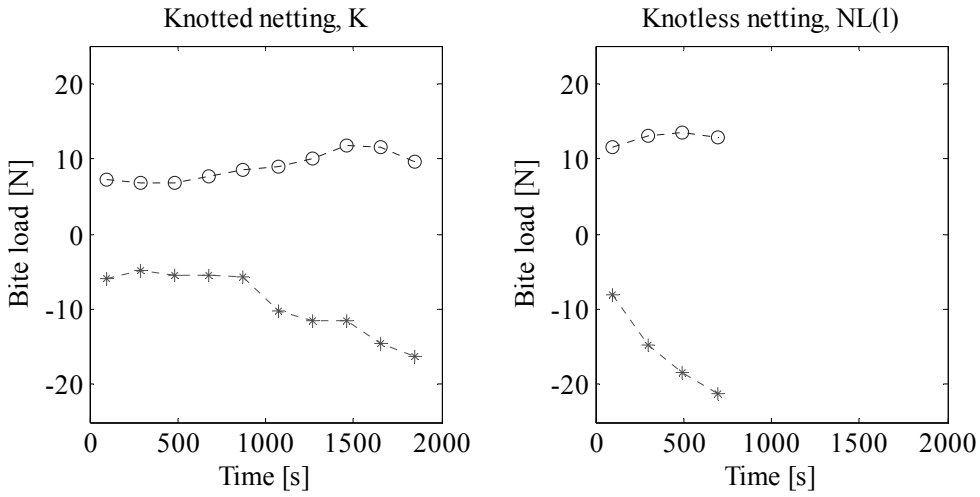

Figure 8: Mean bite load versus time for single test repetitions of knotted netting, K, and loosely laid knotless netting, KL(l). Negative bite force occurred when the netting twine was pushed down by the teeth and the teeth functioned like a barb on a fish hook, while positive forces occurred when the test frame moved downwards.

For netting with UHMWPE-fibres (KL_{UPE}), the bite loads were rather constant the first 2500 seconds (-10 N and 7 N), increasing slightly towards the end. This indicated a close to constant damage in time, which corresponds to the hypothesis that loosely laid netting will make the filaments available ensuring a relatively large interaction between teeth and filament.

The standard deviation in Figure 7 shows that the variation in time and absorbed energy or work until break had large variations between test repetitions. This was probably mainly due to coincidences that determined how many filaments the teeth caught in each bite. If the teeth caught a few filaments at a time, many of these probably broke before the teeth tilted back and released the filaments. In opposite, if many filaments were caught, the netting would follow the relative movement of the tooth until the teeth segment tilted and released the filaments, resulting in few torn filaments. The latter scenario would require performance of relatively much work before break of twine.

4 Conclusions

We conclude that netting materials for cod aquaculture must be resistant to cod bite or be repellent or uninteresting for the cod. The field experiments indicated that cod preferred to bite at materials that were easy to grip over stiff, coated structures and thick filaments. Based on the results, the best choice among the traditional netting materials seems to be hard-laid netting materials, preferably with a primer that glues the filaments together. New netting concepts show promising results, but findings and a general assessment indicate that full-scale testing may reveal challenges in traditional operation (Moe et al., 2008a). Operational aspects and general strength properties are important for many reasons, for instance to prevent escapes and ensure good water quality in the net, and must also be considered when choosing a net for cod aquaculture.

The results from field experiments indicated that cod may have been attracted by structures that made it possible to draw filaments out of the twine. This was observed for the very loosely laid netting with UHMWPE-fibres (KL_{UPE}). On the other hand, primer seemed to glue the filaments together. Although it did not seem to increase the shear and tensile strength of the material, it may have been less interesting for the cod to bite at the netting, or it may actually have been difficult for the cod to get hold of fibres and pull them out of the netting. The PE-netting (K_{PE}) did not obtain any bite damage visible to the eye during field experiments, but valid test results from the bite-jig showed that the local bite resistance was no better than loosely laid knotless netting. However, the resulting damage was abrasion, which has not been observed on materials with actual cod bite damage. In other words, it is not known if the cod will gnaw through solid twines and thick filaments. A hypothesis can be formed that the cod prefer to bite at netting with available, thin filaments.

The bite-jig was designed to simulate damage from cod bite at netting with many thin and available filaments (multifilaments). Loosely laid and medium hard laid netting with thick twines experienced a relative low resistance against simulated cod bite. Increasing the mesh strength did not increase the local cod bite resistance. Hard-laid netting lasted approximately twice as long as loosely laid netting in the bite-jig, and experienced on average 40% more work before break. Knotted netting and netting with UHMWPE- and PES-fibres (KL_{UPE}) endured 2.5 and 4 times more simulated local cod bite than ordinary loosely laid knotless netting respectively.

Other materials have also been tested in the bite-jig (KL6(af), KL6(p), KL6(p+af) and K_{PE}). The results from these tests indicated that cod would be able to damage all these materials if they were attacked in the same way as traditional netting. The question is whether the cod will bite on netting without available, thin filaments. Today's knowledge is not enough to answer this, however the performed field experiments indicate that netting with primer, PE-filaments and PVC coating experience less bite damage than traditional netting materials. This indicates that the cod behaviour will vary towards different types of netting.

In order to achieve more knowledge of cod bite damage and the resistance of various netting materials to cod bite, field experiments with netting panels and bite-jig tests have been performed. However, tests in controlled environments (laboratories) and full scale tests of cages with different netting materials are needed for the complete picture, since both the presented test methods involve several unknown factors and assumptions, and are affected by unrealistic boundary conditions. Surveys of traditional net cages (Moe et al., 2008a) confirm the findings from both field experiments and bite-jig test that traditional multifilament netting materials have a relative low resistance toward cod bite.

5 Acknowledgements

This work was sponsored by Innovation Norway, Hordaland County Council District and Sogn of Fjordane County Council District through the CodNet-project (Torskenot, In Norwegian) and the Norwegian Research Council through the IntelliSTRUCT programme (Intelligent Structures in Fisheries and Aquaculture) at SINTEF Fisheries and Aquaculture. We would like to thank Tim Dempster, Ulf Winther and Leif Magne Sunde at SINTEF Fisheries and Aquaculture for their help and good advice during this work.

6 References

ASTM, 2001. Standard D4158 " Standard Guide for Abrasion Resistance of Textile Fabrics (Uniform Abrasion)". ASTM International, West Conshohocken, PA.

BISFA (The International Bureau for the Standardisation of Man-Made Fibres), 2004b. Testing methods for polyamide filament yarns.

DSM Dyneema BV. Dyneema properties & application brochure. Edition 02/04.

Flory J. F., McKenna H. A., Parsey M. R., 1982. Fiber ropes for ocean engineering in the 21st century. Civil Engineering in the Oceans Conference, American Society of Civil Engineering.

Hatlen B., Grisdale-Helland B., Hjelland S. J., 2006. Growth variation and fin damage in Atlantic cod (*Gadus morhua* L.) fed at graded levels of feed restriction. *Aquaculture* 261, 1212-1221.

ICES Mariculture Committee, 2006. Report of the Working Group on Environmental Interactions of Mariculture (WGEIM).

Klust, Gerhard, 1982. Netting materials for fishing gear. Fishing News Books Ltd., England.

Moe H., Gaarder R., Sunde L.M., Borthen J., Olafsen K. (2005) Escape-free nets for cod. SINTEF report no SFH-A054041 (In Norwegian).

Moe H., Olsen A., 2006. *Codnet –status report 1*. SINTEF report no SFH80-A064067 (In Norwegian).

Moe H., Dempster T., Sunde L. M., Winther U. & Fredheim A., 2007a. Technological solutions and operational measures to prevent escapes of Atlantic Cod (*Gadus morhua*) from sea cages. *Aquaculture Research* 38, 91-99.

Moe H., Olsen A., Hopperstad O. S., Jensen Ø., Fredheim A., 2007b. Tensile properties for netting materials used in aquaculture net cages. Aquacultural Engineering 37, 252–265.

Moe H., Gaarder R. H., Olsen A., 2008a. *Codnet –right choice of nets in cod aquaculture.* SINTEF report no SFH80-A084016 (In Norwegian).

Moe H., Hopperstad O. S., Olsen A., Jensen Ø., Fredheim A., 2008b (submitted for publication). Temporary creep and post creep properties of aquaculture netting materials.

Rhodia Polyamide, 2005. Multifilament product information. (http://www.rhodia-iy.com/RIY/download/ebusiness/Multifil_2005.pdf).

Sala, A., Lucchetti, A., Buglioni, G., 2004. The change in physical properties of some nylon (PA) netting samples before and after use. Fisheries research 69, 181-188.

Standards Norway, 2003. NS 9415 Marine fish farms—Requirements for design dimensioning, production, installation and operation. (In Norwegian).

Steinberg R., 1963. Monofilament Gillnets in Freshwater Experiment and Practice. Fishing Gear of the World 2. Fishing News Books Ltd., England, pp. 111–115.

The International Organization for Standardization, 1973. ISO 1805 Fishing nets - Determination of breaking load and knot breaking load of netting yarns.

The International Organization for Standardization, 1997. ISO 291 Plastics – Standard atmospheres for conditioning and testing.

The International Organization for Standardization, 1998. ISO 12947 Textiles – Determination of the abrasion resistance of fabrics by the Martindale method.

The International Organization for Standardization, 2002. ISO 1806 Fishing nets –Determination of mesh breaking force of netting.

Paper 5

Moe H., Fredheim A. and Hopperstad O. S. (2008c). *Structural analysis of aquaculture net cages in current.* Submitted for possible journal publication.

Structural analysis of aquaculture net cages in current

Heidi Moe [a,b]*, Arne Fredheim [a] and Odd Sture Hopperstad [b]

[a] SINTEF Fisheries and Aquaculture, NO-7465 Trondheim
[b] Structural Impact Laboratory (SIMLab), Centre for Research-based Innovation/ Department of Structural Engineering, Norwegian University of Science and Technology (NTNU), Department of Structural Engineering, NO-7491 Trondheim
* Telephone: +47 4000 5350, Fax: + 47 932 70 701, E-mail: Heidi.Moe@Sintef.no

Abstract

A method for structural analysis of aquaculture net cages has been developed and verified for a netting solidity of 0.23, water current velocities from 0.1-0.5 m/s and relatively large deformations (volume reduction up to 70 %) by comparing the numerical results to tests in a flume tank. A quasi-static analysis was performed, using commercial explicit Finite Element software to calculate distribution of loads in the net cage due to current, weights and gravity. The net cage was modelled using truss elements that represented several parallel twines. Sub-elements allowed the trusses to buckle in compression, and only negligible compressive forces were seen in the numerical results. Resulting drag loads and cage volume were shown to be dependent on the net cage size and weight system. Drag loads increased almost proportional to the current velocity for velocities in the range of 0.2-0.5 m/s, while the cage volume was reduced proportional to the current velocity. The calculated forces in ropes and netting of full-size net cages were well below the design capacity for current velocities up to 0.5 m/s. However, netting seams in the bottom panel of the net cage were identified as a potential problem area as the forces could reach the design capacity.

Keywords: Non-linear structural analysis, net cages, explicit finite element analysis, model tests, loads from water current, Morison's Equation.

1 Introduction

Net cages for aquaculture have traditionally been dimensioned and produced based on empirical data (Standards Norway, 2003). However, the requirements for documentation of net cage strength and volume increases, and the need for development of methods for structural analysis arises. In addition, fish farming is developing outside the borders of experience. The size of net cages increases rapidly, reaching volumes above current experience. More exposed locations are used for fish production, introducing higher loads on the net cage and fish farm from strong water currents and large waves. Strength analysis can also be a useful tool for development of net cage designs (Moe et al. 2005) to avoid escape of fish and ensure sufficient volume for good fish welfare and water quality.

It is not straight forward to analyze a fish farm or a single net cage (Figure 1). The loads acting on the structure will be the result of a fluid-structure interaction between moving sea-water and the deformed net. Analyses of net cages involve a high degree of non-linearity, both in loads, deformation and sometimes also material properties. In addition, loads from waves and current, damping and inertia loads are complex to model for netting materials in a general FEA (Finite Element Analysis) program, while programs with appropriate load-modules often have shortcomings in the structural model. An analysis involving a complete fluid and structure interaction model (CFD and FEA) will be complex and extremely demanding on computational resources, and to our knowledge attempts to perform such analysis on net cages have not been performed. There is ongoing work to verify and develop CFD methods for flow around net structures. This work reveals the complexity of such flows and the need of new knowledge and methods (Klebert, 2008, Enerhaug & Lader, 2008) Thus, the only current options is to use methods to calculate loads from moving fluids on netting structures, such as Morison's equation or equations based on tank test results (Løland, 1991). However, both these methods currently have limitations concerning amongst other the solidity of the net panel (ratio between area of netting material and total area), deformations and current velocity.

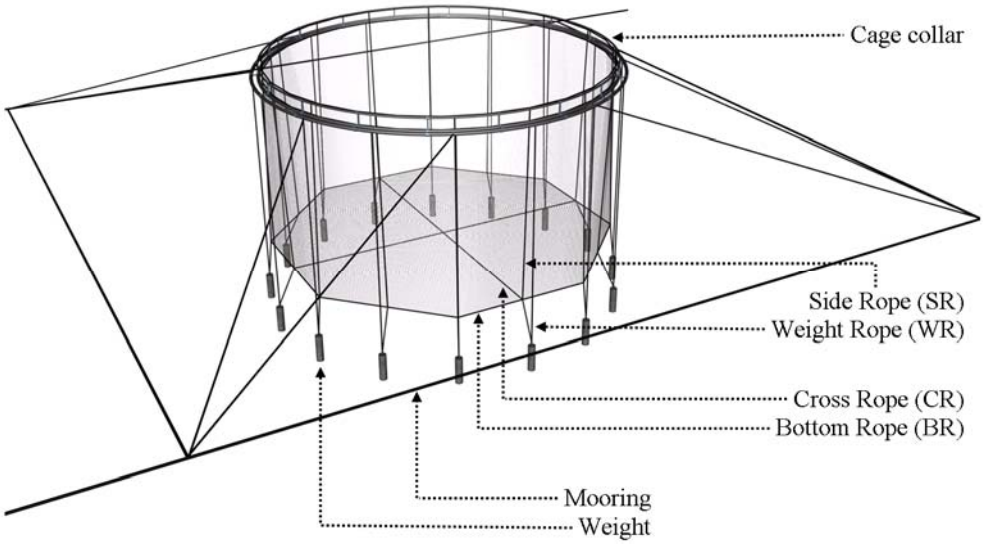

Figure 1: Illustration of traditional circular fish cage.

In the literature, net structures have been modelled using truss, beam, cable or spring elements to represent the twines (Fredheim, 2005, Gignoux & Messier, 1999, Li et al., 2006, Huang et al. 2006), or using 2D membrane elements (Lader & Fredheim, 2006, Tsukrov et al., 2003, Prior, 1999 and Tronstad, 2000). Most of the previous work included custom made software and/or elements, and often focused on the hydrodynamics and displacements rather than the distribution of loads in the model. Our approach to structural analyses was to apply a commercial FEA-software, which could include various material models and ensure effective modelling, processing and post processing. In this work truss elements were applied to model the net cage. The fact that netting and ropes do not take compression was modelled by introducing sub-elements, which combined with an explicit Finite Element code allowed the elements to buckle in compression.

Due to the mentioned limitations in methods for structural analysis of net cages, it is important to validate the methods applied, for instance by comparing results with model tests. The first step will be a static load situation involving a constant and uniform current. This paper presents a method for numerical analysis of net cages in constant uniform current verified for limited solidity, deformations and current velocities, applying

Morison's equation to calculate loads on the deformed net cage. The model was validated by comparing the results to model tests of a cage without bottom performed in a flume tank (Lader & Enerhaug, 2005), and then the method was applied to study deformations and global and local forces on full-scale net cages in uniform current.

2 Materials and methods

2.1 Analysis and modelling

Quasi-static strength analyses were performed using the Finite Element Method software ABAQUS Explicit (Dessault Systèmes, 2007, Moe et al., 2005). A large number of degrees of freedom was required to model the complete geometry of a full-scale net cage. In practice, it was not possible to analyze a model of a standard size net cage including all twines. Thus, major model simplifications had to be performed to reduce the computation time to an acceptable level. The applied square mesh Raschel knitted netting, made out of very thin Nylon (PA6) filaments, had a negligible bending stiffness (Klust, 1982). The net cage model was therefore built up of three-dimensional truss-elements (Dessault Systèmes, 2007) and each truss element represented several parallel twines in the netting. The truss elements were given the combined properties of the represented twines, i.e. the cross section area of the truss element was equal to the sum of the cross section area of the represented twines. The applied netting materials did not carry compressive loads. Therefore, each global truss element was divided into at least two sub-elements, allowing the twines to buckle when subjected to compression. Only negligible compressive loads were seen in the numerical results.

Three different models, described in Table 1, was analysed. Model M1 were similar to the cage without bottom subjected to model tests in a flume tank. Twine thickness, t, and half mesh width $w_{1/2}$ (ISO, 2002) were increased by approximately 8 % compared with given values in Lader & Enerhaug (2005) in order to account for elongation due to water absorption (Moe et al, 2007). The solidity was calculated as $Sn = 2t/w_{1/2}$. For all models, the netting dimensions were equal to typical smolt-nets (for juvenile salmon). M1 was modelled with one truss for each fourth twine. This model was also analyzed using a detailed mesh with one truss for each twine to verify the model simplification (for one load case, Figure 2). This refinement resulted

in drag- and lift-forces less than 0.7% different to the results using the coarser mesh (4 twines per truss). Two full-scale models (Figure 3) represented a cage of standard industry size a few years ago (M2), and a large cage according to present industry standards (M3). M2 and M3 had 80 and 128 elements around the circumference, which should be sufficient to capture the global deformations in the net cage. In comparison, M1 had 63 elements along the circumference, which was proved to be sufficient.

Table 1: Model dimensions.

Model	Circum-ference (m)	Cage depth (m)	Twine thickness, t (mm)	Half mesh width, $w_{1/2}$ (mm)	Solidity, Sn	Truss length (mm)	Twines pr. truss
M1	4.42	1.41	2	17.6	0.23	70.4	4
M2	90	20	2	16	0.25	1125	70.3
M3	160	40	2	16	0.25	1250	78.1

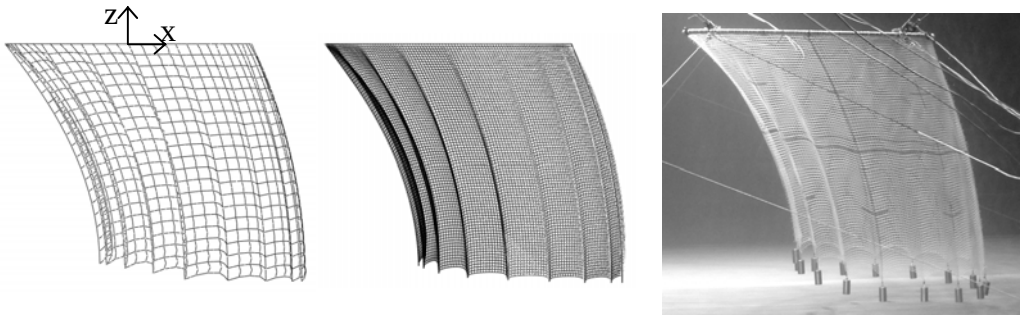

Figure 2: Comparison of deformed shape from numerical models with applied (coarse) and detailed mesh, and physical model of M1 (16 weights of 800g and current velocity of 0.34).

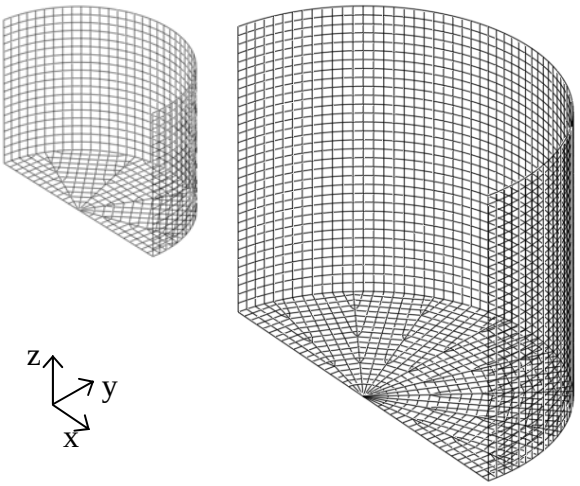

Figure 3: Model M2 and M3. The relative difference in size is maintained in the figure, which shows half of each model.

The full-scale models, M2 and M3, had 16 and 32 side ropes and 4 and 8 cross ropes respectively, in addition to main and bottom rope (Figure 1). M1 consisted of netting only.

The strains in the netting were in general small (less than 10%), and a linear elastic material model was applied for all analyses (Moe et al. (2007), Moe et al. (2008)). The stiffness of the netting material was chosen as 82 MPa, given for a specified pretension in Moe et al. (2007). This simplified netting material model was found sufficient for these global analyses (see Discussion chapter). However, boundary conditions and load cases that induce large strains in the netting would require a more refined material model. Ropes were given a stiffness of 1 GPa (Moe et al., 2005) and a diameter of 18 mm. The bottom of the full-scale net cages consisted of 8 and 16 netting triangles for M2 and M3 respectively. These were joined by seams that were assumed to have a constant stiffness equal to 10 parallel twines. Both netting and ropes are close to neutral in water, and both materials were given a submerged density of 100 kg/m^3.

The net cage volume was estimated by dividing the net cage into sections and summing their approximate volumes. M1, M2 and M3 were divided into 21, 19 and 33 sections over their depth (the possible volume below the bottom rope was not considered). For the unloaded cage configuration the

sections were horizontal, circular disks with a thickness equal to the truss length (except the upper and lower sections, which were half as thick). The volume of a deformed section was calculated as the horizontal cross-section multiplied by the average (vertical) thickness of the section circumference.

2.2 Boundary conditions and loads

The net cage of a circular fish cage (Figure 1) is usually attached to the cage collar at each side rope. In order to get the correct boundary conditions of the net cage, both the bending stiffness of the cage collar and the tensile stiffness of the mooring lines should be modelled. However, for simplicity, neither the cage collar nor the mooring system was modelled in these analyses, but assumed to keep their original shape and position, although this may affect the distribution of loads in the net cage (see Section 4). For M1 both the tank test model and the numerical model were attached to a rigid cage collar over the full circumference, consequently with no effect of mooring stiffness on the net cage response in current. The full-scale models, M2 and M3, were assumed attached to a rigid cage collar at all side ropes, which were 16 and 32 respectively.

In the numerical analysis, loads from current, weights and gravity were applied gradually to ensure that external work was converted to internal energy without introducing significant kinetic or viscous energy. The numerical models were subjected to loads representing a uniformly distributed current with constant velocity, **U**, acting in the x-direction (coordinate system defined in Figure 2 and Figure 3). The cross-flow principle was applied (Hoerner 1965), assuming that the current could be separated into flow tangential and normal to the element axis. The first step in the current load calculation for an element was to decompose **U** into tangential and normal velocity components, $\mathbf{U_T}$ and $\mathbf{U_N}$**,** as shown for an element in the xz-plane in Figure 4. However, most elements were oriented in the xyz-space and subjected to three-dimensional velocity vectors**.** Each truss element was considered as individual, friction free cylinders, with negligible tangential load components. The resulting load acting on each element was the normal load, $\mathbf{F_N}$, calculated using the drag term of Morison's equation (Faltinsen, 1990):

$$\mathbf{F_N} = \frac{1}{2}\rho C_D d w_{1/2} \left|\mathbf{U_N}\right| \mathbf{U_N} \qquad (1)$$

where $\rho = 1025\,kg/m^3$ (density of seawater), C_D is drag coefficient and d is the diameter. $\mathbf{F_N}$ was decomposed in x- y- and z- direction and applied as concentrated loads in adjacent nodes. Drag load ($\mathbf{F_D}$) and lift load ($\mathbf{F_L}$) were found as the x- and z- component of $\mathbf{F_N}$.

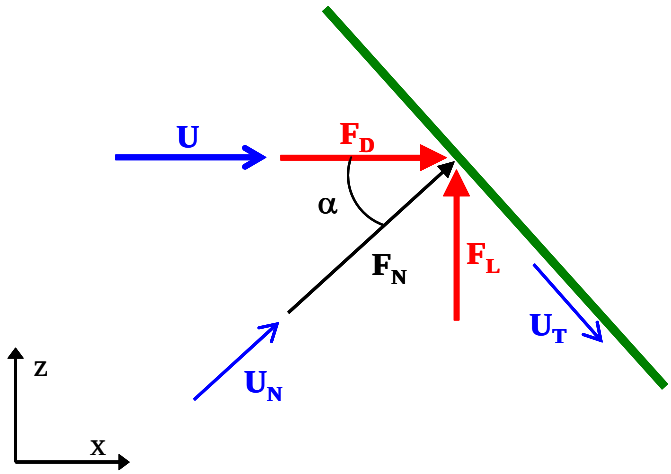

Figure 4: Calculation of current loads for an element in the xz-plane.

For M1 it was assumed that the current velocity was reduced by 20% after passing the first net wall (Lader & Enerhaug, 2005). For the full size cages the velocity reduction was assumed to be 15%, corresponding to findings by Løland (1991). The bottom would in general experience a high degree of shadow effects (see Section 4), and the current velocity was thus reduced by 50 % in the initially horizontal bottom.

Fredheim (2005) presented results implying that the drag term of Morison's equation could be applied with a constant drag coefficient to calculate drag on netting for a limited range of Reynolds number and solidities (less than 0.25). M1, M2 and M3 were analysed for current velocities ranging from 0.1-0.5 m/s, corresponding to Reynolds number $\mathrm{Re} \in [174 - 870]$ ($\mathrm{Re} = Ud/\nu$, where ν is the kinematic viscosity, $\nu = 1.15 \cdot 10^{-6}\, m^2/s$ for seawater). Based on findings in Fredheim (2005), the drag-coefficient was given a constant value $C_D = 1.15$ (valid for the applied solidities, Table 1, and given range of Reynolds number).

Net cage structures are highly flexible and will experience large displacements when subjected to currents. The displacements are dependent on current loads, and the direction and magnitude of current forces are affected by the net cage displacements. An iteration scheme was applied to account for this complex relationship. First, current forces were calculated based on the initial (unloaded) cage geometry and the resulting deformations of the cage model were found. New loads were calculated based on the deformed model, resulting in a new cage configuration. The last step was repeated until the difference in drag and lift was less then 2% between the last two iterations (most often the difference was less than 1 %).

M1 was analyzed using 4 different bottom weight configurations: 16 weights of 400g, 600g and 800g (3.0, 4.5 and 6.0 N submerged weight) and 4 weights of 6.0 N. The weights were attached directly to the netting and equally distributed along the circumference. M2 was subjected to a concentrated load of 1000 N at the end of each side rope, while M3 was analyzed for both 1000 N and 2000 N at all 32 side ropes. Both M2 and M3 were subjected to a weight of 1000 N at the centre of the bottom.

3 Results

3.1 Comparison of numerical analyses and model tests

M1 was analyzed for various weight configurations and current velocities corresponding to load cases presented in Lader & Enerhaug (2005), who performed physical model tests of M1 at the North Sea Centre flume tank in Denmark. The results from the numerical analyses of M1 were compared to the physical model tests.

Figure 5 shows a selection of 2D plots of the deformed shape from the various analyzed load cases compared with the configuration in calm water (dotted lines). The 2D positions of the physical model were measured at 8 points (front, aft and centre of net cage) as indicated in Figure 5 using a video system. The overall impression from these figures was that the deformed shapes achieved from numerical analyses corresponded very well to the shapes of the physical model. It was noted that the tank test model had an initially imperfect geometry (slightly skew in calm water, as shown in Figure 5), that must be assumed had an effect on deformation and loads in current. Most of the tank model tests showed an initial horizontal

displacement in calm water. This was probably due to slight movements in the water, as it would take some time for the water in the tank to be completely calm. The bottom circumference of the physical model was significantly smaller than the upper circumference, which was not the case in the numerical model. This was a consequence of the design of the joint between two twines (not included in the FE model), which makes unloaded netting contract. The vertical deformation of the net was slightly larger in the numerical analyses for cages with large deformations (16x400g, v_c=0.56 m/s and 4x800g, v_c=0.53 m/s). The given deformation of the physical model with 16x800g weights at v_c=0.50 m/s had obvious errors of unknown source in the deformed geometry measurements. The upper two points on the downstream side (right hand side) was registered with an unlikely, probably too small, x-coordinate.

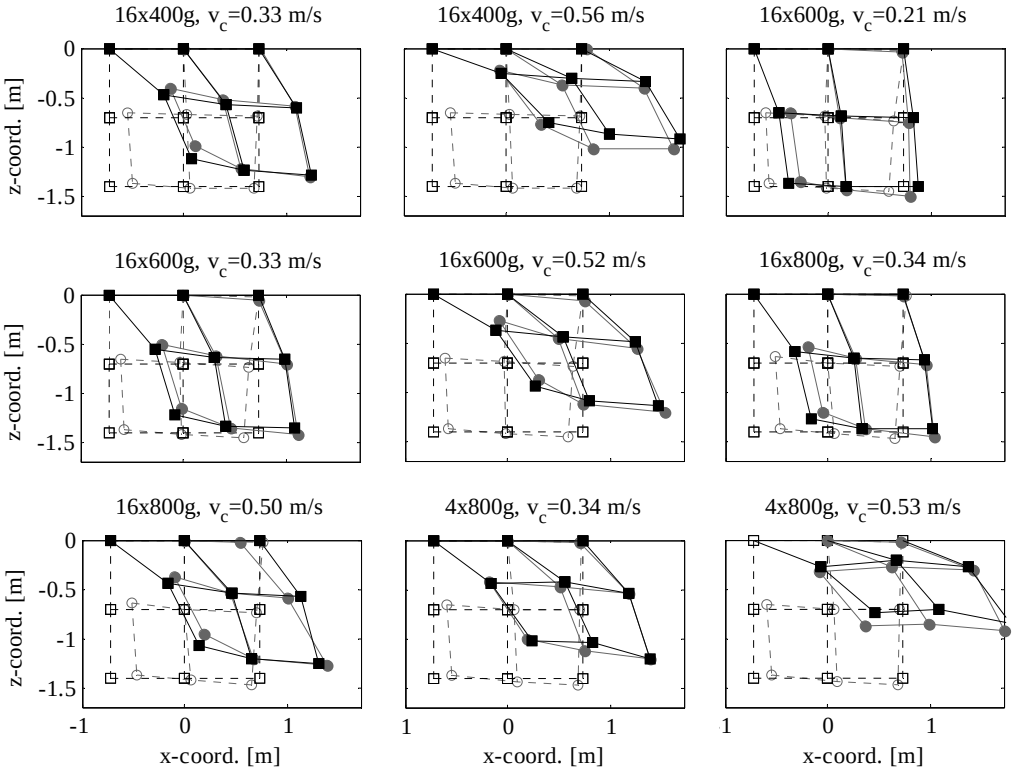

Figure 5: Comparison of 2D shape of net between physical model tests (given as grey circles) and numerical analysis (black squares). Shape with and without current are given in all figures (filled markers for current).

Figure 6 and Figure 7 give the resulting total drag and lift forces acting on M1 from model and numerical tests, and the volume reduction calculated based on the deformed numerical model. As would be expected, drag and lift forces increased with increased current velocity, while the volume decreased. Drag and relative volume seemed to be almost proportional with the current velocity for velocities above 0.2 m/s. There was good coherence in drag force, although the numerical analyses differed more in drag between the various bottom weights for high velocities, indicating that increased bottom weights increased the drag loads acting on the netting (due to reduced deformations). The results from the model tests indicated that there were significant uncertainties in the measured velocities and loads: The drag was measured to be slightly larger for a current velocity of 0.52 than 0.53, the opposite of what should be expected. In addition, the drag was measured to 0.7 N, while lift was 0.5 N in calm water (16x800g weights).

The calculated drag force was $95 \pm 9\%$ of the measured values (mean and standard deviation), while the calculated total lift force was $83 \pm 10\%$ of the measured values (Figure 7), disregarding a couple of the lower values of lift forces where the deviation probably was strongly affected by the mentioned uncertainties in load measurements. Even in the numerical analyses that showed a larger vertical deformation than model tests (Figure 7), the lift forces were lower than the measured values.

The net cage volume was reduced close to proportional with increased current velocity (Figure 6), resulting in a relative volume (volume in current divided by unloaded cage volume) between 40-70% for a current velocity of 0.5 m/s. Preservation of volume increased with increased bottom weights. Lader & Enerhaug (2005) estimated the relative volume based on global deformation of the nets (Figure 5), as a non-linear relationship between relative volume and current velocity. Their relative volume estimates gave smaller values than the calculations presented in Figure 6, probably because they were not able to include the effect of netting displacements on cage volume.

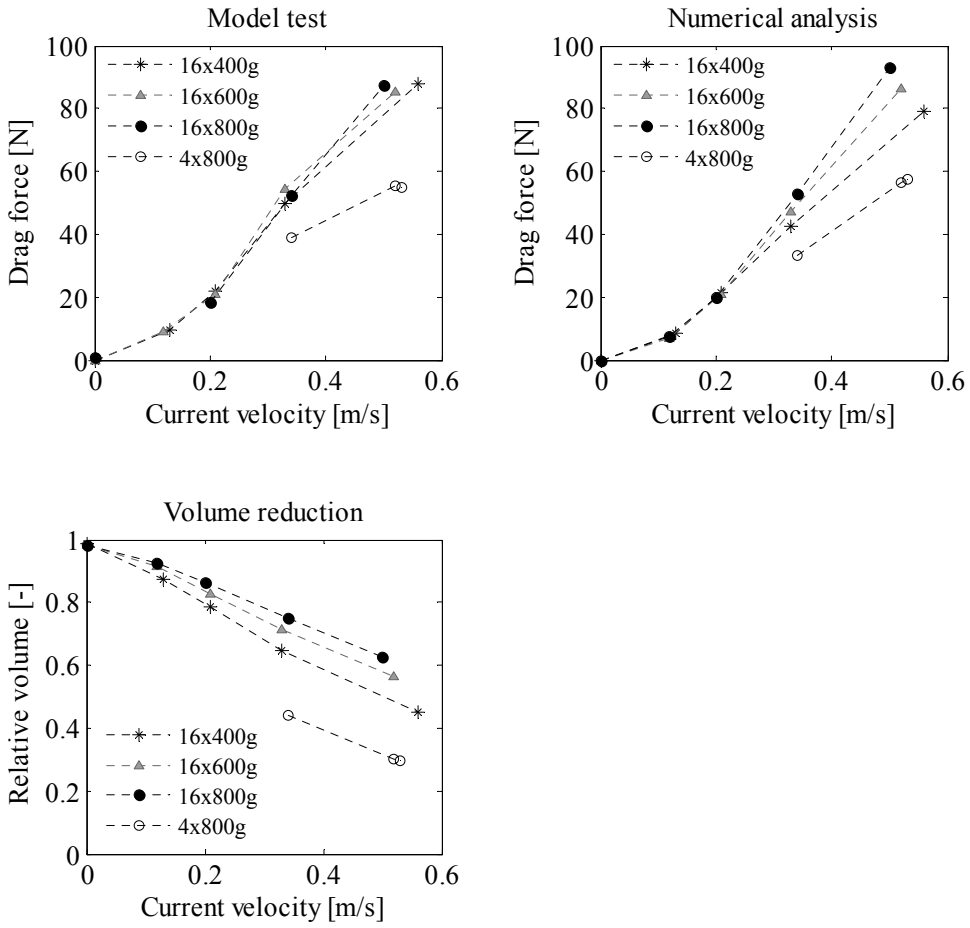

Figure 6: Total drag force measured during model tests and calculated in numerical analysis of net cage M1. Relative volume in net cage M1 as a function of current velocity.

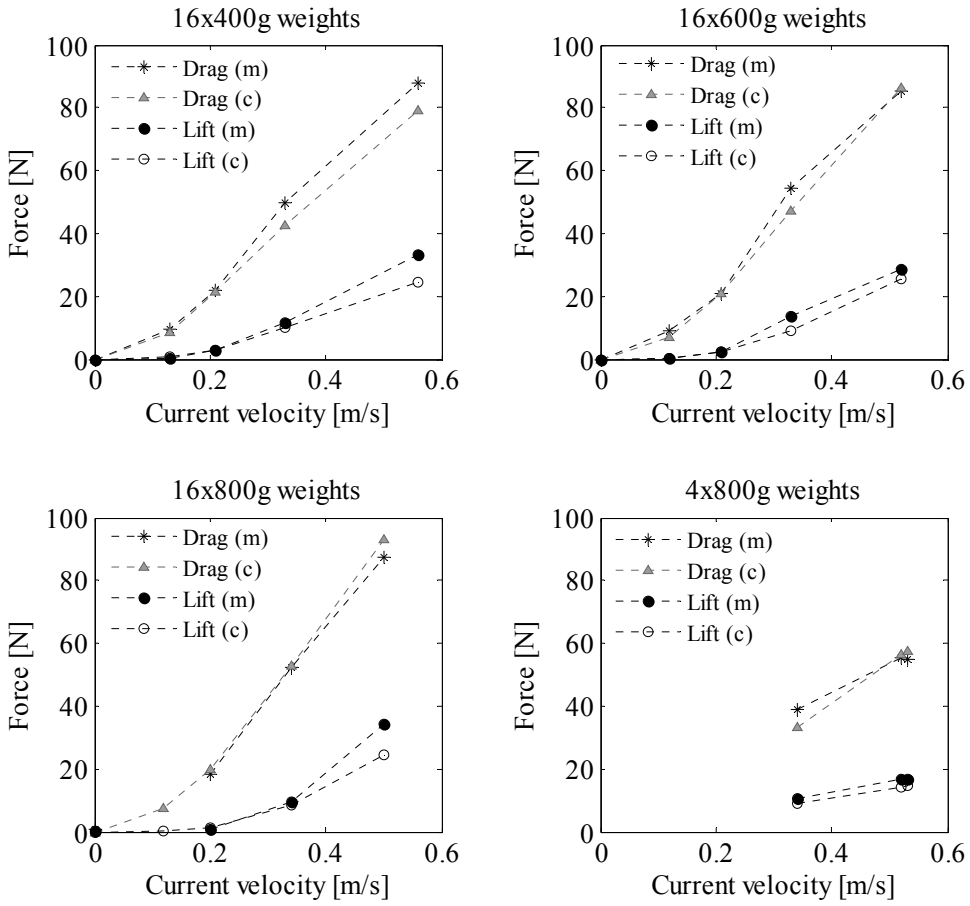

Figure 7: Total drag and lift forces measured during model tests (m) and calculated in numerical analysis of net cage M1 (c) for the various weight configurations.

3.2 Strength analysis of full-scale net cages

Analyses of M1 showed that the numerical analysis corresponded reasonably well to the model test results. The method has thus been verified under the given conditions and corresponding numerical analyses can be performed on FE-models of full-scale net cages. In addition to an evaluation of loads acting on the cage and their deformed shape, maximal values of local forces in the structure were found and compared to the capacity of the various structural components.

The global results from analyses of M2 and M3 are given in Figure 8. In general, drag loads increased with increased cage size, current velocity and bottom weights. For small velocities, the increase in drag force was approximately proportional to the velocity squared, as we would expect for negligible net cage deformations (according to Morison's equation). For larger velocities (>0.2 m/s), the deformation of the net cage resulted in a significant reduction of the normal velocity component ($|\mathbf{U}_N|$, Figure 4) for some of the elements, compared to an undeformed net cage. The total resulting drag loads were almost proportional to the current velocity for velocities between 0.2-0.5 m/s. The lift forces increased with increased velocity, with varying rate of change.

Knowledge of the expected maximal forces acting in the boundaries between net cage and cage collar is important in design and dimensioning of net cages. The connection point with the highest loads in x- and z- direction was found in front of the cage (upper left point in Figure 2). Loads in x-direction, F_x, for this point are given in Figure 8. The horizontal boundary forces increased with increasing velocity. The maximal boundary force was not significantly affected by the increased bottom weights for M3, and not as sensitive to difference in cage size as the drag force. Loads in z-direction, F_z did not vary much with current velocity for the three different models, with mean value and standard deviation of 1.2±0.1 kN, 1.2±0.1 kN and 2.1±0.1 kN for M2 and M3 with 1000 N and 2000 N weights respectively.

The relative volume of the net cages (Figure 8) decreased with increasing current velocity, resulting in a value of 41-55% for a velocity of 0.5 m/s. The linear trend was not as clear in this figure as for M1. However, the volume for cages in currents less than 0.2-0.3 m/s was somewhat underestimated as the method for volume calculation did not consider the volume below the bottom rope of the cage. Figure 9 shows the 2D displacements of M3 with 1000 N weights, and how the central bottom weight increased the depth below the bottom rope of the cage significantly for velocities below 0.3 m/s. The net below the bottom rope formed a conical volume in calm water. Including this volume in the calculation of deformed cage volume gave a total relative volume of 1.0 in calm water. This indicated that the relationship between the total relative volume (including volume below the bottom rope) and current velocity had a linear trend for all net cages in Figure 8.

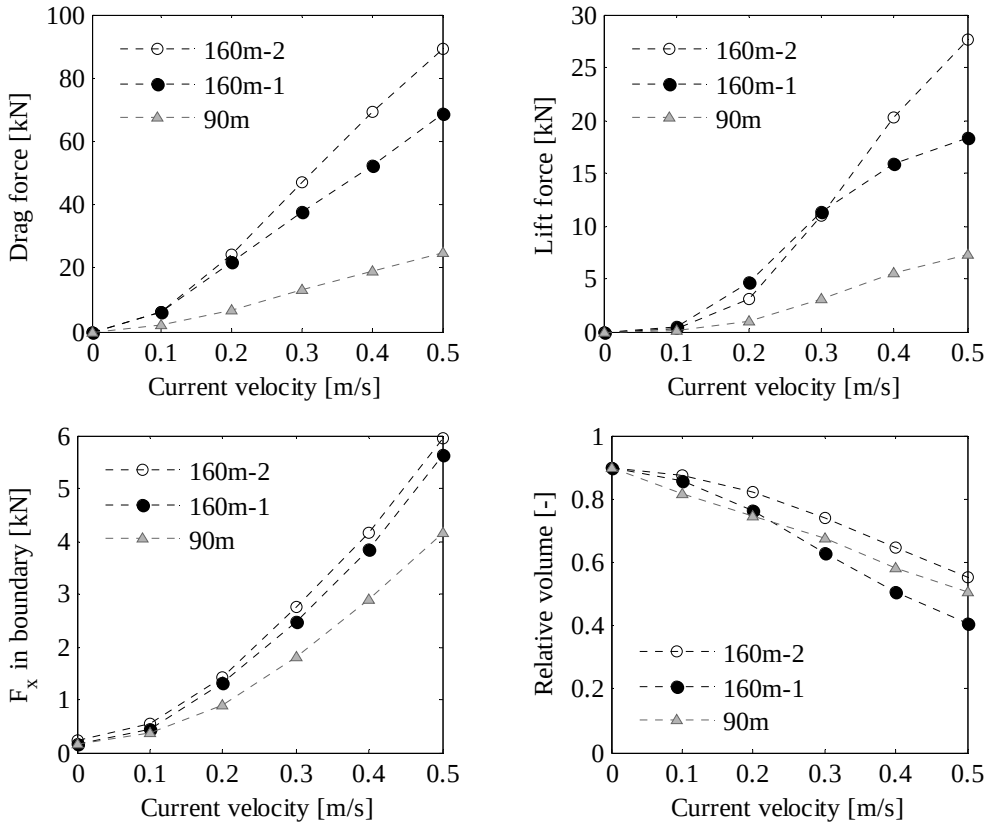

Figure 8: Drag and lift forces, max. forces in x-direction in boundary with cage collar and relative volume for M2 (90m) and M3 with 1000 N weights (160m-1) and 2000N weights (160m-2).

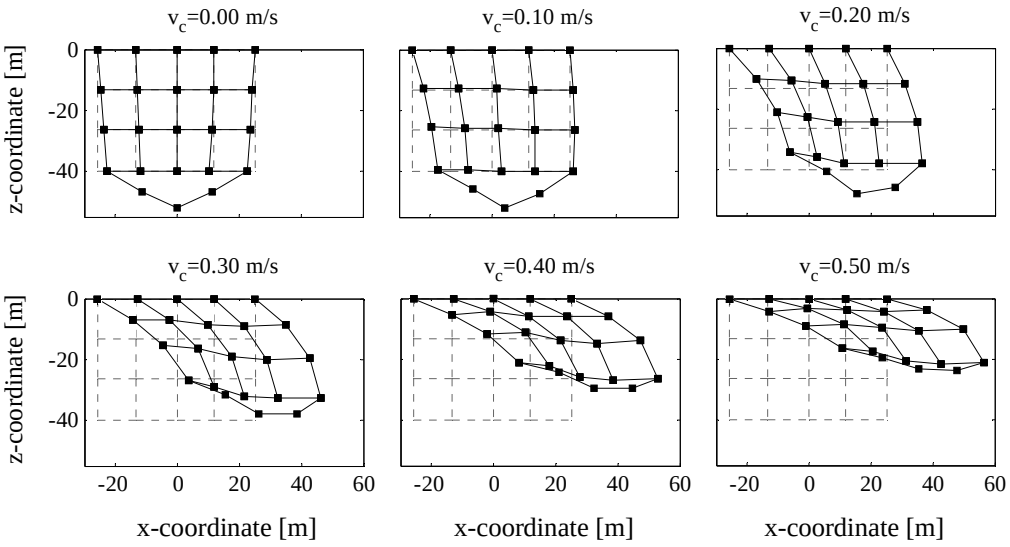

Figure 9: Calculated 2D net cage displacements for M3 with 1000N weights in calm water and various current velocities. Undeformed cage configuration is given as dotted lines.

Maximal forces in various structural components were found and are given for main ropes, side ropes, cross ropes, netting twines and seam in Figure 10. In all components, the maximal forces increased with increasing current velocity. In general the forces in net cage M2 were smaller than the forces in M3, except in the seam for low velocities. This is due to the low number of cross ropes in M2, increasing the stress concentration in the seam. Increasing the bottom weights only had a small effect on the local forces in the net cage, although the drag loads increased significantly (Figure 8). The only significant deviation was in forces in side ropes, where the heavier weights naturally gave a higher tensile force in the side ropes, however the difference in force decreased between the two variations of M3 for increasing velocity.

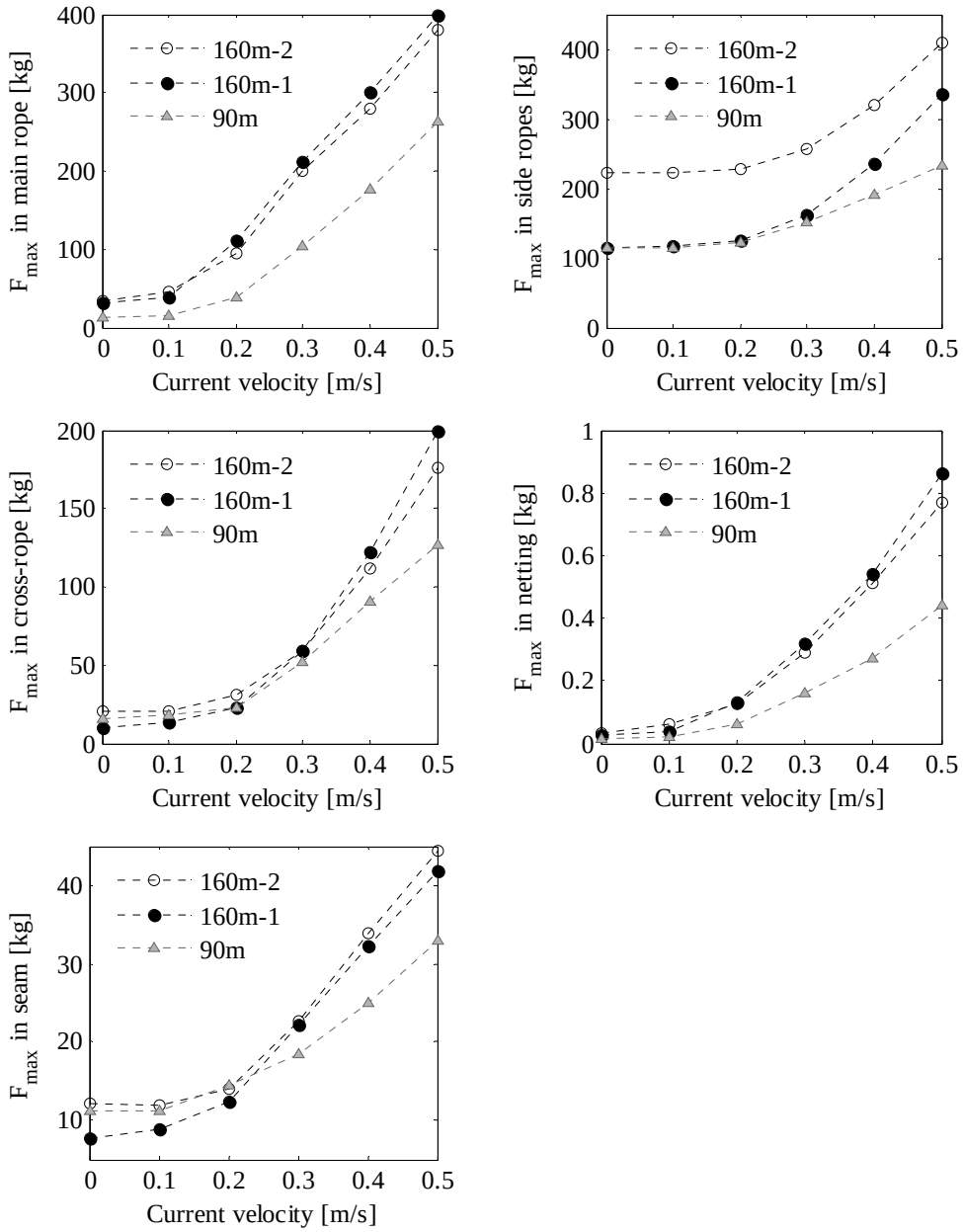

Figure 10: Maximum calculated forces in structural component of net cage: Main rope, side ropes, netting seam in bottom and netting twines for M2 (90m) and M3 with 1000 N weights (160m-1) and 2000N weights (160m-2).

The forces can be compared to the capacity of the various structural components, using the following rule: The force in a component (F) multiplied by a load factor (γ_f) should be equal to or less than the capacity (R) of the component divided by a material factor (γ_m) (Standard Norway, 2003 and 2004): $F \cdot \gamma_f \leq R/\gamma_m$. The percentage of utilized design capacity can be calculated as follows:

$$C_u = \frac{R \cdot \gamma_f \cdot \gamma_m}{F} \qquad (2)$$

Based on NS9415 (Standards Norway, 2003), $f_{load} = 1.3$ and $f_{mat} = 3$ for ropes, while no material factor was given for netting. Based on the results presented in Figure 10, the maximum utilized design capacity was 20 % of the main rope in M2, 31 % of the main rope for M3 with 1000 N weights and 32 % of the side rope for M3 with 2000 N weights. Forces in the netting twines are in general low (less than 1 kg), considering that the breaking strength of each twine will be greater than 20 kg for such netting dimensions (derived from NS9415). It is difficult to establish a material factor for netting, and this is consequently not given in NS9415. The seam was subjected to relatively high forces, up to 44 kg for M3. If our assumption that the seam had 10 times the strength of a netting twine is valid, $C_u = \frac{44 \cdot 1.3 \cdot \gamma_m}{200} = 0.29 \cdot \gamma_m$, i.e. depending on the material factor we are close to or beyond utilizing the design capacity of the seam. One can also raise the question whether a component like a seam should be used as a load carrying member in a structure. Seams are known to be a problem area in the net cage, and it should be considered to increase the number of cross-ropes so that all load carrying points in the net are connected to a cross-rope in the bottom for circular cages, at least for large cages in intermediate to strong currents.

4 Discussion

Results from the numerical analyses corresponded well with the physical model tests. However, some deviations existed, especially in calculated lift forces which on average were 17% lower than the measured values. Several sources of error could have had significant effect on the model test results: The initial model geometry was imperfect, the current velocity varied over the model depth and measurements of loads, current velocities and net configuration involved uncertainties (Enerhaug, 2003). In addition, the simplified numerical model did not give a perfect representation of the model: Local dimensions of wet netting were estimated based on given dry dimensions (possible errors both in measurements of dry netting and estimation of wetting effect). The local netting geometry was not modelled in detail, but was modelled as a mesh of smooth cylinders. Drag calculations involved possible sources of error due to estimation of drag coefficients and shadow effects.

Measurements showed that the current velocity was not constant over the depth of the flume tank (Enerhaug, 2003, Figure 11). The net cage was placed approximately 0.9 m below the water surface and the velocity was measured at three vertical positions as indicated in Figure 11. Approximately 0.25 m above the cage, the velocity was 0.38 m/s, while 0.5 m and 1.0 m below this point the velocity was reduced by approximately 8% and 11%. In the presented results (Figure 5 and Figure 7), the applied current velocity was measured in the intermediate point (1.4 m below the surface). The bottom of the net cage model M1 was lifted when the cage was subjected to loads from current (Figure 5). A larger fraction of the net was thus subjected to the relative high velocities in the upper water levels. This may partly explain the deviation in lift forces for high velocities.

The velocity reduction in the centre of the net cage was given as 20% in Lader & Enerhaug (2005), although close studies of the velocity measurement from the tests indicate that the shadow effect may be lower in the middle of the cage (Enerhaug, 2003). The velocity was measured in front of, in the middle and behind the net cage, and the data on velocity inside the full volume of the cage was thus unknown. Consequently the shadow effect could not be modelled correctly. A lower velocity reduction would probably increase both drag and lift loads.

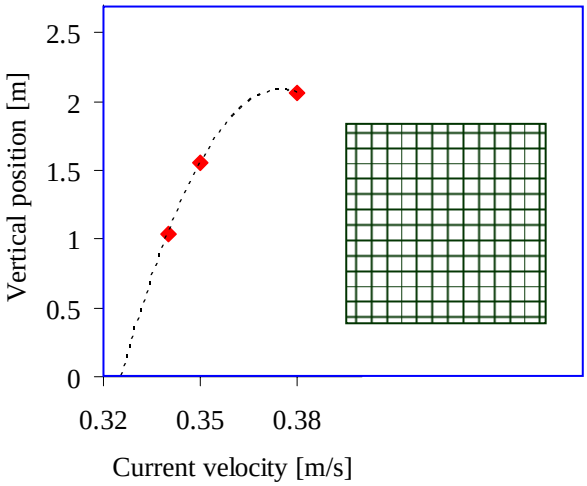

Figure 11: Measurements of horizontal current velocity in 3 points over the depth of the flume tank (2.7 m) given by Enerhaug (2003). A current velocity trend and position and size of the undeformed net cage M1 are indicated.

It was not trivial to find suitable drag coefficients for the netting twines. An overview of data on drag coefficients for netting materials are given in Fredheim (2005), based on experiments performed on knotted netting materials by Rudi et al. (1988). Klebert (2008) have found that the drag-coefficient may not be very different for knotless netting, and that the drag coefficient are close to constant for Reynolds numbers $\mathrm{Re} \in (300,1000)$, which corresponds to data from Rudi et al. (1988). A detailed study of drag coefficients was not included in this work. Based on data in Fredheim (2005) the given drag-coefficient of 1.15 was chosen for the given solidity and velocities.

We conclude that the applied numerical model seem to reflect the results from the model tests as well as could be expected. However, more validation of the method is necessary. It should also be tested for larger current velocities, deformations and solidities. During large net cage deformations, significant fractions of the net cage will be affected by additional shadow effects where some of the twines will be positioned in the wake of one or several twines. The extreme example of this is a horizontal panel of netting (in the xy-plane) subjected to in plane current (in x-

direction). Using Morrison's equation and the cross-flow principle, all elements with axis parallel to the y-axis will be subjected to a drag-load proportional to the current velocity squared ($|\mathbf{U}|^2$), while the elements with axis parallel to the x-axis (α = 90° in Figure 4) will yield no drag load ($|\mathbf{U_N}| = 0$). Thus, we can assume that the drag calculated for a horizontal panel is 50 % less than for a vertical panel (in the yz-plane). According to results from model tests presented in Løland (1991), the drag of a horizontal panel is reduced by approximately 94 % compared to a vertical panel. Thus, it must be assumed that drag loads can be over-predicted for large displacements if this potential shadow effect is not included. The applied method does not include this potential shadow effect. However, we do not see any effect of this in the presented results. In further analysis with even larger net cage deformations, this effect should be considered when calculating the loads.

The forces in the various structural components of the full-scale model were calculated for a geometrical perfect net cage model with perfectly applied loads and boundary conditions from a strength point of view. However, in practice all nets have imperfections like initial stress concentrations in the netting, variations in length of ropes and ends of side ropes and cross ropes that do not connect perfectly. This will introduce significantly larger forces in the netting than indicated in Figure 10, and may also change the distribution of loads in the ropes with the possibility of increased maximal forces. This can be handled in the design process through introduction of increased load and material factors that include modelling uncertainties (γ_F and γ_M, Standards Norway, 2004). The forces in the seams could become critical, and this design should be reconsidered, especially for net cages used at locations with high current velocities. A possible solution could be to increase the number of cross ropes. Introducing a flexible cage collar with a significant deformation during loading would probably change the distribution of loads in the net cage, most likely increasing the maximal forces in side ropes and attachment loop.

Traditional knotless netting materials for aquaculture have a very low stiffness for small tensile loads. In fact, they are so flexible it is hard to define a precise initial length and stiffness. The actual stiffness of the applied netting materials may differ from the assumed 82 MPa. However, according to the numerical analyses, evenly distributed, moderate current loading will only introduce small strains in the netting of the analyzed

cages. (The maximum nominal strain was 3 % for M3 locally, while the major part of the net had strains less than 1 %.) The ropes had a relatively large tensile stiffness, and errors in netting stiffness would not affect the loads in the netting or the deformed shape significantly (dominated by global displacement). In M1, strains in the netting were up to 3% in the twines above the weights, while most of the netting had strains less than 10^{-4}.The assumed value of 82 MPa represents the uniaxial stiffness of the netting materials, which can be applied for netting in net cages, as one load direction often dominates over the other for significant stress levels (Moe et al., 2007). The numerical analysis results showed that in the area with highest loads (upper part of the upstream side of the cage), the initially vertical twines were strained approximately 10 times as much as the initially horizontal elements.

5 Conclusions

This study indicated that quasi-static Finite Element analyses can be applied to estimate deformations and loads acting on net cages. A method for structural analysis of aquaculture net cages was developed using a commercial FEA software and verified for a netting solidity of 0.23, water current velocities from 0.1-0.5 m/s and relatively large deformations (volume reduction up to 70 %). Resulting drag loads were shown to be dependent on the net cage size and weight system, increasing close to proportional with the current velocity for velocities in the range of 0.2-0.5 m/s. The corresponding lift forces increased with increased velocity, with varying rate of change. The cage volume was reduced almost proportionally with the current velocity.

The calculated forces in ropes and netting were well below the design capacity. However, the netting seams in the bottom panel of the net cage were identified as a potential problem area as the forces could reach the design capacity.

6 Acknowledgements

This work was sponsored by the Norwegian Research Council through the IntelliSTRUCT programme (Intelligent Structures in Fisheries and Aquaculture) at SINTEF Fisheries and Aquaculture. We would like to thank Birger Enerhaug, Østen Jensen, Martin Føre and Pål Lader at SINTEF Fisheries and Aquaculture for their help and good advice during this work.

7 References

Dessault Systèmes, 2007. ABAQUS 6.7 Documentation.

Enerhaug, B., 2003. Model tests of net structures. SINTEF report.

Enerhaug & Lader, 2008. Unpublished data.

Fredheim, A., 2005. Doctoral thesis (dr. eng.). Current forces on net structures. Norwegian University of Science and Technology, Norway.

Gignoux, H. & Messier, R. H., 1999. Computational Modelling for Fin-Fish Aquaculture Net Pens. Oceanic Engineering International, Vol. 3, No. 1., 12-22.

Hoerner, S. F., 1965. Fluid-dynamic drag. Hoerner Fluid Dynamics.

Huang, C.-C., Tang H.-J., Liu J.-Y., 2006. Dynamical analysis of net cage structures for marine aquaculture: Numerical simulation and model testing. Aquacultural Engineering, 35, 258-270.

Klust, Gerhard, 1982. Netting materials for fishing gear. Fishing News Books Ltd., England.

Klebert, 2008. Unpublished data.

Moe, H., Fredheim, A., Heide, M., 2005. New net cage designs to prevent tearing during handling. IMAM 2005, Lisbon, Portugal, 26 – 30 September 2005.

Moe, H., Olsen, A., Hopperstad, O. S., Jensen, Ø., Fredheim, A., 2007. Tensile properties for netting materials used in aquaculture net cages. Aquacultural Engineering 37, 252–265.

Moe, H., Hopperstad, O. S., Olsen, A., Jensen, Ø., and Fredheim, A., 2008. Temporary creep and post creep properties of aquaculture netting materials. Submitted for possible journal publication.

Lader, P., Enerhaug, B., 2005. Experimental Investigation of Forces and Geometry of a Net Cage in Uniform Flow. IEEE Journal of Ocean Engineering, vol. 30, no 1.

Lader, P. F. & Fedheim, A., 2006. Dynamic properties of a flexible net sheet in waves and current –A numerical approach. Aquacultural Engineering, 35, 228-238.

Li, Y.-C., Zhao, Y.-P., Gui, F.-K., Teng, B., 2006. Numerical simulation of the hydrodynamic behaviour of submerged plane nets in current. Ocean Engineering, 33, 2352-2368.

Løland, G., 1991. Current forces on flow through fish farms. Doctoral thesis (dr. eng.). The Norwegian Institute og Technology, Norway.

Priour, D., 1999. Calculation of net shapes by the finite element method with triangular elements. Communications in Numerical Methods in Engineering, **15**, 755-763.

Standards Norway, 2004. NS 3490 Design of structures –Requirements to reliability.

Standards Norway, 2003. NS 9415 Marine fish farms –Requirements for design dimensioning, production , installation and operation (In Norwegian).

The International Organization for Standardization, 2002a. ISO 1107 Fishing nets –Netting – Basic terms and definitions.

Tsukrov, I., Eroshkin, O., Fredriksson, D., Swift, M. R., Celikkol, B., 2003. Finite element modelling of net panels using a consistent net element. Ocean Engineering, 30, 251-270.

Paper 6

Moe H., Fredheim A. and Heide M. (2005). *New net cage designs to prevent tearing during handling*. IMAM 2005, Lisboa, Portugal, 26 – 30 September 2005.

New net cage designs to prevent tearing during handling

H. Moe, A. Fredheim & M. A. Heide
SINTEF Fisheries and Aquaculture, Trondheim, Norway

ABSTRACT: This paper presents new designs for aquaculture net cages. The purpose of the new designs is to reduce the probability of escape of fish during lifting of the net cage. Several new designs are compared to a traditional net cage with regard to stresses in the netting material and deformation of the net cage. Topics of major interest are the risk of tearing of the net cage netting during handling and the shape of the net cage subjected to current loading.

A method for strength analysis of net cages is presented, applying an explicit FEM. The material properties are derived from tensile testing of new netting material and modelled using a hyperelastic material model. A critical stress value is established based on the stress-strain curve of the netting material.

1 INTRODUCTION

Escape of fish from fish farms has been identified as a potential environmental risk. Cross breeding of wild and cultured fish like salmon, trout and cod may have a negative impact on the behaviour and genetics of wild stocks of fish. This has resulted in major efforts to reduce the problem of escape in Norwegian aquaculture.

A substantial amount of the escaped fish is a consequence of tearing of the net cage netting during handling of the net cage. The most critical operation in this context is lifting of a net cage containing fish.

The net cage is lifted at regular intervals either as part of the operation to change a net cage, to clean the upper part of the netting for biofouling by marine organisms (such as mussels, hydroids and seaweed) and to reduce the net cage volume when fish are fetched to be sorted or slaughtered.

The net cage is usually lifted by pulling the weight ropes. As shown in Figure 1, one end of the weight rope is connected to the lower end of a side rope, and the other end is connected to the cage collar. Weights are tied to the weight ropes, their function is to maintain volume in the fish cage.

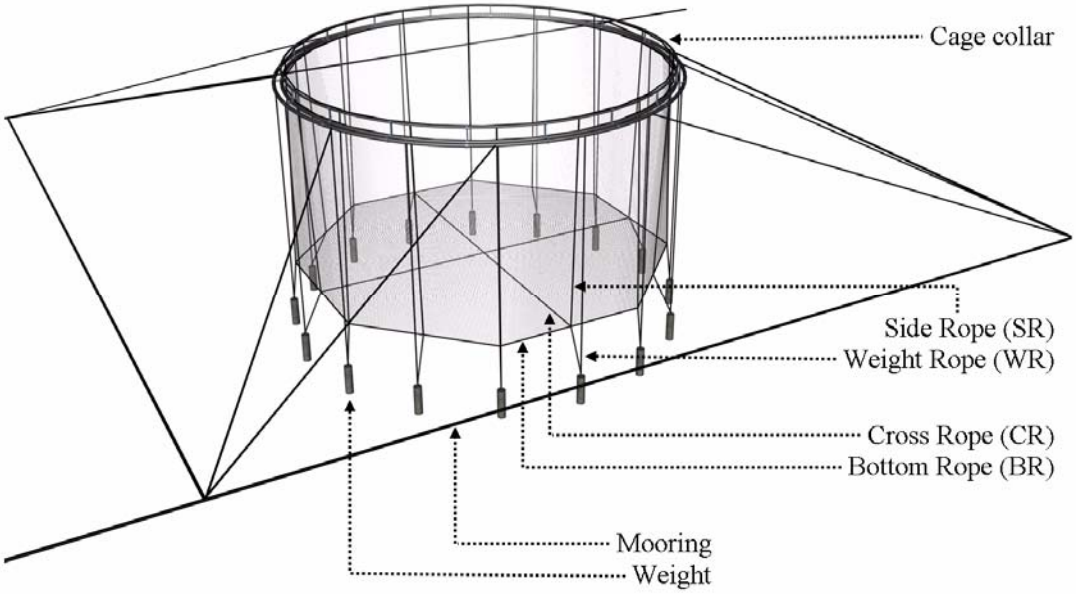

Figure 1. Circular fish farm.

The problem with tearing of net cages during handling is a direct consequence of several factors (Moe 2004a):

- Worn net cages with weak spots
- Unfavourable handling of the net cage
- Weak construction, mainly due to few cross ropes in the bottom
- Large loads during handling due to gravity, drag and mass forces, heavy weights and powerful lifting equipment
- Stress concentrations in the netting due to the net cage production
- Abrasion from adjacent equipment such as weights, cage collar and mooring system

Fish farmers have both the means and the opportunity to tear the net cage during operations, which gives them great responsibility for the integrity of the net cage. The development of net cages has been limited over the last 20 years, although auxiliary equipment for operations has become more powerful and is more frequently in use. The possibility of overloading the net cage combined with the demand for efficient operations is an important reason for escape of fish from fish farms.

Heavy equipment and strong cranes often result in little control of the forces involved during handling of the net cage, and relative motions between the crane vessel and the fish cage makes the situation even worse. In addition, the condition of the net cage with respect to residual strength and biofouling is often not known during lifting. Biofouling has been a critical factor in several cases of escape, as it can induce huge gravity, drag and mass forces during lifting of the net cage.

2 NET CAGE DESIGNS

Most net cages are made out of square mesh knotless nylon netting and polypropylene / polyethylene ropes. They are designed to transfer and carry all major forces through the ropes. The netting is attached to the ropes and its only intended function is to keep the fish in place.

In the process of designing new net cages, the following criteria have been important:

- The new net cages should be based on the same materials and production methods as applied today
- No loads should be transferred directly from the ropes into the netting
- The new net cages must have equal or better properties than a traditional net cage, meaning that the design should be simple and the net cage must have approximately the same weight as a traditional net cage. The shape of the net cage should not be baggy, and the deformed volume in current should be sufficient.

In total, seven variations of three square net cage designs have been defined with the main dimensions (width x length x depth) of 24 x 24 x 12 meters. Illustrations of the different designs are given in Figure 2 to Figure 5. The different designs are numbered as follows:

1. Standard net cage
2. Standard net cage with bending stiff bottom rope
3. Net cage with inclined ropes
4. Net cage with inclined ropes without vertical side ropes and bottom ropes
5. Net cage with twisted bottom
6. Net cage with twisted bottom, including extra side ropes
7. Net cage with twisted bottom, including extra side ropes and weights

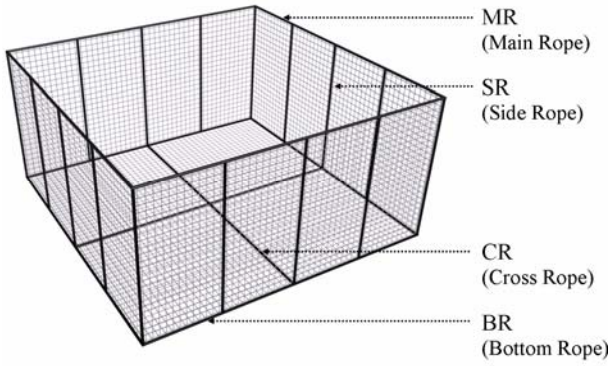

Figure 2. Standard net cage.

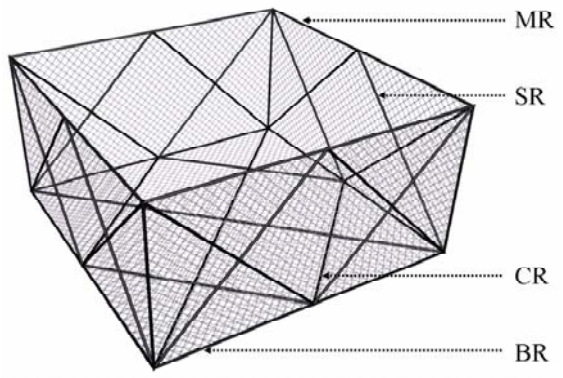

Figure 3. Net cage with inclined ropes

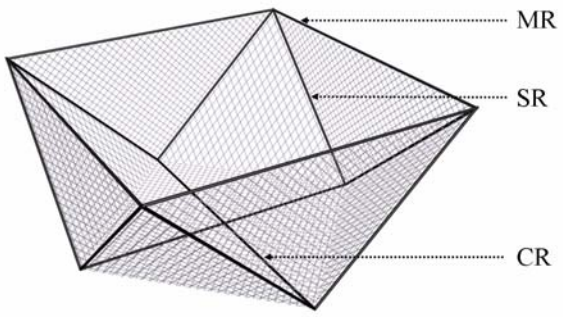

Figure 4. Net cage with twisted bottom (incorrect netting orientation in illustration).

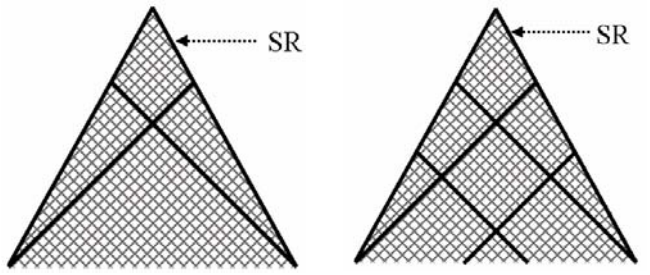

Figure 5. Design 6 (left) and design 7 (right).

The standard net cage (Design 1) represents a common net cage design. It consists of square mesh netting, 16 side ropes, traditional top-, main- and bottom ropes and 2 cross ropes. The motivation for including a bending stiff bottom rope in the standard net cage (Design 2) is to avoid stress concentrations in the bottom of the net cage during lifting.

The new "inclined ropes" design has a diamond mesh netting, 16 inclined side ropes that follow the direction of the netting mesh, a vertical side rope in each corner and a bottom cross rope pattern consisting of 6 cross ropes.

Design 4 is a modification of net cage with inclined ropes, where the ropes that are diagonal to the netting mesh, i.e. bottom ropes and vertical side ropes are removed.

Strength analysis of net the cage with twisted bottom (Design 5) reveals stress concentrations in the side due to the fact that the netting is cut across the twines (as shown in Figure 5). This resulted in design 6, which has extra side ropes that reduce the stress in the netting. Analysis of Design 5 also showed that its volume is greatly reduced in current. Design 7 has an increased number of ropes (6 cross ropes) and weights, which should give increased volume in current.

3 ANALYSIS METHOD

The net cages were modelled in the FEA (Finite Element Analysis) program ABAQUS, and a non-linear dynamic explicit analysis was carried out. The loads were static, but a dynamic analysis was applied in order to avoid zero stiffness when netting elements become slack (netting does not take compression). The inertia will keep the numerical solution stable.

ABAQUS/Explicit uses a central difference rule to integrate the equation of motion explicitly through time, using the kinematics conditions at one increment to calculate the kinematics conditions at the next increment (Hibbit, Karlson & Sorensen, Inc. 2002). At the beginning of the increment the program solves for dynamic equilibrium, which states that the nodal mass matrix, **M**, times the nodal accelerations, **ü**, equals the total nodal forces (the difference between the external applied forces, **P**, and the internal element forces, **I**):

$$\mathbf{M}\ddot{\mathbf{u}} = \mathbf{P} - \mathbf{I} \tag{1}$$

The explicit procedure in ABAQUS always uses a lumped mass matrix and solving for the acceleration is trivial. The velocity at the middle of the current increments is calculated by integration of the accelerations through time assuming constant acceleration and using the central difference rule:

$$\dot{\mathbf{u}}\left(t+\tfrac{\Delta t}{2}\right) = \dot{\mathbf{u}}\left(t-\tfrac{\Delta t}{2}\right) + \tfrac{1}{2}\left(\Delta t\left(t+\Delta t\right)+\Delta t\left(t\right)\right)\cdot\ddot{\mathbf{u}}\left(t\right) \tag{2}$$

Displacement at the end of the increment:

$$\mathbf{u}\left(t+\Delta t\right) = \mathbf{u}\left(t\right) + \Delta t\left(t+\Delta t\right)\cdot\dot{\mathbf{u}}\left(t+\tfrac{\Delta t}{2}\right) \tag{3}$$

The term "explicit" refers to the fact that the state at the end of the increment is based solely on the displacements, velocities and accelerations at the beginning of the increment. The increments must be small, ensuring a nearly constant acceleration during an increment.

Strain is then calculated by integration of the strain rate, which is found for one element as the relationship between velocity at both nodes and the element length:

$$d\varepsilon_{element} = \int \frac{\dot{u}_{node\,1} - \dot{u}_{node\,2}}{l_{element}} \tag{4}$$

Stresses are found using Hook's Law: $\sigma = E \cdot \varepsilon$.

4 MODEL DESCRIPTION

4.1 *FEA model*

Only the net cage is modelled. Top rope and netting between main and top rope (jump netting) is not included in the models.

To model the complete geometry of a net cage requires a vast number of degrees of freedom. Thus, major model simplifications must be performed to reduce the computation time to an acceptable level.

The knitted netting is made out of very thin filaments, and the total bending stiffness of these filaments is thus very small (Slaattelid, 1993). Therefore the bending stiffness is neglected by disregarding all rotational degrees of freedom in the model.

For the global analysis, it is not necessary to model the netting in detail. The netting twines are represented by global elements in the model, each element representing several twines in the netting.

The net cage model is built up of three-dimensional truss-elements (Hibbit, Karlson & Sorensen, Inc. 2002). Each truss element represents several parallel twines in the netting; the number of represented twines is dependent on the refinement of

the mesh. The truss elements have equivalent properties to the combined effect of the represented twines (the cross section area of the truss element is equal to the sum of the cross section areas of the represented twines).

Analyses showed that the model simplifications give negligible errors in global strength analyses of net cage constructions.

Netting does not take compression, and will collapse when subjected to compression. To model this effect, each global truss element is divided into at least two sub-elements, allowing the twines to buckle when subjected to compression.

4.2 *Material properties*

4.2.1 *Netting*

The netting used in net cages varies in material, size and construction. The netting applied in the models is knotless and knitted (Figure 6 and Figure 7), and made of Nylon 6 (Polyamide 6). The mesh width is 25.5 mm. The twines in the netting have a breaking strength of 117 kg.

To perform the strength analyses, the cross section area of the netting twines and their stiffness properties must be known. The cross section area is estimated and the stiffness properties are given from tensile testing.

It is difficult to define a precise cross section area for knitted netting. The structure of the netting twine is shown in Figure 7. The twines are knitted of three threads, each consisting of one or several bundles of very thin filaments (in the order of magnitude 2000 filaments in each bundle).

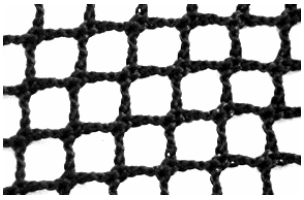

Figure 6. Raschel knitted netting.

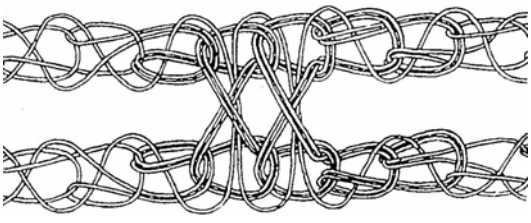

Figure 7: Raschel knitted netting. Illustration of netting construction.

Table 1. Cross section properties for netting twine.

Radius (r)	1	mm
Cross section area (A)	3	mm^2

In the FEA model, the cross section of the twines is assumed to be circular. Based on cross section and strength data for twisted twines and monofilament given in Slaattelid (1993), the cross section of the knitted netting twine is assumed to be 3 mm^2. This diameter is validated by comparing the weight of the actual netting with the weight of the modelled twines with circular cross section, which yields corresponding results.

The stiffness properties of the netting are derived from tensile testing of new netting material. The test is of mesh strength, performed by the netting and net cage producer Mørenot. The result from the test is a non-linear load-extension curve, given as nominal axial stress versus nominal strain in Figure 8.

The important information extracted from the force–strain curve is the axial stiffness, or the sum of cross section area times E-modulus for the netting material.

Unloading of the net cages is not analyzed, and an elastic material model is thus sufficient. The material properties of the netting are modelled using a hyperelastic material model. This material model allows input of test results directly in terms of stress-strain data. Based on the mesh strength test, a stress-strain-curve is established for the FEA-model. This is given in Figure 8.

Based on the stress-strain curve given in Figure 8, a partly linear stiffness is calculated for intervals of nominal strain. This is given in Table 2.

For relatively small strains, i.e. $\varepsilon_{nom} < 10$ %, the netting material can be assumed to behave as a linear elastic material. Then an E-modulus of 50 MPa (Table 2) may be assumed for the netting.

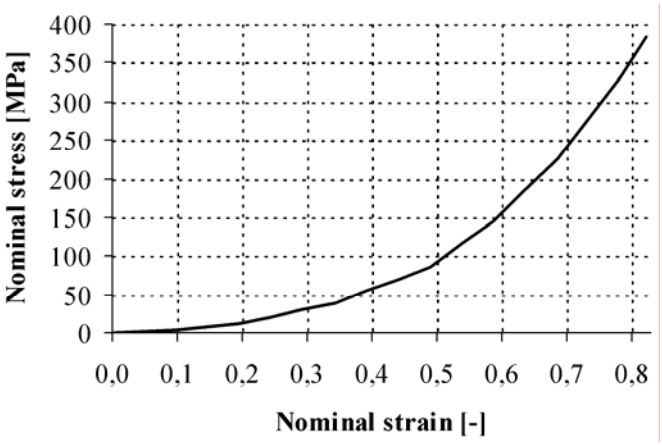

Figure 8. Stress-strain curve for netting material.

Table 2. Partly linear stiffness for netting material.

Nominal strain [%]	Stiffness* [MPa]
0 – 10	50
10 – 30	100
30 – 50	300
50 – 70	750
70 – 82	1100

*Based on tensile testing and nominal cross section area.

To avoid damage of the net cage during handling, it is important that repeated lifting of the net cage does not result in plastic strains in the netting material.

The netting is produced of polyamide 6 (Enkalon ® 540T) fibres. Based on tenacity /elongation curves for these polyamide fibres, the fibres are assumed to have only elastic deformations for strains less than 2 % (Polyamide High Performance, 2004). According to the same curves, this corresponds to a critical stress, or initial yield stress, of approximately 60 MPa and an E-modulus of 3 GPa. These values are confirmed by Ashby & Jones (1980), who state that nylon has a yield stress in the range of 49 – 87 MPa and an E-modulus of 2 – 4 GPa.

Since the netting is made out of knitted fibres, the netting has a global geometric flexibility. This means that the global strain in the netting will be greater than the local strain in the fibres. The yield stress of 60 MPa corresponds to a global axial strain of approximately 40 % in the netting twine, as shown in Figure 8.

The material properties of a net cage in operation will change significantly with time, and have significant local variation. During lifting, the netting will be subjected to large loads that are difficult to quantify due to large mass forces, unknown fouling situations and relative movement between net cage and crane vessel. Thus, it is important to introduce sufficient load and material safety factors when calculating the critical stress value.

In strength analysis of synthetic mooring ropes, a material factor of 3 should be applied according to Norwegian Standard NS 9415. For netting material, no specific material factor is given. Both the ropes and netting are made of polymers, and should thus have a material factor of the same order of magnitude. Thus the material factor of 3 was chosen for the netting. The high material factor was justified through the variations in the material properties for the netting used. In addition, the tensile strength of the twine will be less than the combined tensile strength of the fibres that make up the twine. When the netting is overloaded, it is usually the twines that break. Inspecting the construction of the netting twines (shown in Figure 7), it is obvious that the threads that make up the twine are of varying length. Thus, the tearing of the netting twine will be progressive as threads will break one by one.

There are no load factors given for lifting the net cage. Due to the large uncertainties in applied loads, a load factor of 2 is applied. This gives a total safety factor of 6, which in practice means that the netting should not be subjected to stresses greater than 10 MPa or strain greater than 16 %. The safety factor is based on many assumptions, due to lack of scientific work.

The Enkalon 540T filaments have a specific weight of 1140 kg/m^3.

4.2.2 *Ropes*

The ropes in aquaculture net cages are often made out of a combination of polypropylene and polyethylene (for instance Danline).

We have applied Danline ropes with a diameter of 16 mm, a breaking strength of approximately 44 kN and an elongation at fracture of approximately 20 %. Assuming a linear force-strain curve, the E-modulus will be 1100 MPa. The curve will be slightly non-linear, resulting in a smaller E-modulus for small strains and a larger E-modulus for large strains. Due to small strains in the ropes, elastic material properties will be sufficient. The ropes are given an E-modulus of 1000 MPa and a specific weight of 1000 kg/m^3.

In Design 2 (Standard net cage with bending stiff bottom rope), the bottom rope is modelled as a steel rod with a diameter of 20 mm (circular cross section). The bottom rope is modelled using beam elements to include the bending stiffness. The E-modulus is given as 210 GPa, and the profile is given a specific weight of 8000 kg/m^3.

5 ANALYSES

The different net cage designs are analysed for the following five load cases, as shown in Table 3:

A. Calm water
B. Current
C. Lifting –no cross rope
D. Lifting –cross rope
E. Lifting –corner

Table 3. Design and load case matrix.

Load case	Design						
(Lc)	1	2	3	4	5	6	7
A	X	X	X	X	X	X	X
B	X	X	X	X	X	X	X
C	X	X	NA	NA	NA	NA	NA
D	X	X	X	X	X	X	X
E	X	X	X	X	NA	NA	X

* X analyzed
NA not applicable

In Load Case A (LcA), the net cage is not subjected to any environmental forces or handling. The only forces acting on the net cage are the bottom weights and gravity loading due to biofouling (and the steel rod for Design 2). In LcB, current forces are added. In LcC, LcD and LcE, the net cage with bottom weights is subjected to handling and drag loads due to the velocity induced through the lifting (the net cage has no biofouling). LcC represents lifting of the net cage through a weight rope that has no connection to cross ropes. For Design 3 to 7, LcC is not applicable as all weight ropes are connected to at least one cross rope. LcD is lifting of the net cage through a weight rope that is connected to one or

two cross ropes. LcE is lifting of the corner of the net cage. For Designs 5 and 6, LcE is not applicable as it will be equal to LcD for these two designs.

When interpreting the results of the analyses, focus will be on stresses in the netting, but volume in calm water and current has also been considered and will be commented upon.

6 BOUNDARY CONDITIONS AND LOADS

6.1 *Boundary conditions*

The net cage is attached to the cage collar through the main rope. In practice, the number of connection points between the net cage and cage collar varies between the different fish cages, but as a minimum, the net cage is connected at each side rope. Various boundary conditions have been analysed, with the conclusion that the effect of the boundary condition in most cases is negligible. In all analyses presented in this paper, the net cage is connected to the cage collar at 16 points, which is equal to all connection points between main rope and side rope for a standard net cage.

6.2 *Loads*

6.2.1 *Bottom weights*

Weights with a total submerged weight of 16 kN were applied to the net cages. All weights are modelled as vertical concentrated forces at the lower end of the side ropes. Designs 1 and 2 have 16 weights of 1000 N each. Designs 3, 4 and 7 have eight weights of 2000 N, while Designs 5 and 6 have four weights of 4000 N.

6.2.2 *Gravity loads*

The net cages are assumed to be neutral in water, as the specific weight of the net cage materials are close to the specific weight of water (except for Design 2, where the steel rod will load the net cage). Net cages are often treated with anti-fouling paint, which typically will increase the net cage weight in air by approximately 50 %, but the treated net cage will still be close to neutral in water.

Biofouling can increase the submerged weight of the net cage, dependent on the type of fouling. In LcA, the net cages are subjected to a gravity load from biofouling of approximately 5000 N (equal the weight in air of the net cage model). The fouling is assumed to be evenly distributed over the net cage.

6.2.3 *Current induced loads*

It is assumed that current forces are constant over the depth and width of the net cage. The current load is modelled as a gravitation force in horizontal direction, using Newton's Law and the mass of the net cage to calculate the correct acceleration (g_h in Equation (7)).

The drag and mass force per unit length of a netting twine can, according to Morison's equation (Morrison et al, 1950), be written as:

$$dF = \tfrac{1}{2}\rho \cdot C_D \cdot D \cdot |u| \cdot u + \tfrac{1}{4}\rho \cdot \pi \cdot D^2 \cdot C_M \cdot a \qquad (5)$$

Where ρ = water density
C_D = drag coefficient
D = twine diameter
u = velocity
C_M = mass coefficient
a = acceleration

Assume ρ = 1025 kg/m^3
C_D = 1.2 -
C_M = 1 - (added mass)

This results in the following expression for drag and mass force per unit length of a netting twine [N/m]:

$$dF = 615 \cdot D \cdot u^2 + 805 \cdot D^2 \cdot a \qquad (6)$$

Current loading per unit length of netting twine is equal to the drag term (first term) in equation (6), since there is no acceleration. The biofouling will increase the diameter of the netting twines, and thus the drag forces acting on the net cage will increase. According to Norwegian Standard NS9415, the diameter of the netting should be increased by 50 % to account for bio fouling. A diameter of 3 mm was thus applied in the calculation of drag forces due to current. The total drag load [N] is calculated as given in Equation (7):

$$F_{\text{total drag}} = g_h \cdot M = \frac{dF}{dm} \cdot M = \frac{dF \cdot M}{\rho_t \cdot A} \qquad (7)$$

Where g_h = horizontal "gravitation"
M = total submerged mass of net cage and biofouling (approx. 500 kg)
dm = mass of twine per unit length
ρ_t = twine density, approx. 1000 kg /m^3

Insert given values in Equation (7) and get:

$$F_{\text{total drag}} = \frac{615 \cdot 3 \cdot 10^{-3} \cdot u^2 \cdot 500}{1000 \cdot 3 \cdot 10^{-6}} \approx 300 \cdot 10^3 \cdot u^2$$

A total drag force of 20000 N is assumed, which is equivalent to a current velocity of 0.26 m/s (and an applied horizontal acceleration g_h = 40 m/s^2). All net cage designs are subjected to drag loads due to a current velocity of 0.26 m/s. Due to the smaller surface, the total drag force will be smaller than 20 kN for Design 5, 6 and 7.

6.2.4 *Lifting load*

All net cages are lifted with a constant force of 2000 N, applied as a point load in the bottom node of a side rope. This node is also prevented from moving horizontally for LcC, LcD and LcE.

6.2.5 *Drag load*

During lifting of the net cage, gravity, drag and mass force can give major load contributions. Gravity dominates the part of the net cage above water, where neither the netting, impregnation nor the biofouling is neutral. The tearing of the net is initiated in the area close to the attachment point of the weight rope. In LcC, LcD and LcE, the net cage is assumed to have no biofouling, and gravity forces are thus not included.

Drag and mass forces are important with regard to tearing of the net cage during handling. Drag loads are dependent on the lifting velocity and the diameter of the netting, while mass force depends on lifting acceleration and diameter (as shown in Eq. 6).

When the net cage is lifted with close to constant velocity (small or zero acceleration), the forces acting on the net cage during handling are only dependent on the velocity. However, setting the net cage in motion from a stationary condition may result in huge accelerations and consequently huge mass forces, representing a jerk in the net cage.

In the analysis, the mass forces are not included, mainly because they are hard to quantify. Thus, the analysis is of a lifting operation with constant velocity and does not include the jerk at the initiation of the lifting. The drag force is modelled as a vertical gravitation force. As a simplification, it is equally distributed over the net cage. In practice, the lifting velocity will vary over the net cage, but this effect is difficult to model in a general FEA-program. This way of modelling the drag loads is sufficient for the purpose of these analyses, which is to compare different designs.

A total drag force of 5000N was applied to the net cage. This corresponds to a lifting velocity of 0.2 m/s.

7 RESULTS

The results from the finite element analyses described in Table 3 are given as maximum stress in the netting in Figure 9 and Figure 10. The locations of these maximum stresses are given in Table 4.

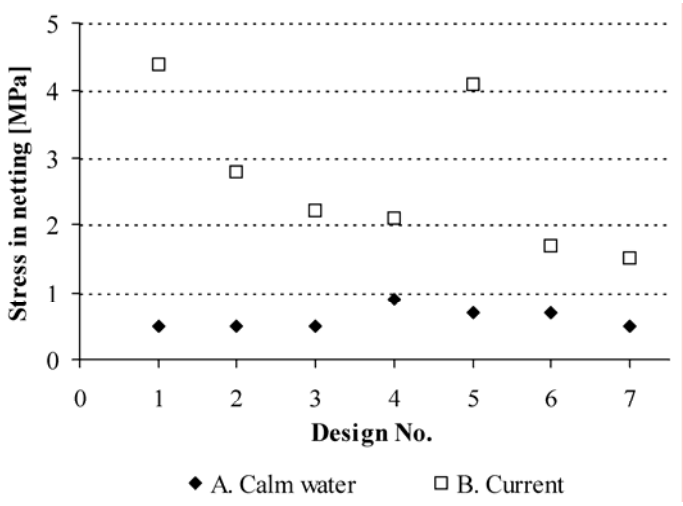

Figure 9. Maximum stress in netting for net cage in calm water and current.

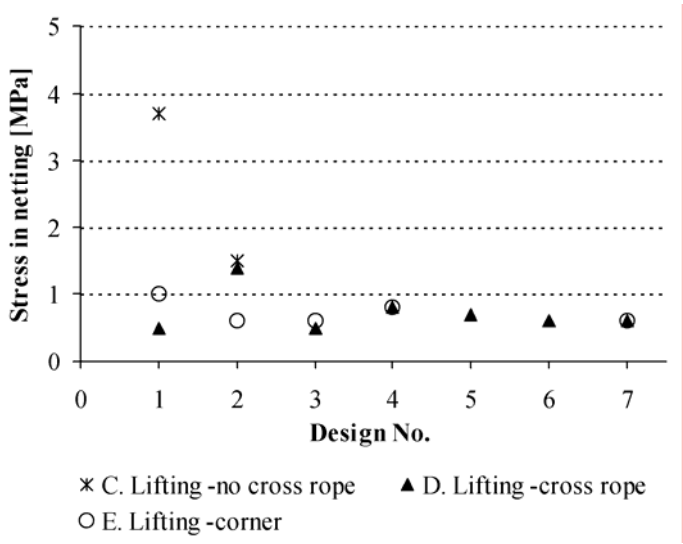

Figure 10. Maximum stress in netting during lifting of the net cage.

Table 4. Location of maxmium stress in netting.

Load case	Design						
	1	2	3	4	5	6	7
A	S	S	S	S	S	S	S
B	B	B	S	S	S	S	S
C	B	B/S	NA	NA	NA	NA	NA
D	B	S	S	BY	S	S	S
E	B	S	S	BY	NA	NA	S

* S Net cage sides
B Net cage bottom
BY Boundary
NA not applicable

8 DISCUSSION AND CONCLUSIONS

The analyses show no stresses above the critical stress of 10 MPa in the netting. However, the loads applied are moderate. It is not unusual that net cages experience current velocities above 0.5 m/s, which in this cage equals a total drag force above 70 kN and a significant increase in the maximum stresses in the netting. Lifting a net cage with heavy biofouling and an initial large acceleration can introduce critical stresses in the netting. In addition, strong currents may occur during lifting (although the farmers try to avoid lifting the net cage in strong currents). Figure 9 and Figure 10 show that all the net cage designs have stresses far below the critical stress range in calm water.

Comparing the results, it is obvious that lifting of the net cage should be performed using weight ropes that are connected to cross ropes. The analyses indicate that lifting the net cage through weight ropes that are connected to cross ropes does not lead to critical stresses in the netting. This has recently been implemented in Norwegian Standard NS9415. The results also indicate that at locations with strong currents, all side ropes should be connected to cross ropes.

Lifting the net cages by the corner does not reveal high stresses in these analyses, but for the standard net cage the stresses in the netting can become critical during fast lifting of a net cage with heavy fouling.

The net cage with inclined ropes experienced smaller or equal stress in the netting compared to the standard net cage. Even though stresses in the netting are limited, practical use of this design will be difficult due to the baggy shape of the net cage. Design 3 and 4 will both have a baggy shape especially in the corners and bottom area. This is a problem, as dead fish may be collected in these baggy areas. On the positive side, the analyses indicate that there will be no problem with abrasion on the netting from the weights in current, as it can be for standard net cages. The leeward side of the net in current will be closer to vertical than in a standard net cage. This is positive as it reduces the chance for propellers on boats to make contact with the netting. Propeller damage to netting is known to have caused several cases of escape of cultured fish.

Except for Design 5, the stresses in the netting are small for all load cases for the net cage with twisted bottom. All three variations of the net cage have a full and smooth shape in calm water, especially Designs 5 and 6, which show no signs of bags in the netting. Designs 5 and 6 experienced large deformations in current, although this is improved by introducing extra ropes and weights in Design 7. The distance the net cage was lifted when applying the given lifting load varied. While Designs 1 to 4 was lifted between 4 and 7 m for the given lifting load, Designs 5 and 6 was lifted 12 m (all the way up to the water surface) without inducing critical stresses in the netting. Design 7 was lifted 7.5 m.

These analyses show that Designs 6 and 7 are the most promising new designs. The maximum stresses in the netting are relatively low, reducing the risk of tearing of the netting and escape of cultured fish. In other aspects, the net cage has similar or better properties than a traditional net cage.

8.1 *Further work*

- Establish plastic material models for Raschel knitted netting (both new and used netting), based on tensile testing. Include damage effects and time dependent behaviour.
- Establish method for fatigue calculations (e.g. SN-curves).
- Establish suitable material and load factors. Analyses with varying lifting loads and more load cases (e.g. combined current and lifting) including dynamic loads (e.g. from waves).
- Dynamic analysis where drag loads are calculated directly from the velocity at each node.

9 ACKNOWLEDGEMENTS

This work is sponsored by the Norwegian Research Council through the SIKTEK (Safe and environmentally friendly fish farming constructions) and the IntelliStruct (Intelligent structures in fisheries and aquaculture) projects, and FHF (Norwegian fishery an aquaculture industry research fund).

10 REFERENCES

Heide, Mats Augdal & Moe, Heidi 2004. *Alternative notkonsepter, Nye rømmingssikre merdkonsept.* (In Norwegian)

Moe, Heidi & Pedersen, Roar & Heide, Mats A. 2004a. *Oversikt over notsystemer, Nye rømmingssikre merdkonsept.* (In Norwegian)

Moe, Heidi & Lien, Egil 2004b. *Modellforsøk, Nye rømmingssikre merdkonsept.* (In Norwegian)

Hibbit, Karlson & Sorensen, Inc. 2002. ABAQUS 6.3-1 Documentation.

MatWeb –Material Property Data. http://www.matweb.com.

Ashby & Jones 1980. *Engineering materials 1, an introduction to their Properties and Applications.* England: Pergamon Press.

Morison, J. R. & O'Brien, M. P. & Johnson, J. W. & Schaaf, S. A: *The force exerted by surface waves on piles.* 1950.

Norwegian Standards NS 9415. 2003. *Marine Fish farm. Requirements for design, dimensioning, production, installation and operation.* (In Norwegian)

Slaattelid, Olav H. 1993. *Materialdata og egenskaper for notlin og tau*. (In Norwegian, Confidential)

Nasjonal tiltaksplan mot rømming. 2000. (In Norwegian)

Polyamide High Performance, 2004. Private communication.

Appendices

Appendix A: Comparing results from uniaxial tensile test and mesh strength tests.

Appendix B: Nominal dimensions of netting materials.

Appendix C: Tensile properties of netting with cod bite damage.

Appendix A: Comparing results from uniaxial tensile test and mesh strength tests.

This appendix compares the force-strain results from the developed uniaxial tensile test (Paper 1) and the standardized mesh strength test (ISO, 2002). The uniaxial tensile test of netting materials was developed in order to determine tensile properties of knotless netting with loads acting along the twines (Figure 1b). The only standardized method for testing of knotless netting materials is the mesh breaking force test, which yields the tensile properties of one mesh (Figure 1a). The mesh breaking force test set-up is illustrated for knotted netting materials in Figure 1a, while Figure 1b shows a part of the test specimen for the uniaxial test.

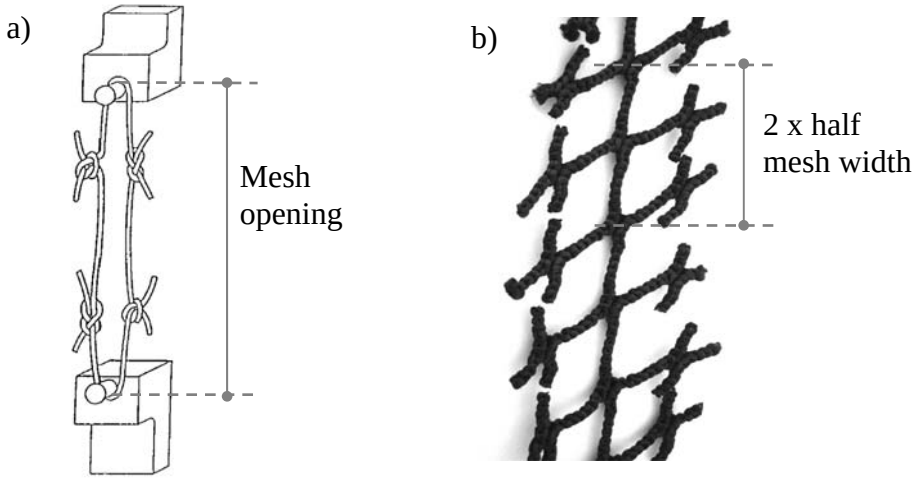

Figure 1: a) Mesh breaking force test (ISO, 2002). b) Uniaxial test specimen (Moe et al., 2007b).

As a part of the validation of the developed tensile test method, three different netting materials were tested using both the mesh breaking force test and the developed uniaxial tensile test. The netting materials are described in Table 1 (for details see Moe et al. 2007b). The test speed of the mesh strength test was 100 mm/s.

Table 1: Properties of tested netting materials (S_m given by producers).

Netting material number	Dry half mesh width $w_{1/2}$ [mm]	Min. wet mesh strength S_m [kg]	Cross sectional area* A [mm^2]	Total linear density [dtex]**	Loops along twine n_l	Hard-ness h [-]	Pre-tension P [N]
1	25	151	3.43	24400	7	1.00	9.6
2	27.2	170	4.13	27200	7	1.01	11.6
3	27.5	180	5.11	30000	7	1.11	14.3

* of solid material
** 1 dtex = 10^{-4} g/m.

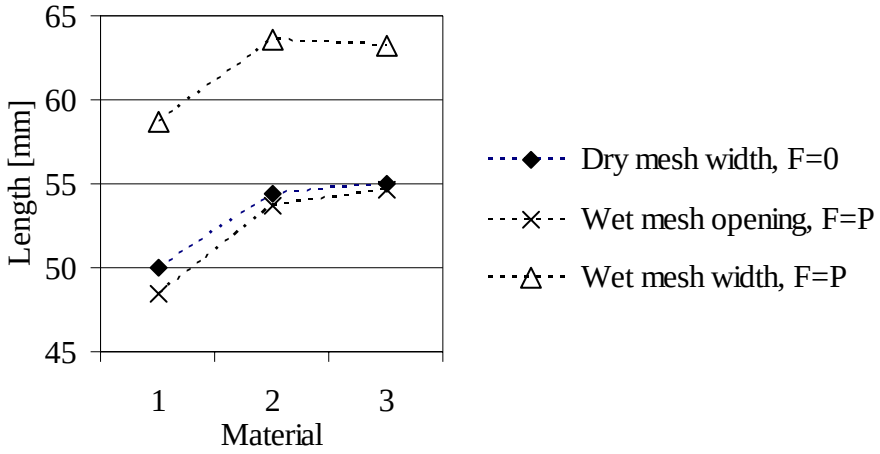

Figure 2: Various measures of mesh size for netting materials 1, 2 and 3 given either for unloaded netting (F=0) or at pretension (F=P).

During the uniaxial test, the elongation over a given number of twines and knots was measured using an extensometer as explained in Moe et al. 2007b. (Due to the limited size of the test piece of netting material 3, the elongation was measured over 2 meshes only. This should not have any significant effect on the results.) In connection with the mesh strength test, the mesh opening was measured prior to stretching (Figure 1a) and the increase in mesh opening was logged during loading. Figure 2 gives the dry mesh width for unloaded materials (ISO 1107, 2002a), the modified wet mesh opening at pretension (2 mm were added to the mesh opening to

account for the twine thickness), and wet mesh width at pretension from the uniaxial test (calculated as 2 times the half mesh width). Wetting of the netting and application of pretension increased the mesh width by 15-17% (discussed in Appendix B), while the modified wet mesh opening at pretension was 1-3% smaller than the dry mesh width.

Figure 3 gives force-strain results for one twine from the two different test methods for netting material number 2. The results from the mesh strength test are presented using two different strain estimates: Based on the (modified) mesh opening at pretension: $\varepsilon_{m\_o}(t) = \Delta L(t) / \left(w_{m\_o} + 2mm\right)$, and based on the mesh width at pretension (from the uniaxial test): $\varepsilon_{m\_w}(t) = \Delta L(t) / w_{m\_w}$. It was assumed that the two parallel twines stretched in the mesh strength test carried equal loads, and the tensile load in one twine was calculated as the measured load divided by 2. The strain during the uniaxial test was calculated as the change in length between extensometer arms, ΔL_e, divided by the nominal length between extensometer arms at pretension, L_{e0}, (Fig. 4 in Moe et al., 2007b): $\varepsilon_e(t) = \Delta L_e(t) / L_{e0}$.

Comparing the results from the mesh strength test and uniaxial test showed that the resulting stiffness was different between the two tests methods. Using the mesh width for mesh strain estimates, opposed to mesh opening, gave a better coherence. However, the difference in stiffness was significant, especially for the lower strains where the stiffness from the mesh strength test was low compared to the uniaxial test results as shown in Table 2. The table also shows that deviation in strain and force at break in one twine was insignificant between the two test methods.

In conclusion, the developed uniaxial tensile test resulted in a force at break corresponding to half the mesh strength, which validates the developed test method. Comparing the stress-strain relations for the two different tests revealed significant differences in stiffness properties, especially if the mesh opening was used in the strain estimates for the mesh strength test.

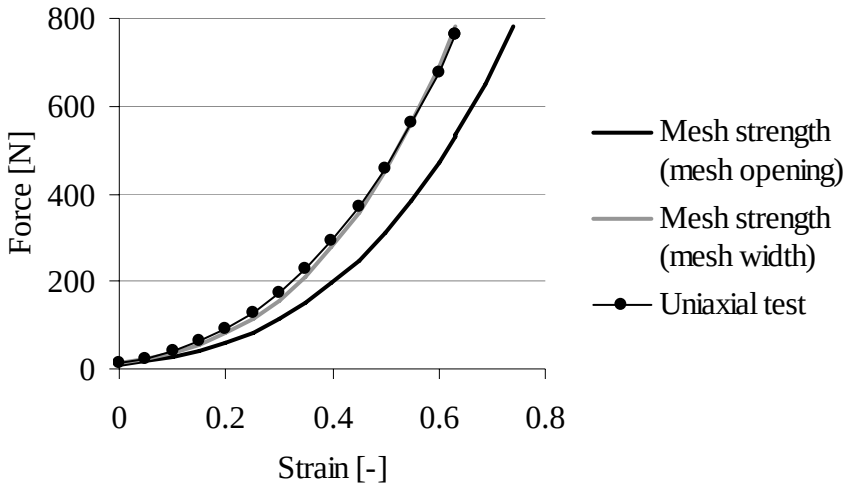

Figure 3: Resulting force-strain curves for a netting twine. Mesh strength (mesh opening): Strain was calculated based on (modified) mesh opening. Mesh strength (mesh width): Strain was calculated based on mesh width. Uniaxial test: Strain was calculated from extensometer measurements.

Table 2: Deviation in tensile properties between results from uniaxial test and mesh strength test (strain based on mesh width) for one twine [%]. (Positive number means uniaxial test yielded the higher value).

	Stiffness			Breaking strain	Twine breaking force
	0-10 % strain	10-30 % strain	30-60 % strain		
Material 1	21	9	-7	0	- 3
Material 2	15	12	-4	0	- 1
Material 3	19	24	3	-3	+ 3

APPENDIX B: Nominal dimensions of netting materials

Traditional knotless netting materials for aquaculture (Raschel knitted Polyamide multifilaments) have a very low stiffness for small tensile loads. In fact, they are so flexible it is hard to define a precise initial length. The traditional way of measuring the initial length of twisted netting twines is to apply a pretension (dependent on mass per length) and measure the length at this level (ISO 3790, 1976). The pretension was calculated according to ISO 3790 for 23 different dimensions (half mesh width and mesh strength) of typical knotless netting materials presented in Moe et al., 2007b. This resulted in pretensions between 5 and 11 N for materials with a twine breaking strength of approximately 270 – 930 N, i.e. the pretension was 1-2 % of the ultimate strength of the material. However, this small pretension resulted in significant strains of several percentages. Wetting of the netting and application of pretension resulted in an average strain of 15±4 % for the 23 materials, approximately 8 % due to wetting (Moe et al., 2007b). The wet half mesh width at pretension is plotted against dry half mesh width in Figure 1. The linear trend, representing the on average 15 % difference is indicated.

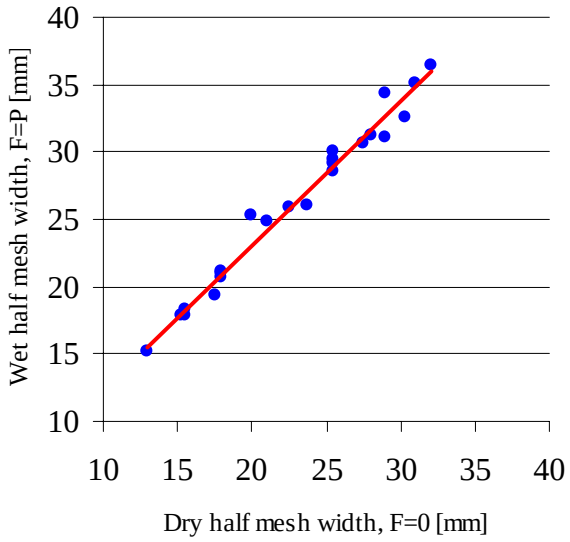

Figure 1: Relationship between half mesh width of wetted knotless netting at pretension and dry, unloaded netting. A linear trend is indicated.

The variation in strain for wet netting materials at pretension did not seem to be significantly dependent on half mesh width, hardness, thickness or number of loops in twine (defined in Moe et al., 2007b). The half mesh width at pretension for wet netting are given for the 23 individual materials in Figure 2 together with the relative increase in mesh width compared to dry and unloaded netting. In Figure 3, estimated hardness is compared to the increase in half mesh width. There is a tendency indicating that the relative increase in half mesh width may be dependent on initial dry half mesh width and hardness. However, the deviation in results are too large to make any hypothesis or conclusions.

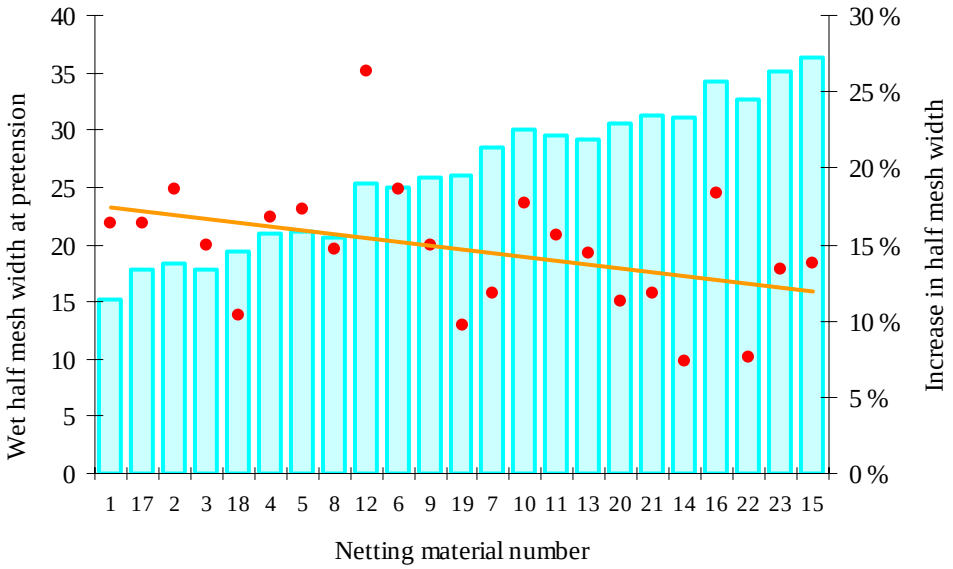

Figure 2: Wet half mesh width at pretension (columns) and percentage increase in half mesh width due to application of water and pretension (dots and indicated linear trend). Netting materials are sorted by increasing dry and unloaded half mesh width.

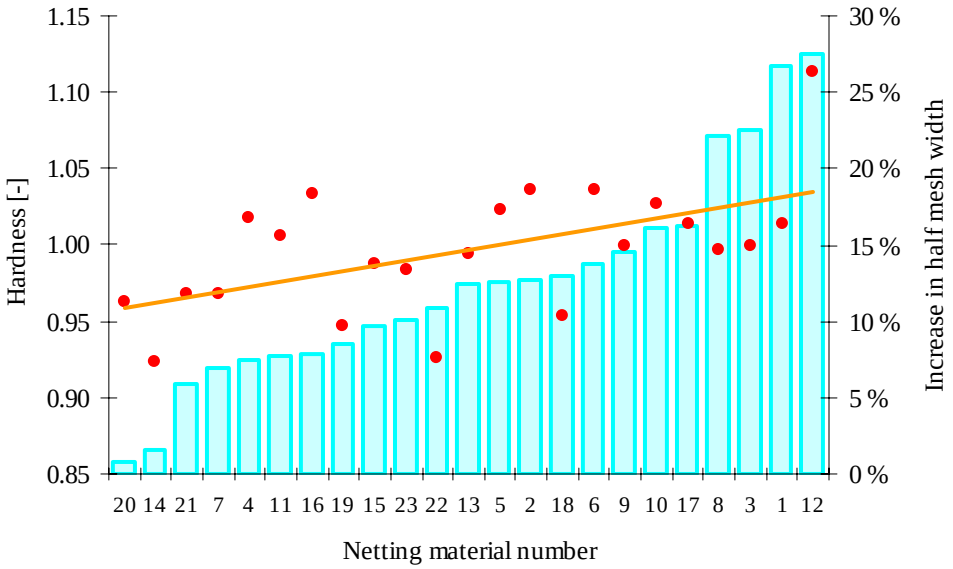

Figure 3: Estimated hardness (columns) and percentage increase in half mesh width due to application of water and pretension (dots and indicated linear trend). Netting materials are sorted by increasing estimated hardness.

The mentioned large flexibility for small loads can be challenging to handle in a structural analysis. Assuming that the elongation due to wetting was 8 % and that the strain increased further by 7 % during introduction of pretension, this initial strain can be included by one of the following methods:

1 The netting can be modelled with the length at pretension, on average 15 % longer than the half mesh width of dry netting materials. This can however be difficult in practice, as the netting dimensions will exceed the dimensions of the ropes.

2 The stiffness of the netting for strains less then 15 % can be modelled as $K = \sigma/\varepsilon = P/(\varepsilon A) = 19MPa$. ($P/A = 2.80MPa$ for all materials, $\varepsilon = 0.15$).

3 The netting can be modelled with wet dimensions, and the stiffness of the netting can then be modelled as $K = 2.80MPa/0.07 = 40MPa$ for strains less then 7 %.

The netting with anti-fouling treatment was impregnated and should in theory not absorb water. It was thus tested in dry condition. Moe et al. (2007b) showed that the anti-fouling treatment reduced the initial twine length. Figure 4 gives the half mesh width at pretension and increase in half mesh width at pretension (compared to dry unloaded and untreated materials) for materials with anti-fouling treatment. Figure 4 shows that at pretension, the half mesh width of treated netting was 2±1 % larger than for dry, untreated and unloaded netting. Thus, materials with anti fouling treatment may be modelled with their dimensions for dry, untreated and unloaded netting materials, using the material properties given in Moe et al. (2007b).

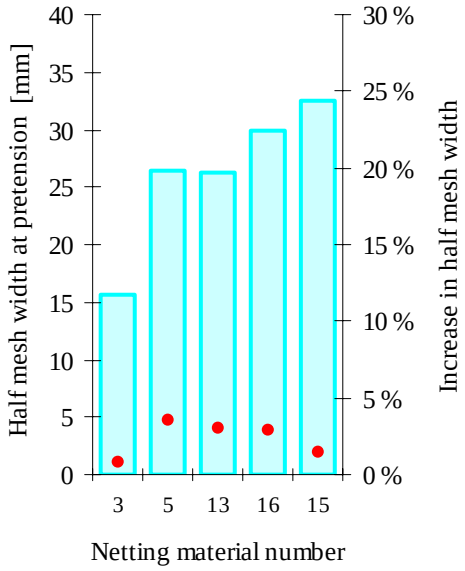

Figure 4: Increase in half mesh width at pretension for materials with anti-fouling treatment. Half mesh width at pretension (columns) and percentage increase in half mesh width due to application and pretension (dots). Netting materials are sorted by increasing dry half mesh width.

APPENDIX C: Tensile properties of netting with cod bite damage

The nature of the cod bite attack on traditional, multifilament netting materials was described based on studies of cod interaction with traditional knotless netting and resulting fracture damage on netting fibres. The cod bite attack was described as follows: The cod bit into the netting and filaments were caught behind its teeth. The cod made powerful movements with head and body, and the filaments were subjected to shear and tensile forces. In this process filaments were pulled out of the netting and torn. After several bite attacks in one area, the netting was visibly frayed and in time holes could be created. Studies of fractured filaments due to natural and simulated cod bite, revealed fractures with signs of tension and shear overloading and very little abrasion damage on the fibres (Figure 1).

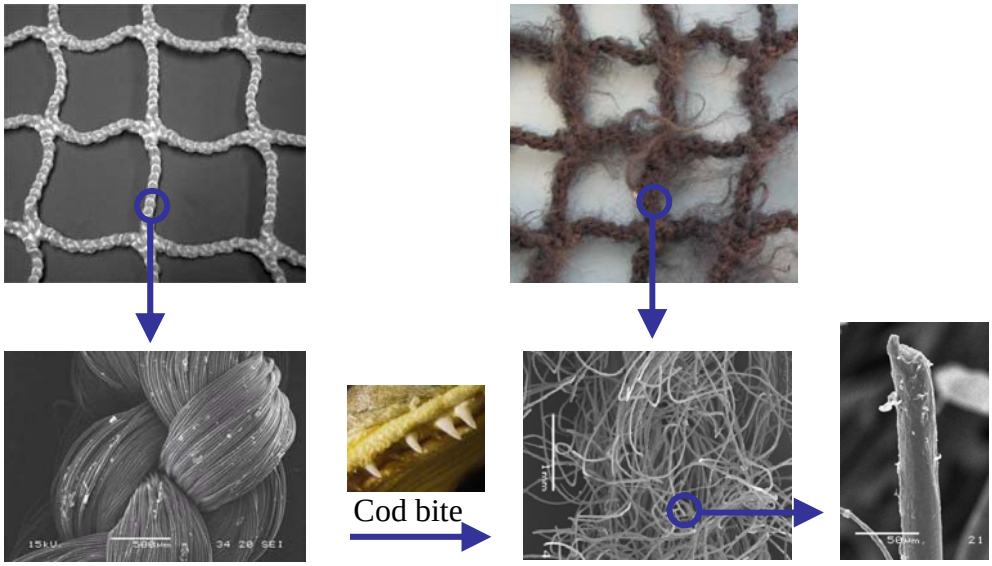

Figure 1: Study of cod bite damage on netting. Undamaged netting to the left, netting subjected to cod bite on the right. (Photo: Heidi Moe, SEM-images: SINTEF Materials and Chemistry).

Three samples of netting from three different net cages used in cod aquaculture were studied in order to get an impression of the effect of cod bite damage on tensile properties. All test samples had areas with signs of wear and tear due to cod bite (frayed netting). Figure 2 shows the three test samples (called A, B and C) after they had been subjected to mesh strength tests. The original mesh strength of the materials, their age and load history was not known.

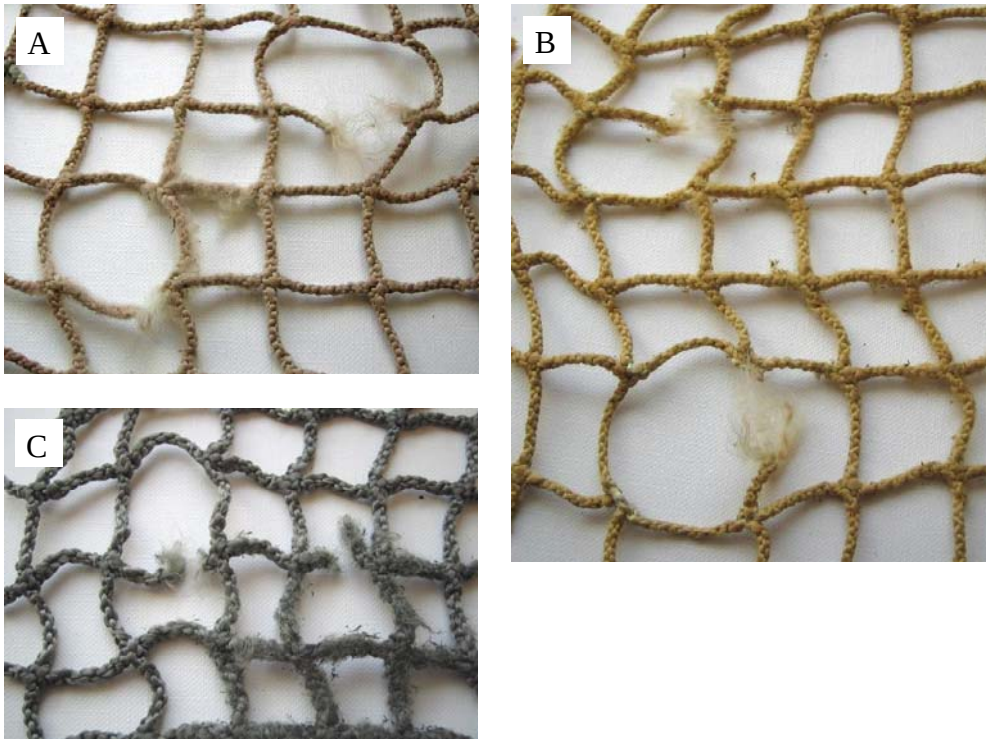

Figure 2: Test sample A, B and C with cod bite damage and broken meshes from mesh strength tests.

Two mesh strength tests were performed on each netting sample: One in an area that was considered to have insignificant cod bite damage (the netting was not visibly frayed), the other using a mesh with frayed twines. The tests were performed as follows:

1. The netting was mounted in a tensile test machine using hooks suitable for mesh strength testing (as described in ISO 1806 and Appendix A).

2. The mesh was applied a small pretension of 2-5 N.
3. The mesh opening was measured as the smallest distance between the inside circumference of the two hooks.
4. The mesh was stretched to fracture at a velocity of 100 mm/min, during which the tensile load and elongation were logged.

The results from the mesh strength tests are shown in Table 1, Figure 3 and Figure 4. The results show that bite damage reduced the mesh opening, i.e. the twine length was reduced when the cod pulled filaments out of the twine. The netting areas that were subjected to cod bite had a significant reduction in strength (35-47%), probably resulting in a strength less than the required 65 % of the mesh strength of new netting (Standard Norway, 2004). The decreased twine length and torn filaments reduced the tensile stiffness of the netting materials and increased the strain at break (based on nominal mesh opening measures). However, the mesh opening at break was reduced to 83-93 % of the mesh opening at break for the undamaged mesh.

Table 1: Properties of used netting with and without bite damage.

	A		**B**		**C**	
	UD*	CB**	UD*	CB**	UD*	CB**
Mesh opening [mm]	36	34	41	36	30	21
Reduction in mesh opening [%]	-	5	-	14	-	31
Mesh strength [kg]	65	34	92	60	90	56
Reduction in mesh strength [%]	-	47	-	35	-	37
Mesh opening at break [mm]	72	65	76	70	71	59
Reduction in mesh opening at break [%]	-	10	-	7	-	17

* Undamaged netting
** Netting with cod bite damage

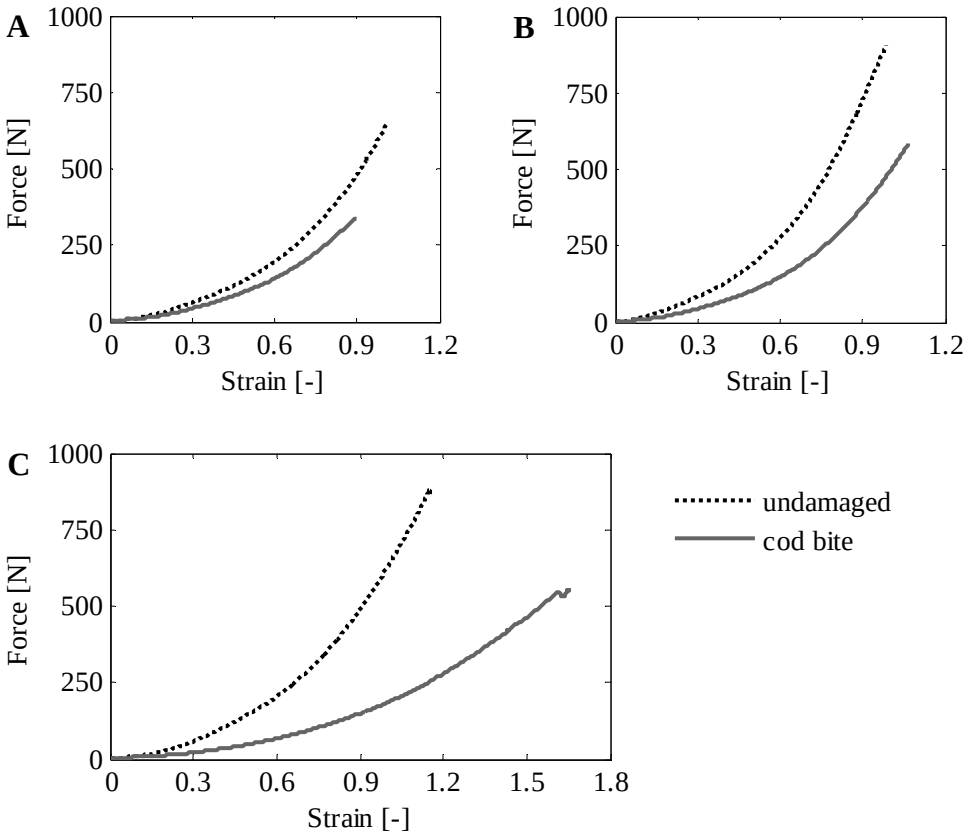

Figure 3: Force-strain curves for test samples A, B and C from single mesh strength tests of undamaged netting and netting with cod bite damage. Strain was calculated based on of measurement of nominal mesh opening of each mesh.

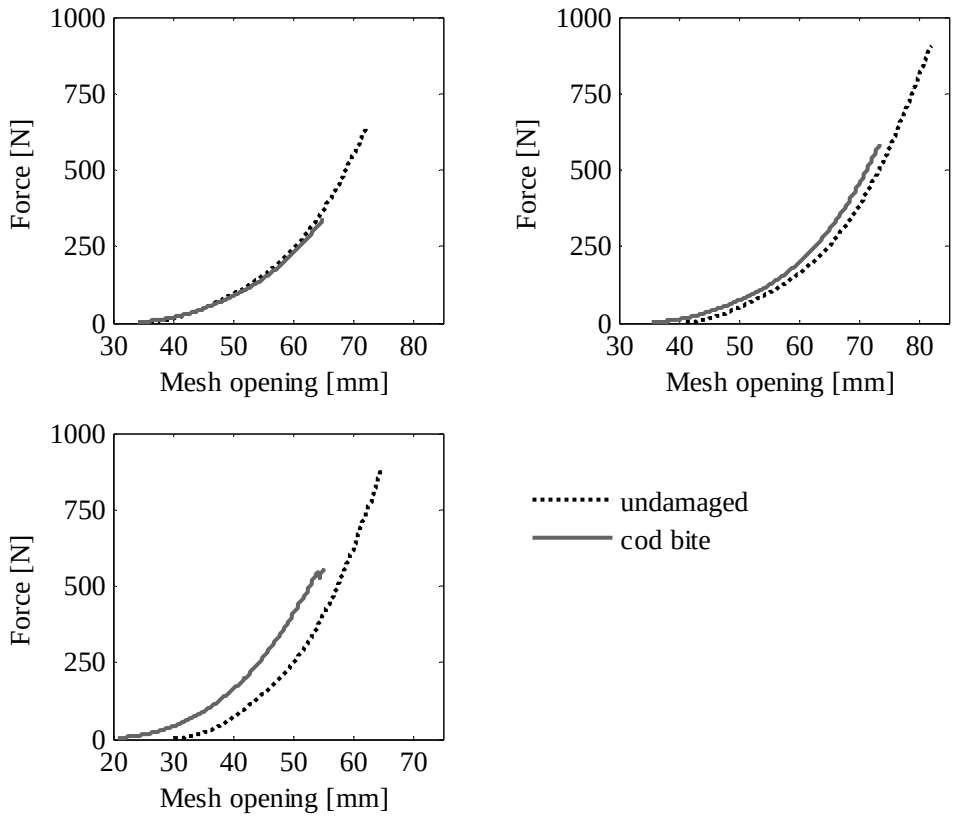

Figure 4: Force-displacement curves for test samples A, B and C from single mesh strength tests of undamaged netting and netting with cod bite damage. Force is given for measured mesh opening.

DEPARTMENT OF STRUCTURAL ENGINEERING
NORWEGIAN UNIVERSITY OF SCIENCE AND TECHNOLOGY

N–7491 TRONDHEIM, NORWAY
Telephone: +47 73 59 47 00 Telefax: +47 73 59 47 01

"Digital Models in Engineering. A Study on why and how engineers build and operate digital models for decisison support", J. Høyte, 1992:75, ISBN 82-7119-429-1, ISSN 0802-3271.

"Sparse Solution of Finite Element Equations",
A. C. Damhaug, 1992:76, ISBN 82-7119-430-5, ISSN 0802-3271.

"Some Aspects of Floating Ice Related to Sea Surface Operations in the Barents Sea",
S. Løset, 1992:95, ISBN 82-7119-452-6, ISSN 0802-3271.

"Modelling of Cyclic Plasticity with Application to Steel and Aluminium Structures",
O. S. Hopperstad, 1993:7, ISBN 82-7119-461-5, ISSN 0802-3271.

"The Free Formulation: Linear Theory and Extensions with Applications to Tetrahedral Elements with Rotational Freedoms", G. Skeie, 1993:17, ISBN 82-7119-472-0, ISSN 0802-3271.

"Høyfast betongs motstand mot piggdekkslitasje. Analyse av resultater fra prøving i Veisliter'n",
T. Tveter, 1993:62, ISBN 82-7119-522-0, ISSN 0802-3271.

"A Nonlinear Finite Element Based on Free Formulation Theory for Analysis of Sandwich Structures", O. Aamlid, 1993:72, ISBN 82-7119-534-4, ISSN 0802-3271.

"The Effect of Curing Temperature and Silica Fume on Chloride Migration and Pore Structure of High Strength Concrete", C. J. Hauck, 1993:90, ISBN 82-7119-553-0, ISSN 0802-3271.

"Failure of Concrete under Compressive Strain Gradients",
G. Markeset, 1993:110, ISBN 82-7119-575-1, ISSN 0802-3271.

"An experimental study of internal tidal amphidromes in Vestfjorden",
J. H. Nilsen, 1994:39, ISBN 82-7119-640-5, ISSN 0802-3271.

"Structural analysis of oil wells with emphasis on conductor design",
H. Larsen, 1994:46, ISBN 82-7119-648-0, ISSN 0802-3271.

"Adaptive methods for non-linear finite element analysis of shell structures",
K. M. Okstad, 1994:66, ISBN 82-7119-670-7, ISSN 0802-3271.

"On constitutive modelling in nonlinear analysis of concrete structures",
O. Fyrileiv, 1994:115, ISBN 82-7119-725-8, ISSN 0802-3271.

"Fluctuating wind load and response of a line-like engineering structure with emphasis on motion-induced wind forces",
J. Bogunovic Jakobsen, 1995:62, ISBN 82-7119-809-2, ISSN 0802-3271.

"An experimental study of beam-columns subjected to combined torsion, bending and axial actions", A. Aalberg, 1995:66, ISBN 82-7119-813-0, ISSN 0802-3271.

"Scaling and cracking in unsealed freeze/thaw testing of Portland cement and silica fume concretes", S. Jacobsen, 1995:101, ISBN 82-7119-851-3, ISSN 0802-3271.

"Damping of water waves by submerged vegetation. A case study of laminaria hyperborea",
A. M. Dubi, 1995:108, ISBN 82-7119-859-9, ISSN 0802-3271.

"The dynamics of a slope current in the Barents Sea",
Sheng Li, 1995:109, ISBN 82-7119-860-2, ISSN 0802-3271.

"Modellering av delmaterialenes betydning for betongens konsistens",
Ernst Mørtsell, 1996:12, ISBN 82-7119-894-7, ISSN 0802-3271.

"Bending of thin-walled aluminium extrusions",
Birgit Søvik Opheim, 1996:60, ISBN 82-7119-947-1, ISSN 0802-3271.

"Material modelling of aluminium for crashworthiness analysis",
Torodd Berstad, 1996:89, ISBN 82-7119-980-3, ISSN 0802-3271.

"Estimation of structural parameters from response measurements on submerged floating tunnels",
Rolf Magne Larssen, 1996:119, ISBN 82-471-0014-2, ISSN 0802-3271.

"Numerical modelling of plain and reinforced concrete by damage mechanics",
Mario A. Polanco-Loria, 1997:20, ISBN 82-471-0049-5, ISSN 0802-3271.

"Nonlinear random vibrations - numerical analysis by path integration methods",
Vibeke Moe, 1997:26, ISBN 82-471-0056-8, ISSN 0802-3271.

"Numerical prediction of vortex-induced vibration by the finite element method",
Joar Martin Dalheim, 1997:63, ISBN 82-471-0096-7, ISSN 0802-3271.

"Time domain calculations of buffeting response for wind sensitive structures",
Ketil Aas-Jakobsen, 1997:148, ISBN 82-471-0189-0, ISSN 0802-3271.

"A numerical study of flow about fixed and flexibly mounted circular cylinders",
Trond Stokka Meling, 1998:48, ISBN 82-471-0244-7, ISSN 0802-3271.

"Estimation of chloride penetration into concrete bridges in coastal areas",
Per Egil Steen, 1998:89, ISBN 82-471-0290-0, ISSN 0802-3271.

"Stress-resultant material models for reinforced concrete plates and shells",
Jan Arve Øverli, 1998:95, ISBN 82-471-0297-8, ISSN 0802-3271.

"Chloride binding in concrete. Effect of surrounding environment and concrete composition",
Claus Kenneth Larsen, 1998:101, ISBN 82-471-0337-0, ISSN 0802-3271.

"Rotational capacity of aluminium alloy beams",
Lars A. Moen, 1999:1, ISBN 82-471-0365-6, ISSN 0802-3271.

"Stretch Bending of Aluminium Extrusions",
Arild H. Clausen, 1999:29, ISBN 82-471-0396-6, ISSN 0802-3271.

"Aluminium and Steel Beams under Concentrated Loading",
Tore Tryland, 1999:30, ISBN 82-471-0397-4, ISSN 0802-3271.

"Engineering Models of Elastoplasticity and Fracture for Aluminium Alloys",
Odd-Geir Lademo, 1999:39, ISBN 82-471-0406-7, ISSN 0802-3271.

"Kapasitet og duktilitet av dybelforbindelser i trekonstruksjoner",
Jan Siem, 1999:46, ISBN 82-471-0414-8, ISSN 0802-3271.

"Etablering av distribuert ingeniørarbeid; Teknologiske og organisatoriske erfaringer fra en norsk ingeniørbedrift", Lars Line, 1999:52, ISBN 82-471-0420-2, ISSN 0802-3271.

"Estimation of Earthquake-Induced Response",

Símon Ólafsson, 1999:73, ISBN 82-471-0443-1, ISSN 0802-3271.

“Coastal Concrete Bridges: Moisture State, Chloride Permeability and Aging Effects”
Ragnhild Holen Relling, 1999:74, ISBN 82-471-0445-8, ISSN 0802-3271.

”Capacity Assessment of Titanium Pipes Subjected to Bending and External Pressure”,
Arve Bjørset, 1999:100, ISBN 82-471-0473-3, ISSN 0802-3271.

“Validation of Numerical Collapse Behaviour of Thin-Walled Corrugated Panels”,
Håvar Ilstad, 1999:101, ISBN 82-471-0474-1, ISSN 0802-3271.

“Strength and Ductility of Welded Structures in Aluminium Alloys”,
Miroslaw Matusiak, 1999:113, ISBN 82-471-0487-3, ISSN 0802-3271.

“Thermal Dilation and Autogenous Deformation as Driving Forces to Self-Induced Stresses in High Performance Concrete”,
Øyvind Bjøntegaard, 1999:121, ISBN 82-7984-002-8, ISSN 0802-3271.

“Some Aspects of Ski Base Sliding Friction and Ski Base Structure”,
Dag Anders Moldestad, 1999:137, ISBN 82-7984-019-2, ISSN 0802-3271.

"Electrode reactions and corrosion resistance for steel in mortar and concrete",
Roy Antonsen, 2000:10, ISBN 82-7984-030-3, ISSN 0802-3271.

"Hydro-Physical Conditions in Kelp Forests and the Effect on Wave Damping and Dune Erosion. A case study on Laminaria Hyperborea",
Stig Magnar Løvås, 2000:28, ISBN 82-7984-050-8, ISSN 0802-3271.

"Random Vibration and the Path Integral Method",
Christian Skaug, 2000:39, ISBN 82-7984-061-3, ISSN 0802-3271.

"Buckling and geometrical nonlinear beam-type analyses of timber structures",
Trond Even Eggen, 2000:56, ISBN 82-7984-081-8, ISSN 0802-3271.

”Structural Crashworthiness of Aluminium Foam-Based Components”,
Arve Grønsund Hanssen, 2000:76, ISBN 82-7984-102-4, ISSN 0809-103X.

“Measurements and simulations of the consolidation in first-year sea ice ridges, and some aspects of mechanical behaviour”, Knut V. Høyland, 2000:94, ISBN 82-7984-121-0, ISSN 0809-103X.

”Kinematics in Regular and Irregular Waves based on a Lagrangian Formulation”,
Svein Helge Gjøsund, 2000-86, ISBN 82-7984-112-1, ISSN 0809-103X.

”Self-Induced Cracking Problems in Hardening Concrete Structures”,
Daniela Bosnjak, 2000-121, ISBN 82-7984-151-2, ISSN 0809-103X.

"Ballistic Penetration and Perforation of Steel Plates",
Tore Børvik, 2000:124, ISBN 82-7984-154-7, ISSN 0809-103X.

"Freeze-Thaw resistance of Concrete. Effect of: Curing Conditions, Moisture Exchange and Materials", Terje Finnerup Rønning, 2001:14, ISBN 82-7984-165-2, ISSN 0809-103X

Structural behaviour of post tensioned concrete structures. Flat slab. Slabs on ground",
Steinar Trygstad, 2001:52, ISBN 82-471-5314-9, ISSN 0809-103X.

"Slipforming of Vertical Concrete Structures. Friction between concrete and slipform panel",
Kjell Tore Fosså, 2001:61, ISBN 82-471-5325-4, ISSN 0809-103X.

"Some numerical methods for the simulation of laminar and turbulent incompressible flows",
Jens Holmen, 2002:6, ISBN 82-471-5396-3, ISSN 0809-103X.

"Improved Fatigue Performance of Threaded Drillstring Connections by Cold Rolling",
Steinar Kristoffersen, 2002:11, ISBN: 82-421-5402-1, ISSN 0809-103X.

"Deformations in Concrete Cantilever Bridges: Observations and Theoretical Modelling",
Peter F. Takâcs, 2002:23, ISBN 82-471-5415-3, ISSN 0809-103X.

"Stiffened aluminium plates subjected to impact loading",
Hilde Giæver Hildrum, 2002:69, ISBN 82-471-5467-6, ISSN 0809-103X.

"Full- and model scale study of wind effects on a medium-rise building in a built up area",
Jónas Thór Snæbjørnsson, 2002:95, ISBN82-471-5495-1, ISSN 0809-103X.

"Evaluation of Concepts for Loading of Hydrocarbons in Ice-infested water",
Arnor Jensen, 2002:114, ISBN 82-417-5506-0, ISSN 0809-103X.

"Numerical and Physical Modelling of Oil Spreading in Broken Ice",
Janne K. Økland Gjøsteen, 2002:130, ISBN 82-471-5523-0, ISSN 0809-103X.

"Diagnosis and protection of corroding steel in concrete",
Franz Pruckner, 20002:140, ISBN 82-471-5555-4, ISSN 0809-103X.

"Tensile and Compressive Creep of Young Concrete: Testing and Modelling",
Dawood Atrushi, 2003:17, ISBN 82-471-5565-6, ISSN 0809-103X.

"Rheology of Particle Suspensions. Fresh Concrete, Mortar and Cement Paste with Various Types of Lignosulfonates",
Jon Elvar Wallevik, 2003:18, ISBN 82-471-5566-4, ISSN 0809-103X.

"Oblique Loading of Aluminium Crash Components", Aase Reyes, 2003:15, ISBN 82-471-5562-1, ISSN 0809-103X.

"Utilization of Ethiopian Natural Pozzolans", Surafel Ketema Desta, 2003:26,
ISSN 82-471-5574-5, ISSN:0809-103X.

"Behaviour and strength prediction of reinforced concrete structures with discontinuity regions",
Helge Brå, 2004:11, ISBN 82-471-6222-9, ISSN 1503-8181.

"High-strength steel plates subjected to projectile impact. An experimental and numerical study",
Sumita Dey, 2004:38, ISBN 82-471-6281-4 (elektr. Utg.), ISBN 82-471-6282-2 (trykt utg.),
ISSN 1503-8181.

"Alkali-reactive and inert fillers in concrete. Rheology of fresh mixtures and expansive reactions."
Bård M. Pedersen, 2004:92, ISBN 82-471-6401-9 (trykt utg.), ISBN 82-471-6400-0 (elektr. utg.),
ISSN 1503-8181.

"On the Shear Capacity of Steel Girders with Large Web Openings". Nils Christian Hagen, 2005:9
ISBN 82-471-6878-2 (trykt utg.), ISBN 82-471-6877-4 (elektr. utg.), ISSN 1503-8181.

”Behaviour of aluminium extrusions subjected to axial loading”. Østen Jensen, 2005:7, ISBN 82-471-6872-3 (elektr. utg.) , ISBN 82-471-6873-1 (trykt utg.), ISSN 1503-8181.

”Thermal Aspects of corrosion of Steel in Concrete”. Jan-Magnus Østvik, 2005:5, ISBN 82-471-6869-3 (trykt utg.) ISBN 82-471-6868 (elektr.utg), ISSN 1503-8181.

”Mechanical and adaptive behaviour of bone in relation to hip replacement.” A study of bone remodelling and bone grafting. Sébastien Muller, 2005:34, ISBN 82-471-6933-9 (trykt utg.) (ISBN 82-471-6932-0 (elektr.utg), ISSN 1503-8181.

“Analysis of geometrical nonlinearities with applications to timber structures”. Lars Wollebæk, 2005:74, ISBN 82-471-7050-5 (trykt utg.), ISBN 82-471-7019-1 (elektr. Utg.), ISSN 1503-8181.

“Pedestrian induced lateral vibrations of slender footbridges”, Anders Rönnquist, 2005:102, ISBN 82-471-7082-5 (trykt utg.), ISBN 82-471-7081-7 (elektr.utg.), ISSN 1503-8181.

“Initial Strength Development of Fly Ash and Limestone Blended Cements at Various Temperatures Predicted by Ultrasonic Pulse Velocity”, Tom Ivar Fredvik, 2005:112, ISBN 82-471-7105-8 (trykt utg.), ISBN 82-471-7103-1 (elektr.utg.), ISSN 1503-8181.

“Behaviour and modelling of thin-walled cast components”, Cato Dørum, 2005:128, ISBN 82-471-7140-6 (trykt utg.), ISBN 82-471-7139-2 (elektr. utg.), ISSN 1503-8181.

“Behaviour and modelling of selfpiercing riveted connections”, Raffaele Porcaro, 2005:165, ISBN 82-471-7219-4 (trykt utg.), ISBN 82-471-7218-6 (elektr.utg.), ISSN 1503-8181.

”Behaviour and Modelling og Aluminium Plates subjected to Compressive Load”, Lars Rønning, 2005:154, ISBN 82-471-7169-1 (trykt utg.), ISBN 82-471-7195-3 (elektr.utg.), ISSN 1503-8181

”Bumper beam-longitudinal system subjected to offset impact loading”, Satyanarayana Kokkula, 2005:193, ISBN 82-471-7280-1 (trykt utg.), ISBN 82-471-7279-8 (elektr.utg.), ISSN 1503-8181.

“Control of Chloride Penetration into Concrete Structures at Early Age”, Guofei Liu, 2006:46, ISBN 82-471-7838-9 (trykt utg.), ISBN 82-471-7837-0 (elektr. utgave), ISSN 1503-8181.

“Modelling of Welded Thin-Walled Aluminium Structures”, Ting Wang, 2006:78, ISBN 82-471-7907-5 (trykt utg.), ISBN 82-471-7906-7 (elektr.utg.), ISSN 1503-8181.

”Time-variant reliability of dynamic systems by importance sampling and probabilistic analysis of ice loads”, Anna Ivanova Olsen, 2006:139, ISBN 82-471-8041-3 (trykt utg.), ISBN 82-471-8040-5 (elektr.utg.), ISSN 1503-8181.

“Fatigue life prediction of an aluminium alloy automotive component using finite element analysis of surface topography”. Sigmund Kyrre Ås, 2006:25, ISBN 82-471-7791-9 (trykt utg.), ISBN 82-471-7791-9 (elektr.utg.), ISSN 1503-8181.

”Constitutive models of elastoplasticity and fracture for aluminium alloys under strain path change”, Dasharatha Achani, 2006:76, ISBN 82-471-7903-2 (trykt utg.), ISBN 82-471-7902-4 (elektr.utg.), ISSN 1503-8181.
“Simulations of 2D dynamic brittle fracture by the Element-free Galerkin method and linear fracture mechanics”, Tommy Karlsson, 2006:125, ISBN 82-471-8011-1 (trykt utg.), ISBN 82-471-8010-3 (elektr.utg.), ISSN 1503-8181.

"Penetration and Perforation of Granite Targets by Hard Projectiles", Chong Chiang Seah, 2006:188, ISBN 82-471-8150-9 (printed ver.), ISBN 82-471-8149-5 (electronic ver.) ISSN 1503-8181.

"Deformations, strain capacity and cracking of concrete in plastic and early hardening phases", Tor Arne Hammer, 2007:234, ISBN 978-82-471-5191-4 (trykt utg.), ISBN 978-82-471-5207-2 (elektr.utg.) ISSN 1503-8181.

"Crashworthiness of dual-phase high-strength steel: Material and Component behaviour", Venkatapathi Tarigopula, 2007:230, ISBN 82-471-5076-4 (trykt utg.) ISBN 82-471-5093-1 (elektr.utg.) ISSN 1503-8181.

"Fibre reinforcement in load carrying concrete structures", Åse Lyslo Døssland, 2008:50, ISBN 978-82-471-6910-0 (trykt utg.), ISBN 978-82-471-6924-7 (elektr.utg.), ISSN 1503-8181.

"Low-velocity penetration of aluminium plates", Frode Grytten, 2008:46, ISBN 978-82-471-6826-4 (trykt utg.) ISBN 978-82-471-6843-1 (elektr. Utg.) ISSN 1503-8181.

"Robustness studies of structures subjected to large deformations", Ørjan Fylling, 2008:24, ISBN 978-82-471-6339-9 (trykt utg.) ISBN 978-82-471-6342-9 (elektro.utg.) ISSN 1503-8181.

"Constitutive modelling of morsellised bone",Knut Birger Lund, 2008:92, ISBN 978-82-471-7829-4 (trykt utg.) ISBN 978-82-471-7832-4 (elektro.utg.) ISSN 1503-8181.

"Experimental Investigations of Wind Loading on a Suspension Bridge Girder", Bjørn Isaksen, 2008:131, ISBN 978-82-471-8656-5 (trykt utg.) ISBN 978-82-471-8673-2 (elektro.utg.) ISSN 1503-8181.

"Cracking Risk of Concrete Structures in The Hardening Phase", Guomin Ji, 2008:198, ISBN 978-82-471-1079-9 (printed ver.), ISBN 978-82-471-1080-5 (electronic ver.) ISSN 1503-8181.

"Modelling and numerical analysis of the porcine and human mitral apparatus", Victorien Emile Prot, 2008:249, ISBN 978-82-471-1192-5 (printed ver.), ISBN 978-82-471-1193-2 (electronic ver.), ISSN 1503-8181.